



Nox protein expression, purification and structure analysis
by Danas Baniulis

A dissertation submitted in partial fulfillment of the requirements for the degree of Doctor of Science
in Microbiology

Montana State University

© Copyright by Danas Baniulis (2004)

Abstract:

Flavocytochrome b558 (Cytb) is a heterodimeric integral membrane protein that serves as the electron transferase of the NADPH oxidase. Six homologues of gp91-phox, the large subunit of Cytb, have been identified (Nox family). Understanding of the structure and function of the Nox proteins is limited. To distinguish solvent-accessible and membrane or conformation sequestered regions on native structure of gp91-phox, a number of proteolytic enzyme cleavage products on the lipid reconstituted protein were identified using mass spectrometry, in this study. Affinity-purified rabbit anti-peptide antibodies binding to intact neutrophils suggested extracellular localization of gp91-phox regions, however, results using control CGD-cells suggested that these antibodies may cross-react with an unusual non-gp91-phox species in the normal and CGD-derived plasma membranes. Further, a monoclonal antibody CL5 epitope was mapped to the region 135-DPYSVALSELGDR on the gp91-phox, the prototype for the Nox family proteins. Epitopes of previously described mAb 54.1 and CL5 in gp91-phox align with Nox family proteins with high degree of identity and the use of these two monoclonal antibodies as immunoprobes for Nox family proteins was evaluated. Ab 54.1 was found to be specifically reactive with homologous Nox protein fragments expressed in *E. coli*. Nox3 protein expressed in HEK293H cells was also detected by 54.1, but not by CL5. Nox1 expression in stably transfected NIH 3T3 was examined using the antibodies, but no detectable binding to Nox1 was observed in immunoblotting assays and by flow-cytometry analysis. The antibodies were also used to probe for presence of potential truncated forms of gp91-phox expressed in chronic granulomatous disease (CGD) affected neutrophils with premature termination of gp91-phox synthesis. Analysis did not detect any smaller size protein fragments by immunoblotting. In addition, two other proteins were found to be crossreactive with 54.1 and CL5, they were identified as GRP58 and gelsolin, respectively, two universally expressed cytosolic proteins with regulated association with the plasma membrane. Finally, to help in ongoing structural biology efforts, a recombinant human Cytb expressing PLB-985 cell line was used to develop process of large-scale production of the protein for application in structural biology experiments.

NOX PROTEIN EXPRESSION, PURIFICATION AND STRUCTURE ANALYSIS

by

Danas Baniulis

A dissertation submitted in partial fulfillment
of the requirements for the degree

of

Doctor of Science

in

Microbiology

MONTANA STATE UNIVERSITY
Bozeman, Montana

April 2004

0378

B2257

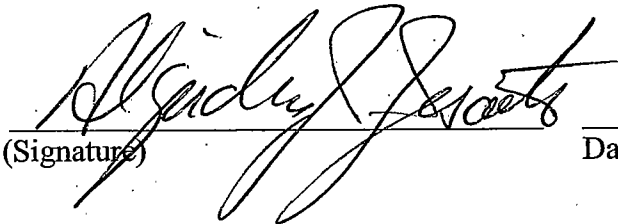
APPROVAL

of a dissertation submitted by

Danas Baniulis


This dissertation has been read by each member of the dissertation committee and has been found to be satisfactory regarding content, English usage, format, citations, bibliographic style, and consistency, and is ready for submission to the College of Graduate Studies.

Dr. Algirdas J. Jesaitis


(Signature) 4/6/04
Date

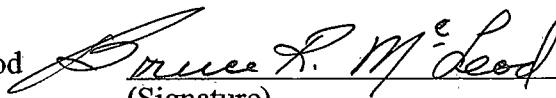
Approved for the Department of Microbiology

Dr. Tim Ford


(Signature) 4/6/04
Date

Approved for the College of Graduate Studies

Dr. Bruce R. McLeod


(Signature) 4-6-04
Date

STATEMENT OF PERMISSION TO USE

In presenting this dissertation in partial fulfillment of the requirements for a doctoral degree at Montana State University, I agree that the Library shall make it available to borrowers under rules of the Library. I further agree that copying of this dissertation is allowable only for scholarly purposes, consistent with "fair use" as prescribed in the U.S. Copyright Law. Requests for extensive copying or reproduction of this dissertation should be referred to Bell & Howell Information and Learning, 300 North Zeeb Road, Ann Arbor, Michigan 48106, to whom I have granted "the exclusive right to reproduce and distribute my dissertation in and from microform along with the non-exclusive right to reproduce and distribute my abstract in any format in whole or in part."

Signature

Bainu

Date

04/05/2004

TABLE OF CONTENTS

1. INTRODUCTION	1
Phagocyte Function and NADPH oxidase.....	1
Structure of NADPH oxidase.....	6
Flavocytochrome b558 Structure and Biosynthesis.....	8
X-linked Chronic Granulomatous Disease	11
Gp91-phox Homologues.....	13
Mammalian Membrane Protein Expression.....	17
Antibody Application for Studies of Cytb Structure and Function	18
Overview of the Dissertation	20
References Cited.....	23
2. TOPOGRAPHY OF GP91-PHOX: COMPUTATIONAL PREDICTIONS AND APPLICATION OF PROTEOLYTIC ENZYME CLEAVAGE AND IMMUNOLOGICAL PROBE BINDING ANALYSIS	40
Introduction.....	40
Materials and Methods.....	42
Materials	42
Computational Amino Acid Sequence Analysis.....	43
Proteolytic Digestion of Relipidated Cytb	44
MALDI Mass Spectrometry	45
Rabbit Polyclonal Antibody Production	46
Polyclonal Antibody Purification	47
SDS-PAGE and Immunoblotting.....	48
ELISA on Cytb Coated Microplates	49
Human Neutrophil Preparation	50
Flow Cytometric Analysis of Surface Antigens	50
Superoxide Anion Production Assay.....	51
Calcium Release Assay.....	52
Results.....	53
Computational Transmembrane Topology Predictions	53
Mass Spectrometry Analysis of Cytb Proteolytic Digests.....	54
Polyclonal anti-peptide antibody binding studies	55
Polyclonal antibody effect on oxidase activity	61
Discussion.....	63
Computational Transmembrane Topology Analysis of Gp91-phox.....	63
Extracellular Domain	66
Cytoplasmic Domain	66
Transmembrane Domain.....	67

TABLE OF CONTENTS – CONTINUED

Limited Proteolysis Followed by Mass Spectrometry	70
Polyclonal Rabbit Anti-peptide Antibodies.....	72
Polyclonal Antibody KIS-1 Effect on Oxidase Activity.....	74
References Cited.....	77
3. ANTI-GP91-PHOX ANTIBODIES (CL5 AND 54.1) AS IMMUNOPROBES FOR NOX FAMILY PROTEINS, GRP58 AND GELSOLIN.....	87
Introduction.....	87
Materials and Methods.....	89
Materials	89
Cloning, Transfection, Cell Culture and Preparation.....	90
Phage-display Epitope Mapping	94
Flow Cytometry Analysis of Surface and Intracellular Antigens.....	95
Protein Purification	96
SDS-PAGE Electrophoresis.....	97
Two-dimensional Gel Electrophoresis.....	98
Immunoblotting.....	99
Protein Identification by MALDI Mass Spectrometry	99
Results and Discussion	100
Monoclonal Antibody Epitope Identification and Characterization of Binding Specificity	100
Monoclonal Antibody CL5 Epitope Identified by Phage Display Epitope Mapping	102
Truncated Gp91-phox Fragments are not Stably Expressed in CGD Neutrophils.....	105
Epitope Alignment with Nox Family Proteins.....	106
Monoclonal Antibody 54.1 Recognizes the Conserved Carboxy-terminal Domain of Nox Family Proteins in Immunoblots.....	108
Attempts at Immunodetection of Nox Protein in Membrane Fraction of HEK-293H and NIH 3T3 Using CL5 and 54.1 on SDS-PAGE and 2-DE Gels	110
Nox1 Expression in NIH 3T3 Cells was not Detected by Flow Cytometry	115
Monoclonal Antibodies 54.1 and CL5 Recognize GRP58 and Gelsolin, Respectively.....	117
References Cited	123
4. HIGH YIELD, INEXPENSIVE BIOREACTOR PRODUCTION OF RECOMBINANT HUMAN FLAVOCYTOCHROME B558	131
Introduction.....	131

TABLE OF CONTENTS – CONTINUED

Materials and Methods.....	134
Materials	134
Cell Culture and Preparation.....	135
Flow Cytometric Analysis	136
Preparation of Cell Membrane Fractions.....	137
SDS-PAGE and Immunoblotting.....	137
Cell Membrane Detergent Extract Preparation and Spectrophotometric Analysis.....	138
Results.....	139
Adaptation to Low Serum Medium	139
Batch and Perfusion Bioreactor Cell Cultures.....	140
Analysis of Cytb Expression.....	143
Discussion.....	145
References Cited	148
 5. FLAVOCYTOCHROME B558 PURIFICATION FROM GP91-PHOX- TRANSFECTED PLB-985 CELLS	 153
Introduction.....	153
Materials and Methods.....	156
Materials	156
Cell Membrane Fraction Isolation	157
Cell Membrane Detergent Extract Preparation and Cytb Purification	157
Spectrophotometric Measurement of Cytb Concentration	159
SDS-PAGE and Immunoblotting.....	159
Results and Discussion	160
References Cited	166
 6. SUMMARY.....	 169

LIST OF TABLES

Table	Page
1.1. Neutrophil Granule Content and Function.....	4
2.1. Results of Gp91-phox Transmembrane Domain Computational Predictions.....	54
2.2. Relipidated Cytb Proteolytic Digestion Peptides Identified by MALDI Mass Spectrometry.....	56
5.1. Cytb Purification from Gp91-PLB-985 Membranes	162

LIST OF FIGURES

Figure	Page
2.1. Antigenicity Profile of Gp91-phox Amino-terminal Half Sequence, Residues 1 to 300, Calculated by the Method of Parker, et al.	57
2.2. Immunoblot Analysis of Polyclonal Antibody Binding to Cytb	58
2.3. Polyclonal Antibody ELISA with Purified Cytb Coated Plates	59
2.4. Flow Cytometry Analysis of Antibody Binding to Intact Neutrophil Cells	60
2.5. The Effect of Antibody KIS-1 on Neutrophil Superoxide Anion Production Rate	62
2.6. The Gp91-phox Topological Model Based on Computational Predictions and Published Experimental Data.....	65
2.7. Soluble Peptides and Protease Cleavage Sites on Gp91-phox Identified by Proteolytic Digestion with Trypsin (panel A) or Endoproteinase Glu-C (panel B) of Lipid Reconstituted Cytb and MALDI Mass spectrometry Analysis.....	71
3.1. Monoclonal Antibody CL5 and 54.1 Immunoreactivity to Neutrophil Cytosol and Membrane Fractions.....	101
3.2. Antibody CL5 Flow Cytometry Analysis of Permeabilized Neutrophils	102
3.3. Phage-display Peptide Sequences Selected on mAb CL5 Affinity Matrix Aligned to the Identified Epitope Sequence on Gp91-phox	103
3.4. CGD Neutrophil Membrane Immunoblotting with mAbs 54.1 (A) and CL5 (B)	107
3.5. Sequence Alignment of Gp91-phox and Nox 1, 3 and 4 Regions Corresponding to mAb 54.1 and CL5 Epitopes Identified by Phage-display	108
3.6. Antibody 54.1 Immunoblotting of Nox 1-4 Fragments (lanes 1-4, respectively).....	109
3.7. Antibody 54.1 and CL5 Immunoblots with HEK-293H Cell Membrane Samples	111

LIST OF FIGURES – CONTINUED

Figure	Page
3.8. Antibody 54.1 and CL5 Immunoblots with NIH 3T3 Cell Membrane Samples.....	113
3.9. Antibody 54.1 Immunoblotting Analysis with NIH 3T3 Cell Membrane Samples Resolved by 2D-electrophoresis.....	114
3.10. Antibody 54.1 and CL5 Flow Cytometry Analysis of Permeabilized NIH 3T3 Cells.....	116
3.11. 2D-electrophoresis Analysis of Partially Purified Mr 57,000 (panel A) and Mr 91,000 (panel B) Protein Samples.....	120
4.1. Flow Cytometry Analysis of Cytb Expression in PLB-985 Cells.....	140
4.2. Repeated Batch Bioreactor Culture of PLB-985 Cells Expressing Cytb.....	142
4.3. Immunoblots of Gp91-PLB-985 and Human Neutrophil Membrane Fractions.....	143
4.4. Reduced-minus-oxidase Absorbance Spectrum of Cytb Expressing PLB-985 Clone.....	144
5.1. Cytb Purification from Gp91-PLB-985 Membranes.....	163
5.2. Absorption Spectrum of Purified Cytb.....	165

GLOSSARY

2-DE, two dimensional electrophoresis;

Ac, acetylated;

ASB-14, amidosulfobetaine-14;

ATP, adenosine 5'-triphosphate;

BCIP/NBT, 5-bromo-4-chloro-3-indolyl phosphate/nitro blue tetrazolium;

BSA, bovine serum albumin;

CHAPS, (3-[(3-cholamidopropyl)dimethylammonio]-1-propanesulfonate);

CGD, chronic granulomatous disease;

Cytb, flavocytochrome b558;

CytC, ferrocytochrome c;

DDM, dodecylmaltoside;

DEAE, diethylaminoethyl;

DMEM, Dulbecco's modified Eagle's medium;

DTT, dithiothreitol;

EDTA, ethylenediaminetetraacetic acid;

EGTA, [ethylenebis(oxyethylenitrilo)]tetraacetic acid;

ELISA, enzyme-linked immunosorbant assay;

FBS, fetal bovine serum;

FAD, flavin adenin dinucleotide;

FITC, fluorescein isothiocyanate;

fMLF, *N*-formyl-methionyl-leucyl-phenylalanine;

gp91-PLB-985, gp91-phox transfected X-CGD PLB-985;

HEPES, *N*-[2-hydroxyethyl]piperazine-*N'*-[2-ethanesulfonic acid];

IEF, isoelectric focusing;

IgG, immunoglobulin G;

IPTG, isopropyl β -D-1-thiogalactopyranoside;

KLH, keyhole limpet hemocyanin;

MAb, monoclonal antibody;

MALDI-TOF, matrix-assisted, laser desorption/ionization - time-of-flight;

Mr, relative molecular mass;

MS, mass spectrometry;

MRB, membrane resuspension buffer (10 mM HEPES, 10 mM NaCl, 100 mM KCl, 1 mM EDTA, 0.1 mM dithiothreitol, 1 mM PMSF, 10 μ g/ml chymostatin, pH-7.4).

NADPH, β -nicotinamide adenine dinucleotidephosphate, reduced;

PBS, phosphate buffered saline (10 mM phosphate, 150 mM NaCl, pH-7.4);

PIPES, 1,4-Piperazinediethanesulfonic acid;

PMA, phorbol myristate acetate;

PMSF, phenylmethylsulfonyl fluoride;

SDS, sodium dodecyl sulfate;

SDS-PAGE, SDS polyacrylamide gel electrophoresis;

SOD, superoxide dismutase;

Tris, tris(hydroxymethyl)aminomethane

YT, yeast extract/tryptone medium.

ABSTRACT

Flavocytochrome b558 (Cytb) is a heterodimeric integral membrane protein that serves as the electron transferase of the NADPH oxidase. Six homologues of gp91-phox, the large subunit of Cytb, have been identified (Nox family). Understanding of the structure and function of the Nox proteins is limited. To distinguish solvent-accessible and membrane or conformation sequestered regions on native structure of gp91-phox, a number of proteolytic enzyme cleavage products on the lipid reconstituted protein were identified using mass spectrometry, in this study. Affinity-purified rabbit anti-peptide antibodies binding to intact neutrophils suggested extracellular localization of gp91-phox regions, however, results using control CGD-cells suggested that these antibodies may cross-react with an unusual non-gp91-phox species in the normal and CGD-derived plasma membranes. Further, a monoclonal antibody CL5 epitope was mapped to the region 135-DPYSVALSELGDR on the gp91-phox, the prototype for the Nox family proteins. Epitopes of previously described mAb 54.1 and CL5 in gp91-phox align with Nox family proteins with high degree of identity and the use of these two monoclonal antibodies as immunoprobes for Nox family proteins was evaluated. Ab 54.1 was found to be specifically reactive with homologous Nox protein fragments expressed in *E. coli*. Nox3 protein expressed in HEK293H cells was also detected by 54.1, but not by CL5. Nox1 expression in stably transfected NIH 3T3 was examined using the antibodies, but no detectable binding to Nox1 was observed in immunoblotting assays and by flow-cytometry analysis. The antibodies were also used to probe for presence of potential truncated forms of gp91-phox expressed in chronic granulomatous disease (CGD) affected neutrophils with premature termination of gp91-phox synthesis. Analysis did not detect any smaller size protein fragments by immunoblotting. In addition, two other proteins were found to be crossreactive with 54.1 and CL5, they were identified as GRP58 and gelsolin, respectively, two universally expressed cytosolic proteins with regulated association with the plasma membrane. Finally, to help in ongoing structural biology efforts, a recombinant human Cytb expressing PLB-985 cell line was used to develop process of large-scale production of the protein for application in structural biology experiments.

INTRODUCTION

Phagocyte Function and NADPH oxidase

Phagocytes are the first line of defense against fungal and bacterial pathogens. Most abundant of this type of immune cells are neutrophils, representing 50-70% of the total number of white blood cells circulating in the blood (1). Neutrophils engulf bacteria by phagocytosis and orchestrate a variety of oxygen dependent and independent systems to kill the ingested pathogens (2). Oxygen-dependent bactericidal species include superoxide anion, hydroxyl radical, hypochlorous acid, nitric oxide, singlet oxygen and ozone (3, 4, 5, 6, 7). Superoxide anion is the common precursor for the production of reactive oxygen species and is generated by the NADPH oxidase in the plasma membrane, phagosomal membrane and at discrete internal membrane sites of these immune cells (8). Recently, the presence of the NADPH oxidase in non-phagocytic cells was also reported and the enzyme activity in such cells may be used for variety of tissue and cell type specific functions, such as host-defense, cell signaling, O₂ sensing or cross-linking reactions (9, 10, 11, 12, 13, 14, 15).

Neutrophils are formed in the bone marrow, where they differentiate to maturity in 7-10 days (1). The cells enter blood stream fully differentiated as polymorphonuclear cells or as nearly mature band cells. Neutrophils have a half life in the blood of approximately 6 hours and ultimately disperse to the tissues in 1-2 days. Mature neutrophils are carried by blood flow but also roll against the blood vessel walls and

sense signals from the underlying endothelium (16). Upregulation of P- and E-selectins and intercellular adhesion molecules, ICAMs, on the endothelial cells is triggered by signals from circulating agents or agents released from the injured cells, e.g. chemokines or bacterial products (17). These interactions enable neutrophil to squeeze between the endothelial cells and to penetrate the basement membrane (an extracellular matrix structure) with the aid of proteolytic enzymes and cell-cell signaling processes. The movement through the vessel wall is known as diapedesis, and enables phagocytes to enter the subepithelial tissues (18). In the tissue they migrate towards infected area along chemical gradients of substances called chemoattractants, such as interleukins, leukotrienes or bacterial products, which are released from bacteria or inflamed cells. This process is called chemotaxis.

Once in an inflammatory site, neutrophils are able to eliminate many pathogens by phagocytosis. One important consequence of the phagocytosis process is the fusion of lysosomes with the phagosome. The process, frequently referred to as phagolysosome fusion, in most cases leads to killing and degradation of the ingested pathogens by peptides, bactericidal enzymes and lipid, protein, and nucleic acid degrading activities (2). Essential to the process is the oxidative degradation of pathogenic components initiated by oxidative metabolites produced via the NADPH oxidase.

Neutrophils contain very few organelles (endoplasmic reticulum, Golgi, mitochondria), apart from the granules. Granule morphogenesis occurs during neutrophil development in the bone marrow as a result of differential expression of granule content proteins during the course of maturation (1, 19, 20). Granules are released selectively

depending on the stimulus (21). Azurophilic granules, also called primary granules, contain proteinases, bactericidal proteins and myeloperoxidase. Gelatinase granules also contain receptors and some proteases (22). The secretory vesicles are the smallest granules and contain plasma proteins, alkaline phosphatase, flavocytochrome b558 (Cytb) and receptors (23). The specific or secondary granules are the most abundant granule type and contain lactoferrin, proteases, components of the NADPH oxidase and receptors for complement and fMLF (24).

The NADPH oxidase plays an essential role in host defensive function of phagocytic cells, i.e., neutrophil granulocytes, monocytes, macrophages and eosinophils (25, 26). Upon phagocytosis, macrophages and neutrophils produce a variety of toxic products that help to kill the microorganisms engulfed into phagosome (3, 5). The NADPH oxidase carries electrons from NADPH across the membrane to oxygen that serves as an electron acceptor and is reduced to superoxide anion. This process is known as the respiratory burst, as it is accompanied by a transient increase in oxygen consumption. Superoxide anion then dismutates to hydrogen peroxide (H_2O_2). Myeloperoxidase, which is released from cytoplasmic granules of neutrophils and monocytes by a degranulation process, reacts with the H_2O_2 to form a complex that can oxidize a large variety of substances (27). Among the latter is chloride, which is oxidized initially to hypochlorous acid, with the subsequent formation of chlorine and chloramines. These products are powerful oxidants that can have profound biological effects, including rapid microbicidal effect or

Table 1. Neutrophil granule content and function (table adapted from (22, 28, 29, 30))

Granule	Factor	Mode of action
Primary (azurophilic)	Microbicidal proteins and peptides (i.e. cathepsin G, defensins, elastase, α_1 -antitrypsin, bactericins)	Destroy bacteria
	Myeloperoxidase	Catalyzes the production of hypochlorous acid
	Lysozyme	Hydrolyzes glycosidic linkages in bacterial cell wall
	Neutral and acidic hydrolases	Activated within the phagosome by pH change and readily breakdown microbial products
Secondary (specific)	Membrane constituents of NADPH oxidase, Cytb, Rap 1A, Rac2; also receptors for laminin, fibronectin, fMLF, TNF, vitronectin and thrombospondin	Provides ROS-producing NADPH oxidase complex proteins, cell surface adhesion molecules and variety of receptors
	Lactoferrin	Iron chelator; may also catalyze production of hydroxyl radical
	Collagenase, gelatinase, histaminase, heparinase, plasminogen activator and sialidase	Breakdown microbial products
	Lysozyme	Hydrolyzes glycosidic linkages in bacterial cell wall
Gelatinase	Gelatinase	Collagen cleavage
	Mac-1, FPR	Provides a reserve of adhesion and chemoattractant receptors
Secretory vesicles	Plasma proteins	
	Cytb, Mac-1, FPR, alkaline phosphatase	Provides a reserve of receptors, adhesion molecules and Cytb

induce damage to adjacent tissue and contribute to the pathogenesis of disease when released to the outside of the cell. It has also been shown that nitrogen species can react with superoxide and form substances important for bacterial killing (7).

Generation of O_2^- by NADPH oxidase is not an exclusive attribute of phagocytic cells. It has been demonstrated in B lymphocytes (31), vascular smooth muscles (12, 14), fibroblasts (11), endothelial cells (12, 32, 33), the carotid body (34), kidney (9, 13) and lung (10, 15). In non-phagocytic cells, NADPH oxidase activity may be used for variety of tissue and cell type specific functions, such as host-defense, cell signaling, O_2 sensing, or cross-linking reactions (12, 35).

A function not involved directly in host defense activity was also suggested for phagocyte NADPH oxidase. Activation of NADPH oxidase in phagocytic cells depends on the binding of specific ligands to receptors expressed in the plasma membrane. The NADPH oxidase can be triggered either by stimulation of adhesion molecules or phagocytic receptors or by chemoattractants such as formyl-methionyl-leucyl-phenylalanine (fMLF), interleukin 8 (IL-8), complement fragment 5a (C5a) and platelet activating factor (PAF) (36, 37, 38, 39). There are also ways of triggering the NADPH oxidase, by-passing the receptors, via stimulation of protein kinase C (PKC) with phorbol myristate acetate (PMA) or elevating Ca^{2+} with ionophores (40). Most (80%) of the membrane-bound components of the NADPH oxidase are located in the specific or secondary granules and the rest in the plasma membrane (41, 42). It has been demonstrated that the two different pools of the oxidase can be activated independently. Stimulating neutrophils with fMLF generates a large, rapid generation of O_2^- from the

plasma membrane pool and a smaller intracellular response (43). Phagocytic stimuli such as bacteria and opsonised yeast induce a mainly intracellular response (44). The function of intracellular activation of the NADPH oxidase in the absence of phagocytosis is not yet understood, but reports have suggested that intracellular oxidative metabolites may have signaling capacity (45).

Structure of the NADPH oxidase

The NADPH oxidase has been shown to consist of several membrane-bound and cytosolic components. Cytb, the core redox active electron transferase, is an integral membrane protein composed of two polypeptides gp91-phox and p22-phox with molecular weights of 91,000 and 22,000 (46, 47). There are also membrane-bound and cytosolic protein-bound prenylated low molecular weight G proteins Rap 1A and Rac2, and cytoplasmic proteins p47-phox, p67-phox and p40-phox (48, 49). Activation of the NADPH oxidase involves translocation of cytosolic oxidase components to the plasma membrane where they associate with each other and Cytb. This association forms an activation regulated, functional multicomponent electron-transfer system.

The membrane protein heterodimer Cytb, with NADPH and FAD binding domains and transmembrane domain-coordinated hemes, serves as an electron transferase of the NADPH oxidase complex (50). Cytosolic proteins p47-phox, p67-phox and Rac2 are needed in the cell-free system to activate Cytb, and have been shown to be required in recombinant systems (8, 51, 52). Human genetic and engineered deficiencies prove that these proteins are required or necessary *in vivo*. The third cytosolic component, p40-

phox, copurifies with p67-phox and p47-phox, suggesting that it may have a regulatory function, as well (53). p47-phox appears to serve as an adaptor protein, transporting the cytosolic protein complex to membrane during activation (54). Neutrophils lacking p47-phox are unable to transfer p67-phox from the cytosol to the membrane during activation. Serving as a switch to trigger oxidase assembly, phosphorylation of p47-phox results in conformational rearrangement, exposing SH3 motifs, proline-rich regions, and a PX domain that together mediate interactions with Cytb and p67-phox (8, 55, 56).

Phosphorylation of p47-phox initially occurs in the cytosol, before translocation of p47-phox to the membrane, and continues after membrane association (57). Besides the SH3 domain, which is important for protein-protein interaction in oxidase assembly, p67-phox contains an NADPH binding domain and an activation domain (amino acids ~200-210) those may be involved in electron flow or regulation of the process within Cytb (8).

Gorzalczany, et al. (58) proposed that the essential event in activation of NADPH oxidase is the interaction between p67-phox and Cytb, and that Rac2 and p47-phox serve as carriers for p67-phox to the membrane. When prenylated, Rac2 can fulfill the carrier function by itself, supporting oxidase activation by p67-phox in the absence of p47-phox and amphiphile. Likewise, Rac2 was shown to regulate electron transfer from NADPH to FAD by Cytb independently of p67-phox (59). The PX domains of p40-phox, as well as p47-phox, have been demonstrated to bind to specific phosphoinositides and may thus mediate in part the assembly of the oxidase at the plasma or phagosomal membrane (60, 61, 62).

Flavocytochrome b558 Structure and Biosynthesis

The electron transferase function of the glycosylated, heterodimeric, bis-heme, transmembrane Cytb arises from the union of its structural characteristics. The large subunit of Cytb, gp91-phox, is encoded by gene CYBB which is comprised of 13 exons spread over a total of 30 kb on the X chromosome at locus Xp21.1 (63). The gene encoding p22-phox CYBA is localized on chromosome 16 at 16q24 and is divided in 6 exons spanning 8.5 kb. Two subunits of Cytb are tightly associated and required for the active NADPH oxidase complex and integrity of its characteristic heme spectrum (64, 65). In myeloid cells, the absence of p22-phox protein due to genetic defects results in the loss of gp91-phox expression and vice versa, indicating that each of these proteins requires the other for mutual stability (66, 67). Neither gp91-phox alone nor the combination of individual gp91-phox and p22phox subunits, when expressed in COS-7 cell line, are able to replace the intact gp91/p22 heterodimer in supporting superoxide production in cell-free NADPH oxidase reconstitution assays, indicating that assembly of the fully functional enzyme complex requires specific interactions between subunits (65). However, gp91-phox and p22-phox have been stably expressed in the absence of their partner subunit in non-phagocytic cells lines (65, 68).

Heterodimer formation is also important for gp91-phox carbohydrate chain maturation (69). Gp91-phox is a glycoprotein (46, 70) and it has five potential N-linked glycosylation consensus sites. Glycosylation of three asparagine residues (131, 148 and 239) was supported by mutagenesis analysis of these positions in a recombinant expression system (71). The protein core of gp91-phox is 58 kDa and its maturation to

form the highly-glycosylated protein proceeds first in the endoplasmic reticulum and then in the Golgi apparatus. The specific function of the glycosylation, whether it is to protect protein from proteolysis, shield it from immunologic surveillance, or some unknown lectin-like interaction, remains unknown.

Cytb contains at least two non-identical, bis histidinyl coordinated heme groups that are believed to be located in either the transmembrane or extracellular domain of the protein (or possibly in both locations) and mediate the final steps of electron transfer to molecular oxygen (47, 72, 73, 74). The function of the Cytb as an electron transporting component of the NADPH oxidase is completely dependent on the presence of FAD (75, 76, 77, 78) which probably receives electrons directly from NADPH, acting like ferredoxin or nitrate reductase (79). It is uncertain how the enzyme functions as a single electron donor to molecular oxygen from a two electron oxidation of NADPH, although intermolecular electron tunnelling has been proposed (80). The substrate, NADPH, was shown to bind to the large subunit of Cytb (81, 82, 83), although some evidence exists suggesting it binds to p67-phox as well (84, 85).

Cytb biosynthesis studies have demonstrated that the heme incorporation is a critical step in the assembly of Cytb subunits. PLB-985 myeloid leukemia cells in which heme synthesis was prevented by addition of succinyl acetone to cell culture medium had decreased expression levels of both p22-phox and the mature glycosylated form of gp91-phox, but not that of the 65 kDa precursor (86, 87). When the histidine residues 101, 115, 209 and 222, putative ligands for the two heme prosthetic groups in gp91-phox, are

replaced by Leu or Arg, p65 is no longer processed and the p65 does not form a heterodimer with p22-phox, resulting in cells that lack functional Cytb (88).

Little is known of secondary structure, transmembrane topological organization or function of the small subunit of Cytb, p22-phox. Primary structure of p22-phox has three hydrophobic domains in the N-terminal two-thirds of the molecule, and a proline-rich domain in the C-terminal cytoplasmic tail. Such proline-rich regions can mediate protein-protein association by binding to SH3 domains that are found in variety of proteins involved in signal transduction, including cytosolic phox proteins. The proline-rich domains 156-PPRPP and 177-GGPPGGP of p22-phox binds the N-terminal SH3 domain of p47-phox, and this interaction is believed to play a dominant role in promoting the association of cytosolic complex, containing p40-phox, p47-phox, and p-67-phox, with flavocytochrome b558 (52, 89). Surface features of p22-phox were mapped with antibodies raised in rabbits against synthetic peptides corresponding to various regions of the protein or monoclonal antibodies which epitopes were identified using phage display libraries. In this way, conclusions were drawn that the amino and carboxy termini of the p22-phox subunit are exposed to the cytosol (90, 91). Moreover, the phage mapping analysis combined with nuclear magnetic resonance (NMR) spectroscopy provided a low-resolution view of the tertiary structure of p22-phox around the epitope of monoclonal antibody 44.1. The results of the study inferred close spatial proximity of the epitope components 29-TAGRF and 183-PQVNPI from discontinuous regions of p22-phox separated apart in the sequence by 150 residues (92). Analysis of the cytochrome using lithium dodecyl sulfate-polyacrylamide gel electrophoresis followed by

tetramethylbenzidine heme staining demonstrated the presence of heme in both the 91- and 22-kDa subunits (93) suggesting that Cytb is bi-heme molecule with at least one heme residing in the large subunit and one shared between both subunits. However, co-expression of gp91-phox with p22-phox harboring leucine, tyrosine, or methionine amino acid substitutions at histidine 94, the only invariant histidine residue within the p22-phox subunit, did not affect heterodimer formation or Cytb function. The heme spectrum in purified preparations of flavocytochrome b558 containing the p22-phox derivative was unaffected. These findings demonstrate conflicting views about the distribution and coordination of the hemes within the Cytb.

X-linked Chronic Granulomatous Disease

Chronic granulomatous disease (CGD) is an immunodeficiency syndrome characterized clinically by severe recurrent bacterial and fungal infections (94, 95, 96). The persistence of catalase positive bacteria and fungal conidia and hyphal forms, often within the phagosomal vacuoles of neutrophils or macrophages, is the stimulus to a chronic inflammatory state with granuloma formation. The most common pathogens encountered in CGD patients are *Staphylococcus aureus*, various *Aspergillus* species and variety of Gram-negative enteric bacilli.

CGD is rare disease, with an estimated incidence of 1 in about 250,000 individuals. Biochemically, CGD is characterized by the inability of phagocytic leukocytes (neutrophils, eosinophils, monocytes and macrophages) to activate the

NADPH oxidase and to generate superoxide as the needed precursor for reactive oxygen species involved in the killing of phagocytosed microorganisms (97).

CGD is a very heterogeneous disorder clinically, because of many antimicrobial systems that can partially compensate for the defect in oxygen-dependent killing systems, and biochemically, because of the complicated genetic origin of CGD (94). The disease is caused by mutations in any one of four genes encoding subunits of the NADPH oxidase, resulting in an absence or low levels of enzyme activity. More than two thirds of all cases are X-linked recessive and results from defects in the CYBB gene that encodes the gp91-phox subunit. A broad distribution of defects in patients with X-linked CGD include small and large deletions, insertions, nonsense and missense mutations, splice-site defects and, rarely, mutations in the 5' regulatory region. The remaining CGD mutation cases are autosomal recessive and caused by defects in CYBA, NCF-1 and NCF-2, which encode p22-phox, p47-phox and p67-phox, respectively (98). To date, there are no reports of CGD caused by defects in the gene for a fifth oxidase subunit, p40-phox. A single patient has been identified with a related immunodeficiency resulting from a defect in the gene for Rac2 (99, 100). Of the 410 known defects in the four affected genes only 19 result in normal level of inactive or weakly active protein: 17 out of 358 mutations in CYBB, 1 out of 25 in CYBA, 1 out of 17 in NCF-2 and none out of 10 in NCF-1 (98, 101, 102). Some of these mutations provide evidence for the function of specific domains in affected subunits and their roles in oxidase activation. The remaining 95% of CGD mutations result in a complete absence or greatly diminished level of protein, either

because the affected gene is partially or completely deleted, or because the aberrant protein product (or mRNA) is unstable.

Gp91-phox Homologues

Homologues of human gp91-phox have been identified in a variety of tissues. Based on their sequence similarity four different mammalian proteins were identified and assigned to the Nox family, two larger proteins were identified and assigned to the Duox family (35, 103, 104, 105). As shown by a survey of genome data, the Nox and Duox proteins are widely distributed in nature. Nox orthologues have been identified in *Drosophila* and *Dictyostelium discoideum* (104). A protein related to Duox1 has been found in *Caenorhabditis elegans* (106). Moreover, plants possess homologues of gp91-phox as well. The *Arabidopsis thaliana* gene called RBOHA (Respiratory Burst Oxidase Homology A) encodes a protein of 108 kDa, which has carboxy-terminal region highly similar to the human neutrophil gp91-phox, and a smaller protein (~69 kDa) was identified in rice (107). A subsequent study revealed the presence in *A. thaliana* of five other genes encoding homologues of human gp91-phox protein (108). These homologues are of approximately the same size between 897 and 948 amino acids and their carboxy-domains are of 60% identity to human gp91-phox. These proteins may be responsible for NADH-dependent ferricytochrome c reductase activity by plasma membrane cytochrome b558 in *Z. mais* (109).

The Nox proteins have a relatively specific tissue distribution in human. Nox 1 is predominantly expressed in colon with lower levels in the prostate, uterus and vascular

smooth muscle cells, where it is induced by platelet derived growth factor (110, 111). Nox2, which designates the gp91-phox, is present mostly in phagocytic and other cell types as described in previous section. Nox3 was cloned from fetal kidney (112), Nox4 also named Renox was found in kidney cortex (113, 114) and osteoclasts (115). Nox5 is expressed in variety of fetal tissues and adult spleen, lymph nodes, uterus, testis (116). The Duox1, also designated as Thox1, is present in the thyroid gland, tracheal, bronchial epithelial cells (117, 118, 119) and Duox2 also designated Thox2 present in thyroid gland and also in the small intestine, colon, epithelial cells in salivary excretory ducts and rectal glands (117, 119, 120).

All of the identified homologues contain a cluster of up to six putative hydrophobic transmembrane domains similar to the gp91-phox transmembrane helices at amino-terminal part of the protein including conserved histidine residues implicated in heme ligation by gp91-phox. There also is significant similarity in the carboxy-terminal domain of Nox/Duox family proteins with consensus sequences comprising putative flavin- and NAD(P)H-binding sites found in a variety of FAD-bound redox proteins. Nox5, Duox proteins and homologous plant proteins also contain larger hydrophilic N-terminal domain not present in other Nox proteins (107, 108, 116, 117, 118). This domain contains two Ca^{2+} -binding EF-hand motifs. In addition, Duox proteins possess a unique, amino-terminal hydrophobic transmembrane α -helix and putative extracellular domain homologous to peroxidase (117, 118). The extended N-terminal domain of plant RbohA also contains EF-hand motifs, and in addition, a region with extended sequence similarity to the human RanGTPase-activating protein (107).

Although neutrophil NADPH oxidase can be activated by Ca^{2+} because of the activation of Ca^{2+} -sensitive second messenger systems as described before (121, 122, 123), it was also shown that another gp91-phox homologue, Nox5, contains an N-terminal extension with three EF hands and when heterologously expressed is able to generate superoxide and conduct H^+ ions in response to cytosolic free Ca^{2+} concentration elevations (116). Activation of Duox enzymes by elevations of the cytosolic free Ca^{2+} concentration has been also suggested based on presence of EF hand motifs and the previously described Ca^{2+} -activated superoxide generation in thyroid cells (124).

The biological function and its mechanism of gp91-phox homologues is scarcely based on experimental data and mostly hypothetical. The Nox, Duox family protein, as well as NADPH oxidase function, may vary depending on the cell type involved. First studies of Nox1 suggested its function in mitogenic regulation and cell transformation (111), and it was shown that production of O_2^- was not enhanced by addition of p47-phox, p67-phox or Rac in cell-free system (125). However, later it was shown that Nox1 expression is induced during differentiation in colon cells and that did not affect the proliferation of colon carcinoma cells (126). Furthermore, coexpression of cytosolic components, p47-phox and p67-phox, augments Nox1 activity in reconstituted K562 or HEK293 cells, and it suggest that Nox1 is likely to be involved in host-defense system of colon epithelium (126, 127). Also it was suggested that the Nox1 activity might be regulated by novel proteins homologous to p47-phox and p67-phox, designated p42-phox and p51-phox, respectively (127, 128, 129).

Primarily, Duox proteins were identified in thyroid gland (118). It was suggested that the proteins possibly complementing function to other thyroid peroxidase and NADPH oxidase enzymes involved in iodination thyroglobulin as they possess amino-terminal peroxidase homologous domain in addition to gp91-phox homologous domains involved in O_2^- production. Later the protein expression was identified in salivary glands, rectum, trachea, and bronchium and Geiszt M et al. postulated that Duox1 and Duox2 might serve as a source of H_2O_2 for lactoperoxidase-mediated antimicrobial defense mechanisms on mucosal surfaces (119).

As a major source of ROS production in kidney, Nox4 has been implicated to have a role under pathological conditions (113, 114). The increase of expression levels and tissue distribution of Nox4 and p22-phox correlated with localization of 8-hydroxydeoxyguanosine, which is a marker of ROS-induced DNA damage, in the kidney of diabetic rats (130). The other homologue, Nox5, is likely to be involved in Ca^{2+} -activated, redox-dependent processes of spermatozoa and lymphocytes such as sperm-oocyte fusion, cell proliferation, and cytokine secretion (116).

Rapid generation of oxidants has been shown in many plant-pathogen interactions and is a characteristic feature in the so called hypersensitive response. Plants possess an NADPH oxidase system similar to that of neutrophils (131, 132, 133). Immunological identification of the soybean proteins corresponding to NADPH oxidase components p22-phox, p47-phox and p67-phox has been described. *A. thaliana* protein RbohA amino-terminal Ca^{2+} binding EF hand motifs have been implicated in the rapid stimulation of the oxidative burst in cells challenged to prime the hypersensitive response (132, 134).

Interplay between the Ca^{2+} activation and GTP-ase mediated signal dumping of domain, similar to human GTPase activating protein, at the N-terminus of RbohA may contribute to stringent regulation of the plant NADPH oxidase (107).

Mammalian Membrane Protein Expression

A fundamental requirement of structural biology experiments is to be able to obtain high quantities of pure protein. An analysis of the mammalian membrane protein structures published shows that the majority of the proteins were purified from naturally abundant sources (reviewed by Tate (135)). In contrast, the majority of new soluble protein structural studies utilized recombinant material (136). These statistics reflect the fact that recombinant membrane proteins are difficult to obtain. Currently, four major expression systems can be distinguished: those using bacteria, yeast, insect cells, or mammalian cells. Although overexpression strategies typically have been developed for soluble proteins, these generally perform poorly with integral membrane proteins. However, several cases of successful mammalian integral membrane protein expression in broadly used prokaryotic and lower eukaryotic expression systems, such as *E. coli*, *P. pastoris*, *S. cerevisiae* and baculovirus-mediated expression in insect cells, have been reported during last decade (reviewed in (136, 137)). These include several G-protein coupled receptors, monoamine oxidase, Ca^{2+} -ATPase and the adrenergic receptor.

Use of prokaryotic or lower eukaryotic expression systems for mammalian proteins can lead to misfolding or loss of functionality of the protein expressed. Inclusion bodies are an attractive way of producing large amounts of protein, but this naturally

requires the refolding of the protein into a functional form, which has been achieved for only relatively few membrane proteins (136). Mammalian membrane proteins often require specific lipid requirements, the presence of certain chaperones, and specific post-translational modifications. Although in some cases glycosylation may play a crucial role in correct protein folding and insertion to membrane, reports of successful expression of functional glycoproteins exist. Several G-protein-coupled receptors were expressed in *E. coli* (138, 139), prostaglandin H2 synthase-2 was expressed in insect cells (140), monoamine oxidase-B in yeast (141), and fatty acid amide hydrolase in bacteria (142). However, these three later proteins have relatively small hydrophobic surface area and do not involve more than one subunit.

Obviously, recombinant protein can be best expressed in the expression system that most closely resembles the natural environment of the protein. For mammalian proteins, therefore, mammalian expression systems are likely to give the best results in terms of structure and functionality of the protein. Transient expression in mammalian cells and the creation of stable cell lines are widely used for protein function and physiological studies, though these systems are complex and relatively expensive for production of milligram quantities of protein. Recent progress in this area may make the mammalian expression systems more popular. An efficient system based upon Semliki Forest virus is now available which appears to be capable of producing large quantities of protein from variety of eukaryotic cells (143). In addition, temperature-regulated, inducible Sindbis virus replicon-based expression system has been developed which should prove useful in cases where large doses of the target protein are toxic (144).

Antibody Application for Studies of Cytb Structure and Function

Anti-Cytb antibodies have found variety of applications in research related to NADPH oxidase structure and function. In the absence of crystallographic data, a variety of experimental approaches have been utilized to explore the arrangements of polypeptide chains of the two subunits of Cytb, include analysis of antibody directed against specific sequences access to the epitope. An antibody raised against residues Glu150-Ser172 in the large subunit bound to intact neutrophils, indicating that this region is exposed to the outside of the cells, while the antibodies raised against any of the carboxyl-terminal regions of the large and small subunits or the amino-terminal region of the small subunit, bound to neutrophils only after the cells were made permeable by freezing and thawing (91).

Biochemical analysis combined with epitope mapping of monoclonal antibodies has confirmed aspects of transmembrane topology. An epitope bound by monoclonal antibody 7D5 has been mapped using phage display analysis to include residues Arg159-Glu164 and Arg226-Gln231 on gp91-phox and further antibody binding analysis revealed location of the regions on the non-cytosolic aspect of neutrophil membrane (145, 146). Epitopes of monoclonal antibodies NL7 (Glu498-Lys506 on gp91-phox); 44.1 (including regions Ser29-Phe33 and Pro183-Ile188 on p22-phox) and 449 (Gly182-Val185 on p22-phox) were shown to be located in neutrophil cytosol and indicate cytosolic location of the segments on the two Cytb subunits (90, 92, 147, 148). The phage mapping analysis combined with nuclear magnetic resonance (NMR) spectroscopy revealed intramolecular interaction features in the tertiary structure of the Cytb (92). The results of the study

inferred close spatial proximity of the epitope components Ser29-Phe33 and Pro183-Ile188 from discontinuous regions of p22-phox separated apart in the sequence by 150 residues.

Also, it was shown that antibody NL7 epitope Glu498-Lys506 represents a region of gp91-phox important for oxidase function (148). In a cell-free assay, NL7 inhibited *in vitro* activation of the NADPH oxidase though it bound its epitope on gp91(phox) independently of cytosolic factor or Rac translocation. However, after assembly of the NADPH oxidase complex, mAb NL7 bound the epitope but did not inhibit the generation of superoxide. Three-dimensional modeling of the C-terminal domain of gp91(phox) on a corn nitrate reductase template suggests close proximity of the NL7 epitope to the proposed NADPH binding site, but significant separation from the proposed p47-phox binding sites, suggesting that the Glu498-Lys506 segment resides on the cytosolic surface of gp91-phox and represents a region important for oxidase function, but not substrate or cytosolic component binding.

Except for structural analysis anti Cytb antibodies have a found variety of other important applications, such as Cytb purification (149), identification and quantitative analysis in Cytb expression experiments and chronic granulomatous disease (CGD) studies (13, 33, 65, 66, 146, 150, 151, 152, 153, 154, 155). Moreover, such antibodies are used in studies involving biochemical and physiological assays of Cytb and NADPH oxidase function (148, 156); (R.M. Taylor, A.J. Jesaitis, unpublished data).

Overview of the Dissertation

Nox protein-produced reactive oxygen species participate in variety of biological functions, including host-defense, cell signaling and O₂ sensing. They are also involved in non-specific tissue damage in a variety of inflammatory diseases. Understanding of the structural design of NADPH oxidase core functional element, the prototypical electron transferase flavocytochrome b558 (Cytb) is essential for comprehension and effective control of the ROS mediated processes initiated by Cytb or the recently discovered and widely expressed Nox family proteins. Thus, the fundamental goal of this research was to extend knowledge of Nox protein structure and function by analysis of elementary features of the Cytb structure. In addition, significant effort was extended toward the development of experimental tools required for the Nox protein detection and detailed structure analysis.

To address important structural issues about gp91-phox, transmembrane topology and protein surface features of the protein were characterized in study described in Chapter 2. Amino acid sequence computational analysis was employed to identify hydrophobic segments of the sequence forming transmembrane domains. Further, analysis of published experimental data was used to refine mathematical predictions to Cytb transmembrane topology model. To support topological predictions and to study functional aspects of the Cytb, a classical approach was employed to produce anti-peptide antibodies against synthetic peptides mimicking segments on N-terminal half of the gp91-phox. Proteolytic digestion of purified and lipid-reconstituted Cytb product analysis

by mass spectrometry extended understanding of hydrophilic, solvent exposed segments on gp91-phox.

Anti-Cytb antibodies have found variety of applications in research related to NADPH oxidase structure and function. Similarities of Nox family protein amino acid sequences also suggested the possibility for application of anti-Cytb antibodies in the detection of other Nox proteins. This perspective was explored by the characterization of binding features for two anti-Cytb antibodies and the immunological analysis of Nox protein expression and is described in Chapter 3. In that study, epitope identification of a new monoclonal anti-Cytb antibody to amino-terminal half of the large subunit of the Cytb provided means to investigate the possibility of expression of truncated gp91-phox forms in neutrophils with CGD mutations resulting in premature termination of the large subunit transcription.

In Chapter 4, a new methodology is described for large-scale production of human neutrophil Cytb in a recombinant expression system. Efficient production and purification techniques are essential to obtain quantities of the protein required for detailed structure analysis. Thus, design of high-yield recombinant protein expression systems would be an attractive alternative source for a functional Cytb. Further development of this system is described in Chapter 5. This section includes an unpublished description of attempts to develop a purification procedure for recombinant Cytb.

References Cited

1. Bainton DF, Ulliyot JL, Farquhar MG. 1971. The development of neutrophilic polymorphonuclear leukocytes in human bone marrow. *J. Exp. Med.* 134:907-34
2. Stickle JE. 1996. The neutrophil. Function, disorders, and testing. *Vet. Clin. North. Am. Small. Anim. Pract.* 26:1013-21
3. Babior BM. 2000. Phagocytes and oxidative stress. *Am. J. Med.* 109:33-44
4. Hampton MB, Kettle AJ, Winterbourn CC. 1998. Inside the neutrophil phagosome: oxidants, myeloperoxidase, and bacterial killing. *Blood* 92:3007-17
5. Rossi F, Zatti M. 1964. Biochemical aspects of phagocytosis in polymorphonuclear leucocytes. NADH and NADPH oxidation by the granules of resting and phagocytizing cells. *Experientia.* 20:21-3
6. Shepherd VL. 1986. The role of the respiratory burst of phagocytes in host defense. *Semin. Respir. Infect.* 1:99-106
7. Shiloh MU, MacMicking JD, Nicholson S, Brause JE, Potter S, Marino M, Fang F, Dinauer M, Nathan C. 1999. Phenotype of mice and macrophages deficient in both phagocyte oxidase and inducible nitric oxide synthase. *Immunity.* 10:29-38
8. Babior BM, Lambeth JD, Nauseef W. 2002. The neutrophil NADPH oxidase. *Arch. Biochem. Biophys.* 397:342-4
9. Cui XL, Douglas JG. 1997. Arachidonic acid activates c-jun N-terminal kinase through NADPH oxidase in rabbit proximal tubular epithelial cells. *Proc. Natl. Acad. Sci. U. S. A.* 94:3771-6
10. Fu XW, Wang D, Nurse CA, Dinauer MC, Cutz E. 2000. NADPH oxidase is an O₂ sensor in airway chemoreceptors: evidence from K⁺ current modulation in wild-type and oxidase-deficient mice. *Proc. Natl. Acad. Sci. U. S. A.* 97:4374-9

11. Meier B, Jesaitis AJ, Emmendorffer A, Roesler J, Quinn MT. 1993. The cytochrome b-558 molecules involved in the fibroblast and polymorphonuclear leucocyte superoxide-generating NADPH oxidase systems are structurally and genetically distinct. *Biochem. J.* 289 (Pt 2):481-6
12. Munzel T, Hink U, Heitzer T, Meinertz T. 1999. Role for NADPH/NADH oxidase in the modulation of vascular tone. *Ann. N. Y. Acad. Sci.* 874:386-400
13. Radeke HH, Cross AR, Hancock JT, Jones OT, Nakamura M, Kaever V, Resch K. 1991. Functional expression of NADPH oxidase components (alpha- and beta-subunits of cytochrome b558 and 45-kDa flavoprotein) by intrinsic human glomerular mesangial cells. *J. Biol. Chem.* 266:21025-9
14. Ushio-Fukai M, Zafari AM, Fukui T, Ishizaka N, Griendling KK. 1996. p22phox is a critical component of the superoxide-generating NADH/NADPH oxidase system and regulates angiotensin II-induced hypertrophy in vascular smooth muscle cells. *J. Biol. Chem.* 271:23317-21
15. Youngson C, Nurse C, Yeger H, Cutz E. 1993. Oxygen sensing in airway chemoreceptors. *Nature.* 365:153-5
16. Tonnesen MG. 1989. Neutrophil-endothelial cell interactions: mechanisms of neutrophil adherence to vascular endothelium. *J. Invest Dermatol.* 93:53S-8S
17. Albelda SM, Smith CW, Ward PA. 1994. Adhesion molecules and inflammatory injury. *FASEB. J.* 8:504-12
18. Parkos CA. 1997. Molecular events in neutrophil transepithelial migration. *Bioessays.* 19:865-73
19. Arnljots K, Sorensen O, Lollike K, Borregaard N. 1998. Timing, targeting and sorting of azurophil granule proteins in human myeloid cells. *Leukemia.* 12:1789-95
20. Le C, V, Calafat J, Borregaard N. 1997. Sorting of the specific granule protein, NGAL, during granulocytic maturation of HL-60 cells. *Blood.* 89:2113-21

21. Bainton DF. 1993. Neutrophilic leukocyte granules: from structure to function. *Adv. Exp. Med. Biol.* 336:17-33
22. Kjeldsen L, Bjerrum OW, Askaa J, Borregaard N. 1992. Subcellular localization and release of human neutrophil gelatinase, confirming the existence of separate gelatinase-containing granules. *Biochem. J.* 287 (Pt 2):603-10
23. Borregaard N, Miller LJ, Springer TA. 1987. Chemoattractant-regulated mobilization of a novel intracellular compartment in human neutrophils. *Science.* 237:1204-6
24. Bainton DF, Miller LJ, Kishimoto TK, Springer TA. 1987. Leukocyte adhesion receptors are stored in peroxidase-negative granules of human neutrophils. *J. Exp. Med.* 166:1641-53
25. Pick E, Gadba R. 1988. Certain lymphoid cells contain the membrane-associated component of the phagocyte-specific NADPH oxidase. *J. Immunol.* 140:1611-7
26. Segal AW, Garcia R, Goldstone H, Cross AR, Jones OT. 1981. Cytochrome b-245 of neutrophils is also present in human monocytes, macrophages and eosinophils. *Biochem. J.* 196:363-7
27. Klebanoff SJ. 1999. Myeloperoxidase. *Proc. Assoc. Am. Physicians* 111:383-9
28. Borregaard N, Lollike K, Kjeldsen L, Sengelov H, Bastholm L, Nielsen MH, Bainton DF. 1993. Human neutrophil granules and secretory vesicles. *Eur. J. Haematol.* 51:187-98
29. DeLeo FR. 1996. *Molecular interaction of human neutrophil NADPH oxidase proteins.* Doctor of Philosophy thesis. Montana State University, 6 pp.
30. Sengelov H, Follin P, Kjeldsen L, Lollike K, Dahlgren C, Borregaard N. 1995. Mobilization of granules and secretory vesicles during in vivo exudation of human neutrophils. *J. Immunol.* 154:4157-65

31. Volkman DJ, Buescher ES, Gallin JI, Fauci AS. 1984. B cell lines as models for inherited phagocytic diseases: abnormal superoxide generation in chronic granulomatous disease and giant granules in Chediak-Higashi syndrome. *J. Immunol.* 133:3006-9
32. Bayraktutan U, Blayney L, Shah AM. 2000. Molecular characterization and localization of the NAD(P)H oxidase components gp91-phox and p22-phox in endothelial cells. *Arterioscler. Thromb. Vasc. Biol.* 20:1903-11
33. Meyer JW, Holland JA, Ziegler LM, Chang MM, Beebe G, Schmitt ME. 1999. Identification of a functional leukocyte-type NADPH oxidase in human endothelial cells :a potential atherogenic source of reactive oxygen species. *Endothelium.* 7:11-22
34. Cross AR, Henderson L, Jones OT, Delpiano MA, Hentschel J, Acker H. 1990. Involvement of an NAD(P)H oxidase as a pO₂ sensor protein in the rat carotid body. *Biochem. J.* 272:743-7
35. Vignais PV. 2002. The superoxide-generating NADPH oxidase: structural aspects and activation mechanism. *Cell. Mol. Life. Sci.* 59:1428-59
36. Daniels RH, Finnen MJ, Hill ME, Lackie JM. 1992. Recombinant human monocyte IL-8 primes NADPH oxidase and phospholipase A2 activation in human neutrophils. *Immunology.* 75:157-63
37. Dewald B, Baggiolini M. 1985. Activation of NADPH oxidase in human neutrophils. Synergism between fMLP and the neutrophil products PAF and LTB₄. *Biochem. Biophys. Res. Commun.* 128:297-304
38. Rossi F, Grzeskowiak M, Della B, V, Calzetti F, Gandini G. 1990. Phosphatidic acid and not diacylglycerol generated by phospholipase D is functionally linked to the activation of the NADPH oxidase by FMLP in human neutrophils. *Biochem. Biophys. Res. Commun.* 168:320-7
39. Wymann MP, Von T, V, Deranleau DA, Baggiolini M. 1987. The onset of the respiratory burst in human neutrophils. Real-time studies of H₂O₂ formation reveal a rapid agonist-induced transduction process. *J. Biol. Chem.* 262:12048-53

40. Henderson LM, Chappel JB. 1996. NADPH oxidase of neutrophils. *Biochim. Biophys. Acta.* 1273:87-107
41. Borregaard N, Heiple JM, Simons ER, Clark RA. 1983. Subcellular localization of the b-cytochrome component of the human neutrophil microbicidal oxidase: translocation during activation. *J. Cell. Biol.* 97:52-61
42. Borregaard N, Tauber AI. 1984. Subcellular localization of the human neutrophil NADPH oxidase. b-Cytochrome and associated flavoprotein. *J. Biol. Chem.* 259:47-52
43. Dahlgren C. 1987. Polymorphonuclear leukocyte chemiluminescence induced by formylmethionyl-leucyl-phenylalanine and phorbol myristate acetate: effects of catalase and superoxide dismutase. *Agents. Actions.* 21:104-12
44. Hed J, Stendahl O. 1982. Differences in the ingestion mechanisms of IgG and C3b particles in phagocytosis by neutrophils. *Immunology.* 45:727-36
45. Brumell JH, Burkhardt AL, Bolen JB, Grinstein S. 1996. Endogenous reactive oxygen intermediates activate tyrosine kinases in human neutrophils. *J. Biol. Chem.* 271:1455-61
46. Parkos CA, Allen RA, Cochrane CG, Jesaitis AJ. 1987. Purified cytochrome b from human granulocyte plasma membrane is comprised of two polypeptides with relative molecular weights of 91,000 and 22,000. *J. Clin. Invest.* 80:732-42
47. Parkos CA, Allen RA, Cochrane CG, Jesaitis AJ. 1988. The quaternary structure of the plasma membrane b-type cytochrome of human granulocytes. *Biochim. Biophys. Acta.* 932:71-83
48. Babior BM. 1999. NADPH oxidase: an update. *Blood.* 93:1464-76
49. Leusen JH, Verhoeven AJ, Roos D. 1996. Interactions between the components of the human NADPH oxidase: intrigues in the phox family. *J. Lab. Clin. Med.* 128:461-76

50. Cross AR, Parkinson JF, Jones OT. 1985. Mechanism of the superoxide-producing oxidase of neutrophils. O₂ is necessary for the fast reduction of cytochrome b-245 by NADPH. *Biochem. J.* 226:881-4
51. Abo A, Boyhan A, West I, Thrasher AJ, Segal AW. 1992. Reconstitution of neutrophil NADPH oxidase activity in the cell-free system by four components: p67-phox, p47-phox, p21rac1, and cytochrome b-245. *J. Biol. Chem.* 267:16767-70
52. DeLeo FR, Quinn MT. 1996. Assembly of the phagocyte NADPH oxidase: molecular interaction of oxidase proteins. *J. Leukoc. Biol.* 60:677-91
53. Wientjes FB, Hsuan JJ, Totty NF, Segal AW. 1993. p40phox, a third cytosolic component of the activation complex of the NADPH oxidase to contain src homology 3 domains. *Biochem. J.* 296 (Pt 3):557-61
54. Heyworth PG, Curnutte JT, Nauseef WM, Volpp BD, Pearson DW, Rosen H, Clark RA. 1991. Neutrophil nicotinamide adenine dinucleotide phosphate oxidase assembly. Translocation of p47-phox and p67-phox requires interaction between p47-phox and cytochrome b558. *J. Clin. Invest.* 87:352-6
55. el Benna J, Park JW, Ruedi JM, Babior BM. 1995. Cell-free activation of the respiratory burst oxidase by protein kinase C. *Blood. Cells. Mol. Dis.* 21:201-6
56. Faust LR, el Benna J, Babior BM, Chanock SJ. 1995. The phosphorylation targets of p47phox, a subunit of the respiratory burst oxidase. Functions of the individual target serines as evaluated by site-directed mutagenesis. *J. Clin. Invest.* 96:1499-505
57. Heyworth PG, Shrimpton CF, Segal AW. 1989. Localization of the 47 kDa phosphoprotein involved in the respiratory-burst NADPH oxidase of phagocytic cells. *Biochem. J.* 260:243-8
58. Gorzalczany Y, Alloul N, Sigal N, Weinbaum C, Pick E. 2002. A prenylated p67phox-Rac1 chimera elicits NADPH-dependent superoxide production by phagocyte membranes in the absence of an activator and of p47phox: conversion of a pagan NADPH oxidase to monotheism. *J. Biol. Chem.* 277:18605-10

59. Diebold BA, Bokoch GM. 2001. Molecular basis for Rac2 regulation of phagocyte NADPH oxidase. *Nat. Immunol.* 2:211-5
60. Ellson CD, Gobert-Gosse S, Anderson KE, Davidson K, Erdjument-Bromage H, Tempst P, Thuring JW, Cooper MA, Lim ZY, Holmes AB, Gaffney PR, Coadwell J, Chilvers ER, Hawkins PT, Stephens LR. 2001. PtdIns(3)P regulates the neutrophil oxidase complex by binding to the PX domain of p40(phox). *Nat. Cell. Biol.* 3:679-82
61. Hiroaki H, Ago T, Ito T, Sumimoto H, Kohda D. 2001. Solution structure of the PX domain, a target of the SH3 domain. *Nat. Struct. Biol.* 8:526-30
62. Kanai F, Liu H, Field SJ, Akbary H, Matsuo T, Brown GE, Cantley LC, Yaffe MB. 2001. The PX domains of p47phox and p40phox bind to lipid products of PI(3)K. *Nat. Cell. Biol.* 3:675-8
63. Hossle JP, Berthet F, Erny C, Seger RA. 1993. Molecular genetic analysis of phagocyte oxidase cytochrome b558 mutations leading to chronic granulomatous disease. *Immunodeficiency.* 4:303-6
64. Parkos CA, Dinauer MC, Walker LE, Allen RA, Jesaitis AJ, Orkin SH. 1988. Primary structure and unique expression of the 22-kilodalton light chain of human neutrophil cytochrome b. *Proc. Natl. Acad. Sci. U. S. A.* 85:3319-23
65. Yu L, Quinn MT, Cross AR, Dinauer MC. 1998. Gp91(phox) is the heme binding subunit of the superoxide-generating NADPH oxidase. *Proc. Natl. Acad. Sci. U. S. A.* 95:7993-8
66. Parkos CA, Dinauer MC, Jesaitis AJ, Orkin SH, Curnutte JT. 1989. Absence of both the 91kD and 22kD subunits of human neutrophil cytochrome b in two genetic forms of chronic granulomatous disease. *Blood.* 73:1416-20
67. Roos D, de Boer M, Kuribayashi F, Meischl C, Weening RS, Segal AW, Ahlin A, Nemet K, Hossle JP, Bernatowska-Matuszkiewicz E, Middleton-Price H. 1996. Mutations in the X-linked and autosomal recessive forms of chronic granulomatous disease. *Blood* 87:1663-81

68. Yu L, Zhen L, Dinauer MC. 1997. Biosynthesis of the phagocyte NADPH oxidase cytochrome b558. Role of heme incorporation and heterodimer formation in maturation and stability of gp91phox and p22phox subunits. *J. Biol. Chem.* 272:27288-94
69. Porter CD, Kuribayashi F, Parkar MH, Roos D, Kinnon C. 1996. Detection of gp91-phox precursor protein in B-cell lines from patients with X-linked chronic granulomatous disease as an indicator for mutations impairing cytochrome b558 biosynthesis. *Biochem. J.* 315 (Pt 2):571-5
70. Harper AM, Chaplin MF, Segal AW. 1985. Cytochrome b-245 from human neutrophils is a glycoprotein. *Biochem. J.* 227:783-8
71. Wallach TM, Segal AW. 1997. Analysis of glycosylation sites on gp91phox, the flavocytochrome of the NADPH oxidase, by site-directed mutagenesis and translation in vitro. *Biochem. J.* 321 (Pt 3):583-5
72. Foubert TR, Burritt JB, Taylor RM, Jesaitis AJ. 2002. Structural changes are induced in human neutrophil cytochrome b by NADPH oxidase activators, LDS, SDS, and arachidonate: intermolecular resonance energy transfer between trisulfopyrenyl-wheat germ agglutinin and cytochrome b(558). *Biochim. Biophys. Acta.* 1567:221-31
73. Parkos CA, Quinn MT, Jesaitis AJ. 1992. The structure of human neutrophil plasma membrane b-type cytochrome involved in superoxide production. In *Molecular Basis of Oxidative Damage by Leukocytes*, ed. AJ Jesaitis, EA Dratz, pp. 45-46. Boca Raton: CRC Press
74. Segal AW, Shatwell KP. 1997. The NADPH oxidase of phagocytic leukocytes. *Ann. N. Y. Acad. Sci.* 832:215-22
75. Escriou V, Laporte F, Vignais PV. 1996. Assessment of the flavoprotein nature of the redox core of neutrophil NADPH oxidase. *Biochem. Biophys. Res. Commun.* 219:930-5
76. Nisimoto Y, Otsuka-Murakami H, Lambeth DJ. 1995. Reconstitution of flavin-depleted neutrophil flavocytochrome b558 with 8-mercapto-FAD and characterization of the flavin-reconstituted enzyme. *J. Biol. Chem.* 270:16428-34

77. Rotrosen D, Yeung CL, Leto TL, Malech HL, Kwong CH. 1992. Cytochrome b558: the flavin-binding component of the phagocyte NADPH oxidase. *Science*. 256:1459-62
78. Sumimoto H, Sakamoto N, Nozaki M, Sakaki Y, Takeshige K, Minakami S. 1992. Cytochrome b558, a component of the phagocyte NADPH oxidase, is a flavoprotein. *Biochem. Biophys. Res. Commun.* 186:1368-75
79. Glass GA, DeLisle DM, DeTogni P, Gabig TG, Magee BH, Markert M, Babior BM. 1986. The respiratory burst oxidase of human neutrophils. Further studies of the purified enzyme. *J. Biol. Chem.* 261:13247-51
80. Jesaitis AJ. 1992. Organization of the leukocyte plasma membrane components of superoxide production. In *Molecular Basis of Oxidative Damage by Leukocytes*, ed. AJ Jesaitis, EA Dratz, pp. 91-98. Boca Raton: CRC Press
81. Doussiere J, Brandolin G, Derrien V, Vignais PV. 1993. Critical assessment of the presence of an NADPH binding site on neutrophil cytochrome b558 by photoaffinity and immunochemical labeling. *Biochemistry*. 32:8880-7
82. Ravel P, Lederer F. 1993. Affinity-labeling of an NADPH-binding site on the heavy subunit of flavocytochrome b558 in particulate NADPH oxidase from activated human neutrophils. *Biochem. Biophys. Res. Commun.* 196:543-52
83. Tsunawaki S, Mizunari H, Namiki H, Kuratsuji T. 1994. NADPH-binding component of the respiratory burst oxidase system: studies using neutrophil membranes from patients with chronic granulomatous disease lacking the beta-subunit of cytochrome b558. *J. Exp. Med.* 179:291-7
84. Smith RM, Connor JA, Chen LM, Babior BM. 1996. The cytosolic subunit p67phox contains an NADPH-binding site that participates in catalysis by the leukocyte NADPH oxidase. *J. Clin. Invest.* 98:977-83
85. Dang PM, Johnson JL, Babior BM. 2000. Binding of nicotinamide adenine dinucleotide phosphate to the tetratricopeptide repeat domains at the N-terminus of p67PHOX, a subunit of the leukocyte nicotinamide adenine dinucleotide phosphate oxidase. *Biochemistry*. 39:3069-75

86. DeLeo FR, Burritt JB, Yu L, Jesaitis AJ, Dinauer MC, Nauseef WM. 2000. Processing and maturation of flavocytochrome b558 include incorporation of heme as a prerequisite for heterodimer assembly. *J. Biol. Chem.* 275:13986-93
87. Yu L, DeLeo FR, Biberstine-Kinkade KJ, Renee J, Nauseef WM, Dinauer MC. 1999. Biosynthesis of flavocytochrome b558 . gp91(phox) is synthesized as a 65-kDa precursor (p65) in the endoplasmic reticulum. *J. Biol. Chem.* 274:4364-9
88. Biberstine-Kinkade KJ, DeLeo FR, Epstein RI, LeRoy BA, Nauseef WM, Dinauer MC. 2001. Heme-ligating histidines in flavocytochrome b(558): identification of specific histidines in gp91(phox). *J. Biol. Chem.* 276:31105-12
89. DeLeo FR, Yu L, Burritt JB, Loetterle LR, Bond CW, Jesaitis AJ, Quinn MT. 1995. Mapping sites of interaction of p47-phox and flavocytochrome b with random-sequence peptide phage display libraries. *Proc. Natl. Acad. Sci. U. S. A.* 92:7110-4
90. Burritt JB, Quinn MT, Jutila MA, Bond CW, Jesaitis AJ. 1995. Topological mapping of neutrophil cytochrome b epitopes with phage-display libraries. *J. Biol. Chem.* 270:16974-80
91. Imajoh-Ohmi S, Tokita K, Ochiai H, Nakamura M, Kanegasaki S. 1992. Topology of cytochrome b558 in neutrophil membrane analyzed by anti-peptide antibodies and proteolysis. *J. Biol. Chem.* 267:180-4
92. Burritt JB, Busse SC, Gizachew D, Siemsen DW, Quinn MT, Bond CW, Dratz EA, Jesaitis AJ. 1998. Antibody imprint of a membrane protein surface. Phagocyte flavocytochrome b. *J. Biol. Chem.* 273:24847-52
93. Quinn MT, Mullen ML, Jesaitis AJ. 1992. Human neutrophil cytochrome b contains multiple hemes. Evidence for heme associated with both subunits. *J. Biol. Chem.* 267:7303-9
94. Smith RM, Curnutte JT. 1991. Molecular basis of chronic granulomatous disease. *Blood* 77:673-86
95. Curnutte JT. 1992. Molecular basis of the autosomal recessive forms of chronic granulomatous disease. *Immunodef. Rev.* 3:149-72

96. Dinauer MC, Lekstrom-Himes JA, Dale DC. 2000. Inherited Neutrophil Disorders: Molecular Basis and New Therapies. *Hematology (Am. Soc. Hematol. Educ. Program.)* 303-18
97. Segal BH, Leto TL, Gallin JI, Malech HL, Holland SM. 2000. Genetic, biochemical, and clinical features of chronic granulomatous disease. *Medicine. (Baltimore.)* 79:170-200
98. Heyworth PG, Cross AR, Curnutte JT. 2003. Chronic granulomatous disease. *Curr. Opin. Immunol.* 15:578-84
99. Ambruso DR, Knall C, Abell AN, Panepinto J, Kurkchubasche A, Thurman G, Gonzalez-Aller C, Hiester A, deBoer M, Harbeck RJ, Oyer R, Johnson GL, Roos D. 2000. Human neutrophil immunodeficiency syndrome is associated with an inhibitory Rac2 mutation. *Proc. Natl. Acad. Sci. U. S. A.* 97:4654-9
100. Williams DA, Tao W, Yang F, Kim C, Gu Y, Mansfield P, Levine JE, Petryniak B, Derrow CW, Harris C, Jia B, Zheng Y, Ambruso DR, Lowe JB, Atkinson SJ, Dinauer MC, Boxer L. 2000. Dominant negative mutation of the hematopoietic-specific Rho GTPase, Rac2, is associated with a human phagocyte immunodeficiency. *Blood.* 96:1646-54
101. Cross AR, Noack D, Rae J, Curnutte JT, Heyworth PG. 2000. Hematologically important mutations: the autosomal recessive forms of chronic granulomatous disease (first update). *Blood. Cells. Mol. Dis.* 26:561-5
102. Heyworth PG, Curnutte JT, Rae J, Noack D, Roos D, van Koppen E, Cross AR. 2001. Hematologically important mutations: X-linked chronic granulomatous disease (second update). *Blood. Cells. Mol. Dis.* 27:16-26
103. Lambeth JD, Cheng G, Arnold RS, Edens WA. 2000. Novel homologs of gp91phox. *Trends. Biochem. Sci.* 25:459-61
104. Lambeth JD. 2002. Nox/Duox family of nicotinamide adenine dinucleotide (phosphate) oxidases. *Curr. Opin. Hematol.* 9:11-7
105. Bokoch GM, Knaus UG. 2003. NADPH oxidases: not just for leukocytes anymore! *Trends. Biochem. Sci.* 28:502-8

106. Edens WA, Sharling L, Cheng G, Shapira R, Kinkade JM, Lee T, Edens HA, Tang X, Sullards C, Flaherty DB, Benian GM, Lambeth JD. 2001. Tyrosine cross-linking of extracellular matrix is catalyzed by Duox, a multidomain oxidase/oxidoreductase with homology to the phagocyte oxidase subunit gp91phox. *J. Cell. Biol.* 154:879-91
107. Keller T, Damude HG, Werner D, Doerner P, Dixon RA, Lamb C. 1998. A plant homolog of the neutrophil NADPH oxidase gp91phox subunit gene encodes a plasma membrane protein with Ca²⁺ binding motifs. *Plant. Cell.* 10:255-66
108. Torres MA, Onouchi H, Hamada S, Machida C, Hammond-Kosack KE, Jones JD. 1998. Six *Arabidopsis thaliana* homologues of the human respiratory burst oxidase (gp91phox). *Plant. J.* 14:365-70
109. Jesaitis AJ, Heners PR, Hertel R, Briggs WB. 1977. Characterization of a membrane fraction containing a b-type cytochrome. *Plant. Physiol.* 59:941-7
110. Kikuchi H, Hikage M, Miyashita H, Fukumoto M. 2000. NADPH oxidase subunit, gp91(phox) homologue, preferentially expressed in human colon epithelial cells. *Gene.* 254:237-43
111. Suh YA, Arnold RS, Lassegue B, Shi J, Xu X, Sorescu D, Chung AB, Griendling KK, Lambeth JD. 1999. Cell transformation by the superoxide-generating oxidase Mox1. *Nature.* 401:79-82
112. Cheng G, Cao Z, Xu X, van Meir EG, Lambeth JD. 2001. Homologs of gp91phox: cloning and tissue expression of Nox3, Nox4, and Nox5. *Gene.* 269:131-40
113. Geiszt M, Kopp JB, Varnai P, Leto TL. 2000. Identification of renox, an NAD(P)H oxidase in kidney. *Proc. Natl. Acad. Sci. U. S. A.* 97:8010-4
114. Shiose A, Kuroda J, Tsuruya K, Hirai M, Hirakata H, Naito S, Hattori M, Sakaki Y, Sumimoto H. 2001. A novel superoxide-producing NAD(P)H oxidase in kidney. *J. Biol. Chem.* 276:1417-23
115. Yang S, Madyastha P, Bingel S, Ries W, Key L. 2001. A new superoxide-generating oxidase in murine osteoclasts. *J. Biol. Chem.* 276:5452-8

116. Banfi B, Molnar G, Maturana A, Steger K, Hegedus B, Demaurex N, Krause KH. 2001. A Ca(2+)-activated NADPH oxidase in testis, spleen, and lymph nodes. *J. Biol. Chem.* 276:37594-601
117. De Deken X, Wang D, Many MC, Costagliola S, Libert F, Vassart G, Dumont JE, Miot F. 2000. Cloning of two human thyroid cDNAs encoding new members of the NADPH oxidase family. *J. Biol. Chem.* 275:23227-33
118. Dupuy C, Ohayon R, Valent A, Noel-Hudson MS, Deme D, Virion A. 1999. Purification of a novel flavoprotein involved in the thyroid NADPH oxidase. Cloning of the porcine and human cdnas. *J. Biol. Chem.* 274:37265-9
119. Geiszt M, Witta J, Baffi J, Lekstrom K, Leto TL. 2003. Dual oxidases represent novel hydrogen peroxide sources supporting mucosal surface host defense. *FASEB. J.* 17:1502-4
120. Dupuy C, Pomerance M, Ohayon R, Noel-Hudson MS, Deme D, Chaaoui M, Francon J, Virion A. 2000. Thyroid oxidase (THOX2) gene expression in the rat thyroid cell line FRTL-5. *Biochem. Biophys. Res. Commun.* 277:287-92
121. Christiansen NO, Larsen CS, Esmann V. 1988. A study on the role of protein kinase C and intracellular calcium in the activation of superoxide generation. *Biochim. Biophys. Acta.* 971:317-24
122. Elzi DJ, Bjornsen AJ, MacKenzie T, Wyman TH, Silliman CC. 2001. Ionomycin causes activation of p38 and p42/44 mitogen-activated protein kinases in human neutrophils. *Am. J. Physiol. Cell. Physiol.* 281:C350-C360
123. Nakamura T, Suchard SJ, Abe A, Shayman JA, Boxer LA. 1994. Role of diradylglycerol formation in H₂O₂ and lactoferrin release in adherent human polymorphonuclear leukocytes. *J. Leukoc. Biol.* 56:105-9
124. Nakamura Y, Makino R, Tanaka T, Ishimura Y, Ohtaki S. 1991. Mechanism of H₂O₂ production in porcine thyroid cells: evidence for intermediary formation of superoxide anion by NADPH-dependent H₂O₂-generating machinery. *Biochemistry.* 30:4880-6

125. Arnold RS, Shi J, Murad E, Whalen AM, Sun CQ, Polavarapu R, Parthasarathy S, Petros JA, Lambeth JD. 2001. Hydrogen peroxide mediates the cell growth and transformation caused by the mitogenic oxidase Nox1. *Proc. Natl. Acad. Sci. U. S. A.* 98:5550-5
126. Geiszt M, Lekstrom K, Brenner S, Hewitt SM, Dana R, Malech HL, Leto TL. 2003. NAD(P)H oxidase 1, a product of differentiated colon epithelial cells, can partially replace glycoprotein 91phox in the regulated production of superoxide by phagocytes. *J. Immunol.* 171:299-306
127. Banfi B, Clark RA, Steger K, Krause KH. 2003. Two novel proteins activate superoxide generation by the NADPH oxidase NOX1. *J. Biol. Chem.* 278:3510-3
128. Geiszt M, Lekstrom K, Witta J, Leto TL. 2003. Proteins homologous to p47phox and p67phox support superoxide production by NAD(P)H oxidase 1 in colon epithelial cells. *J. Biol. Chem.* 278:20006-12
129. Takeya R, Ueno N, Kami K, Taura M, Kohjima M, Izaki T, Nunoi H, Sumimoto H. 2003. Novel human homologues of p47phox and p67phox participate in activation of superoxide-producing NADPH oxidases. *J. Biol. Chem.* 278:25234-46
130. Etoh T, Inoguchi T, Kakimoto M, Sonoda N, Kobayashi K, Kuroda J, Sumimoto H, Nawata H. 2003. Increased expression of NAD(P)H oxidase subunits, NOX4 and p22phox, in the kidney of streptozotocin-induced diabetic rats and its reversibility by interventive insulin treatment. *Diabetologia.* 46:1428-37
131. Dwyer SC, Legendre L, Low PS, Leto TL. 1996. Plant and human neutrophil oxidative burst complexes contain immunologically related proteins. *Biochim. Biophys. Acta.* 1289:231-7
132. Lamb C, Dixon RA. 1997. THE OXIDATIVE BURST IN PLANT DISEASE RESISTANCE. *Annual Review of Plant Physiology and Plant Molecular Biology* 48:251-75
133. Tenhaken R, Levine A, Brisson LF, Dixon RA, Lamb C. 1995. Function of the oxidative burst in hypersensitive disease resistance. *Proc. Natl. Acad. Sci. U. S. A.* 92:4158-63

134. Shirasu K, Nakajima H, Rajasekhar VK, Dixon RA, Lamb C. 1997. Salicylic acid potentiates an agonist-dependent gain control that amplifies pathogen signals in the activation of defense mechanisms. *Plant Cell* 9:261-70
135. Tate CG. 2001. Overexpression of mammalian integral membrane proteins for structural studies. *FEBS Lett.* 504:94-8
136. Loll PJ. 2003. Membrane protein structural biology: the high throughput challenge. *J. Struct. Biol.* 142:144-53
137. Grisshammer R, Tate CG. 1995. Overexpression of integral membrane proteins for structural studies. *Q. Rev. Biophys.* 28:315-422
138. Grisshammer R, Averbeck P, Sohal AK. 1999. Improved purification of a rat neurotensin receptor expressed in *Escherichia coli*. *Biochem. Soc. Trans.* 27:899-903
139. Weiss HM, Grisshammer R. 2002. Purification and characterization of the human adenosine A(2a) receptor functionally expressed in *Escherichia coli*. *Eur. J. Biochem.* 269:82-92
140. Barnett J, Chow J, Ives D, Chiou M, Mackenzie R, Osen E, Nguyen B, Tsing S, Bach C, Freire J, . 1994. Purification, characterization and selective inhibition of human prostaglandin G/H synthase 1 and 2 expressed in the baculovirus system. *Biochim. Biophys. Acta* 1209:130-9
141. Binda C, Newton-Vinson P, Hubalek F, Edmondson DE, Mattevi A. 2002. Structure of human monoamine oxidase B, a drug target for the treatment of neurological disorders. *Nat. Struct. Biol.* 9:22-6
142. Bracey MH, Hanson MA, Masuda KR, Stevens RC, Cravatt BF. 2002. Structural adaptations in a membrane enzyme that terminates endocannabinoid signaling. *Science* 298:1793-6
143. Lundstrom K. 2002. Semliki forest virus-based expression for versatile use in receptor research. *J. Recept. Signal. Transduct. Res.* 22:229-40

144. Boorsma M, Hoenke S, Marrero A, Fischer R, Bailey JE, Renner WA, Bachmann MF. 2002. Bioprocess applications of a Sindbis virus-based temperature-inducible expression system. *Biotechnol. Bioeng.* 79:602-9
145. Burritt JB, DeLeo FR, McDonald CL, Prigge JR, Dinauer MC, Nakamura M, Nauseef WM, Jesaitis AJ. 2001. Phage display epitope mapping of human neutrophil flavocytochrome b558. Identification of two juxtaposed extracellular domains. *J. Biol. Chem.* 276:2053-61
146. Yamauchi A, Yu L, Potgens AJ, Kuribayashi F, Nunoi H, Kanegasaki S, Roos D, Malech HL, Dinauer MC, Nakamura M. 2001. Location of the epitope for 7D5, a monoclonal antibody raised against human flavocytochrome b558, to the extracellular peptide portion of primate gp91phox. *Microbiol. Immunol.* 45:249-57
147. Burritt JB, Fritel GN, Dahan I, Pick E, Roos D, Jesaitis AJ. 2000. Epitope identification for human neutrophil flavocytochrome b monoclonals 48 and 449. *Eur. J. Haematol.* 65:407-13
148. Burritt JB, Foubert TR, Baniulis D, Lord CI, Taylor RM, Mills JS, Baughan TD, Roos D, Parkos CA, Jesaitis AJ. 2003. Functional epitope on human neutrophil flavocytochrome b558. *J. Immunol.* 170:6082-9
149. Taylor RM, Burritt JB, Foubert TR, Snodgrass MA, Stone KC, Baniulis D, Gripenrog JM, Lord C, Jesaitis AJ. 2003. Single-step immunoaffinity purification and characterization of dodecylmaltoside-solubilized human neutrophil flavocytochrome b. *Biochim. Biophys. Acta* 1612:65-75
150. Emmendorffer A, Nakamura M, Rothe G, Spiekermann K, Lohmann-Matthes ML, Roesler J. 1994. Evaluation of flow cytometric methods for diagnosis of chronic granulomatous disease variants under routine laboratory conditions. *Cytometry* 18:147-55
151. Ginsel LA, Onderwater JJ, Fransen JA, Verhoeven AJ, Roos D. 1990. Localization of the low-Mr subunit of cytochrome b558 in human blood phagocytes by immunoelectron microscopy. *Blood* 76:2105-16

152. Johansson A, Jesaitis AJ, Lundqvist H, Magnusson KE, Sjolin C, Karlsson A, Dahlgren C. 1995. Different subcellular localization of cytochrome b and the dormant NADPH oxidase in neutrophils and macrophages: effect on the production of reactive oxygen species during phagocytosis. *Cell. Immunol.* 161:61-71
153. Kuijpers TW, Tool AT, van der Schoot CE, Ginsel LA, Onderwater JJ, Roos D, Verhoeven AJ. 1991. Membrane surface antigen expression on neutrophils: a reappraisal of the use of surface markers for neutrophil activation. *Blood* 78:1105-11
154. Kummer W, Acker H. 1995. Immunohistochemical demonstration of four subunits of neutrophil NAD(P)H oxidase in type I cells of carotid body. *J. Appl. Physiol* 78:1904-9
155. Steinbeck MJ, Appel WHJ, Verhoeven AJ, Karnovsky MJ. 1994. NADPH oxidase expression and in situ production of superoxide by osteoclasts actively resorbing bone. *J. Cell. Biol.* 126:765-72
156. Batot G, Martel C, Capdeville N, Wientjes F, Morel F. 1995. Characterization of neutrophil NADPH oxidase activity reconstituted in a cell-free assay using specific monoclonal antibodies raised against cytochrome b558. *Eur. J. Biochem.* 234:208-15

TOPOGRAPHY OF GP91-PHOX: COMPUTATIONAL PREDICTIONS AND
APPLICATION OF PROTEOLYTIC ENZYME CLEAVAGE AND
IMMUNOLOGICAL PROBE BINDING ANALYSIS

Introduction

Flavocytochrome b558 (Cytb) is the central component of the NADPH oxidase, a multi-subunit enzyme system that produces superoxide ($O_2^{\cdot-}$) (1, 2). The oxidase is important in host defense by phagocytic cells such as neutrophils, monocytes and eosinophils. Dysfunction of the NADPH oxidase causes chronic granulomatous disease (CGD), a clinical disorder characterized by severe recurrent infections (3). Recently, structural homologues of Cytb large subunit have been discovered in a variety of tissues and other organisms suggesting alternate functions for superoxide and Cytb-like proteins (reviewed by Lambeth (4)).

The NADPH oxidase complex consists of membrane-bound Cytb, the low molecular weight G proteins Rap1A and Rac2, and the cytoplasmic proteins p47-phox, p67-phox and p40-phox (5). Activation of the NADPH oxidase involves translocation of cytosolic oxidase components to the plasma membrane where they associate with Cytb. The translocation of these components in the cell occurs as a result of activation by a variety of agents (reviewed by Leusen et al. (5)). In addition, anionic lipids such as arachidonate are sufficient to activate the cell-free oxidase or isolated functional Cytb. As a result of this activation, electrons are transferred from NADPH to molecular oxygen,

forming superoxide. CGD, caused by a deficiency in one of the cytosolic components, demonstrates their regulatory role in superoxide production by the oxidase. However, Cytb is the only obligate electron transporting component known in this enzyme system (6, 7).

Cytb is an integral membrane protein composed of two polypeptides (gp91-phox and p22-phox) with molecular weights of 91,000 and 22,000 (8, 9). The subunits are closely associated and required for the active NADPH oxidase complex (10, 11). Cytb contains at least two non-identical, bis histidinyl coordinated heme groups that are believed to be located in either the transmembrane or extracellular domain of the protein (or possibly in both locations) and mediate the final steps of electron transfer to molecular oxygen (12, 13, 14, 15, 16). The function of Cytb as an electron transporting component of the NADPH oxidase is absolutely dependent on the presence of FAD (17, 18, 19), which probably receives electrons directly from NADPH (20). The substrate NADPH was shown to bind to the large subunit of Cytb (21, 22, 23, 24), although some evidence exists suggesting it also binds to the cytosolic oxidase component p67-phox (24, 25, 26). Comparison of the gp91-phox sequence with members of the ferredoxin-NADP⁺ reductase family suggests possible sites for NADPH and FAD binding (13, 19, 26, 27, 28).

Little is known of the topological organization of the membrane-bound, N-terminal portion of gp91-phox. In earlier attempts to model secondary structure of this subunit, four to six membrane-spanning helices were assigned to the amino-terminal half of the protein (14, 26, 27, 28, 29, 30). Studies employing synthetic peptide inhibition of

NADPH oxidase activity and mutagenesis suggested interaction sites for p47-phox (30, 31, 32), therefore localizing such regions to the cytoplasmic surface of the enzyme. Further, mutagenesis studies have identified (31, 33) carbohydrate attachment sites at the amino-terminal region of the gp91-phox (28) localizing such residues to the extracellular surface. Antibody binding studies have also revealed residues located extracellularly (34, 35). However, even with the studies described, assessment of the topology of gp91-phox awaits further investigation.

In the current study, computational analysis of the gp91-phox amino acid sequence was used to predict transmembrane topology. In addition, proteolytic digestion and mass spectrometry analysis on purified and lipid-reconstituted Cytb extended data about hydrophilic, solvent exposed segments on the protein. To further support topological features of the predicted model and to study functional aspects of the Cytb, an attempt was made to produce and characterize anti-peptide antibodies against synthetic peptides mimicking segments on N-terminal half of the gp91-phox.

Materials and Methods

Materials

Horseradish peroxidase conjugated goat anti-rabbit IgG and alkaline phosphatase conjugated goat anti-rabbit IgG were from BioRad Laboratories (Hercules, CA). Mass spectrometry grade porcine trypsin was purchased from Promega Corporation (Madison, WI), sequencing grade endoproteinase Glu-C from *Staphylococcus aureus* V8 and 2,2'-

azino-bis-[3-ethylbenzthiazoline-6-sulfonic acid) (ABTS) were from Boehringer Mannheim (Indianapolis, IN). Synthetic peptides (with acetylated (Ac) or free (NH₂) amino-terminus) Ac-MGNWAVNEGC-COOH (MGN), Ac-YRVYDIPPKFFYTRKC-COOH (YRV), Ac-ESYLNFAKRC-COOH (ESY), Ac-ARKRIKNPEGGC-COOH (ARK) and NH₂-KISEWGKIKEC-COOH (KIS) were from Macromolecular Resources (Fort Collins, CO). Keyhole Limpet Hemocyanin (KLH), sulfo-GMBS crosslinker, Inject maleimide-activated ovalbumin and SulfoLink Coupling gel were from Pierce (Rockford, IL). Prestained protein molecular weight standards were obtained from Life Technologies (Grand Island, NY). ProSieve Protein Markers were from BMA (Rockland, ME). SOL-GRADE n-Dodecyl- β -D-Maltoside (DDM) was from Anatrace (Maumee, OH). SeroClear reagent, octylglucoside, diisopropyl fluorophosphate, phenylmethylsulfonyl fluoride were from Calbiochem-Novabiochem (La Jolla, CA). 5-bromo-4-chloro-3-indolyl phosphate/nitro blue tetrazolium (BCIP/NBT) chromogen was from Kirkegaard and Perry Laboratories (Gaithersburg, MD). Fura-2/AM was obtained from Molecular Probes (Eugene, OR). GammaBind Plus Sepharose was from Pharmacia Biotech (Piscataway, NJ). Unless otherwise specified, all other reagents were purchased from Sigma-Aldrich (St. Louis, MO).

Mathematical Amino Acid Sequence Analysis

Antigenic regions on the gp91-phox protein N-terminal half were determined using a method developed by Parker, et al. (36) included in the Antheprot software

package of protein sequence analysis (Institute of Biology and Chemistry of Proteins, Lyon, France; <http://antheprot-pbil.ibcp.fr>).

To analyze gp91-*phox* transmembrane topology, six on-line transmembrane helix/topology prediction tools were used:

DAS (<http://www.biokemi.su.se/~server/DAS/>);

HMMTOP 1.1 (<http://www.enzim.hu/hmmtop/>);

PHDhtm (<http://dodo.cpmc.columbia.edu/predictprotein/>);

SOSUI 1.0/10 (<http://www.tuat.ac.jp/~mitaku/sosui/>);

TMHMM 1.0 (<http://www.cbs.dtu.dk/krogh/TMHMM/>);

TMpred (http://www.ch.embnet.org/software/TMPRED_form.html).

For HMMTOP 1.1 the length of helices was used from 10 to 35 a.a., start point of iterations - random, number of iterations -10, while other adjustable settings were selected as default. The length of helices for TMpred was used from 10 to 35 a.a. Other programs were used with default settings.

Proteolytic Digestion of Relipidated Cytb

Cytb was purified using an immunoaffinity method as described by Taylor, et al. (37). Phosphatidylcholine was dissolved at 5 mg/mL in 50 mM NaH₂PO₄, 1 mM EGTA, 1 mM MgCl₂, 20% (v/v) glycerol, 0.05 mM DTT, pH-7.4 (reconstitution buffer) with 1% dodecylmaltoside (DDM) and lipids were dispersed by sonication. Forty µg of purified Cytb were combined with 400 µg of dissolved phosphatidylcholine (~ 400 µL total

sample volume) to obtain a 10:1 lipid to protein ratio (w/w). Samples were then dialyzed for 48 h at 4 °C against 1 L of reconstitution buffer without DDM.

For proteolytic digestion, relipidated Cytb samples were dialyzed against 10,000 volumes of 40 mM NH_4CO_3 , pH-7.8. Lyophilized mass spectrometry grade trypsin was resuspended at 1 $\mu\text{g}/\mu\text{L}$ in 50 mM acetic acid, then diluted in 40 mM NH_4CO_3 /10% CH_3CN to 20 $\mu\text{g}/\text{mL}$ and added to Cytb at a final protease:protein ratio of 1:20 (w/w). Lyophilized endoproteinase Glu-C was reconstituted at 50 $\mu\text{g}/\text{mL}$ in distilled water and added to Cytb samples to a final ratio of 1:15 (w/w). Proteolytic digests were carried out for 24 hours at 37 °C. Lipid vesicles were then pelleted by centrifugation at $114,000 \times g$ for 30 min to isolate the water-soluble peptide fraction. Samples were stored at -20 °C until further analyses were conducted.

MALDI Mass Spectrometry

Cytb proteolytic digestion samples prepared as described above were diluted at a 1:1 ratio with a saturated solution of α -cyano-4-hydroxy-cinnamic acid (in 50% (v/v) CH_3CN , 0.1% (v/v) trifluoroacetic acid), and 1 μL was spotted on a MALDI target. MS analysis was performed in the positive ion mode with Bruker Biflex III MALDI-TOF spectrometer (Bruker Daltonics, Billerica, MA) incorporating a 337-nm nitrogen laser. Spectra were averaged over ~200 laser scans. Angiotensin II ($\text{MH}^+ = 1046.2$ Da) and insulin ($\text{MH}^+ = 3495.65$ Da) were used for external calibration. Spectra processing was carried out using Bruker Daltonics XMASS software (Bruker Daltonics, Bellerica, MA). Peptide peak masses were extracted from MALDI-TOF spectra of proteolysed protein

with Bruker Daltonics XMASS software (Bruker Daltonics, Bellerica, MA). Cytb proteolytic digestion peptides were identified by match of mass spectrometry data to results obtained by theoretical proteolytic enzyme cleavage calculated with the on-line tool PeptideMass (38) (<http://us.expasy.org/tools/peptide-mass.html>).

Rabbit Polyclonal Antibody Production

Immunogens for polyclonal antibody MGN, YRV, ESY, ARK and KIS-1 production were prepared by coupling synthetic peptides Ac-MGNWAVNEGC-COOH, Ac-YRVYDIPPKFFYTRKC-COOH, Ac-ESYLNFAKRC-COOH and Ac-ARKRIKNPEGGC-COOH, NH₂-KISEWGKIKEC-COOH (Ac-, acetylation at the N-terminus of the peptide), respectively, to KLH using sulfo-GMBS bifunctional crosslinker as described by the manufacturer. For antibody KIS-2, immunogen was prepared using glutaraldehyde as follows. Equal mass amounts of peptide NH₂-KISEWGKIKEC-COOH and KLH were dissolved in 0.1 M borate/NaOH buffer, pH 8.5, and glutaraldehyde was added to 0.1% (w/v). After mixing for 30 min at room temperature, the reaction was stopped by adding glycine to a 0.2 M concentration. The mixture was then dialyzed against phosphate buffered saline, PBS (10 mM phosphate, 150 mM NaCl, pH-7.4).

Immunogens were mixed with Hunter's Titer Max adjuvant and injected to New Zealand White rabbits subcutaneously. The second immunization was performed four weeks later, and the rabbits were then immunized six more times at three week intervals.

The antibody titer in rabbit serum was monitored by enzyme-linked immunosorbant assay (ELISA) (39), using a detection antigen prepared by coupling the immunogen corresponding synthetic peptide to Inject maleimide-activated ovalbumin with sulfo-GMBS or glutaraldehyde as described above. Each of the antigens was used to determine the titer of the respective antisera corresponding to immunogen preparation method. For ELISA experiments wells were coated with 100 μ l of antigen at 10 μ g/ml in 50 mM NaCl overnight at 4 °C. Wells were then rinsed twice with PBS and blocked with a blocking buffer (2% (w/v) BSA in PBS) for one hour at 20 °C. Serial dilutions of rabbit serum were made in the blocking buffer and exposed to the antigen for 1 hour at 37 °C. After rinsing with PBS five times, bound antibody was detected after incubation for 30 min at 37 °C with horseradish peroxidase-conjugated goat anti-rabbit IgG diluted 1:2000 in blocking buffer. Plates were rinsed five times with PBS and color development was measured at 405 nm following exposure to the ABTS/H₂O₂ reagent using SpectraMax 250 micro-plate spectrophotometer supplied with SoftMax Pro 3.1.1 software (Molecular Devices Corp., Sunnyvale, CA).

Polyclonal Antibody Purification

Rabbit polyclonal antibodies were purified using affinity columns made by coupling synthetic peptides, corresponding to immunogen, to iodacetate-activated SulfoLink Coupling gel (Pierce, Rockford, IL) as described by Wisniewski, et al. (40). For antibody purification, rabbit serum was delipidated with SeroClear reagent and mixed with the peptide-conjugated gel at 4 °C overnight. Unbound proteins were washed off

with PBS, whereas the bound antibodies were eluted with 0.5 M acetic acid/NaOH, pH-3.0 and neutralized with 2 M Tris/HCl, pH-8.1. Fractions containing eluted antibodies were identified by absorbance at 280 nm and dialyzed in PBS containing 0.02% (w/v) sodium azide.

Preimmune serum IgG was isolated from SeroClear reagent delipidated serum on a sepharose-conjugated protein G (GammaBind Plus Sepharose, Pharmacia Biotech, Piscataway, NJ) column using manufacturer's protocol, and then dialyzed in PBS containing 0.02% (w/v) sodium azide.

SDS-PAGE and Immunoblotting

Samples of human neutrophil Cytb purified as described (41) were mixed with an equal volume of SDS-PAGE sample buffer (3.3% (w/v) SDS, 167 mM Tris-HCl, pH-6.8, 33% (v/v) glycerol, 0.03% (w/v) bromphenol blue, and 500 mM 2-mercaptoethanol) and boiled for 1 min. The samples were then separated by SDS-PAGE on 12% or 7-15% Tris/glycine polyacrylamide slab gels containing 0.1% (w/v) SDS as described (42) and electrophoretic mobility of the sample proteins was compared to prestained protein standards. Electrophoresis was conducted using a vertical slab gel electrophoresis system (Bio-Rad, Richmond, CA) at 40 V while the bromphenol blue tracking dye migrated through stacking gel and then at 80 V until the tracking dye reached the bottom of the resolving gel.

Following electrophoresis, protein samples were transferred to nitrocellulose membranes as described previously (8), using Bio-Rad TransBlot system (Bio-Rad,

Richmond, CA). Membranes were blocked with blocking buffer (5% (w/v) milk protein, 0.2% (v/v) Tween 20 in PBS) for 1 h at room temperature or at 4 °C overnight.

Antibodies were diluted in diluting buffer (3% (v/v) normal goat serum, 1% (w/v) BSA, 0.2% (v/v) Tween 20, 10 mM sodium phosphate, 150 mM NaCl, pH-7.4) and incubated with the nitrocellulose membrane blots for 1 h at room temperature with continuous rocking. The blots were then rinsed with wash buffer (250 mM NaCl, 10 mM HEPES, 0.2% (v/v) Tween 20, pH-7.4) and incubated with a alkaline phosphatase-conjugated secondary antibody diluted 1:1000 ratio in diluting buffer. The blots then were rinsed three times with wash buffer, equilibrated in 250 mM NaCl, 30 mM Tris-HCl, pH-8.0, and developed using a BCIP/NBT phosphatase substrate system.

ELISA on Cytb Coated Microplates

Microplate wells were coated with 40 μ L of 10 nM Cytb purified as described (41) and diluted in Hank's Balanced Salts (1.26 mM CaCl₂, 0.8 mM MgSO₄, 5.4 mM KCl, 0.44mM KH₂PO₄, 0.14 mM NaCl, 0.34 mM Na₂HPO₄, 5.6 mM D-glucose, pH-7.4) with 10mM HEPES. After a 12 hour incubation at 4 °C wells were rinsed three times with PBS and blocked with blocking buffer (0.17 M H₂BO₃, 0.17 M NaCl, 1mM EDTA, 0.05% (v/v) Tween 20, 0.25% (w/v) BSA, 0.02% (w/v) NaN₃, pH-8.5) for one hour at 4 °C. Wells were then rinsed with PBS. Serial dilutions of purified polyclonal antibodies or preimmune serum IgG (concentration range 0.6 - 45 μ g/mL) were made in the blocking buffer and added to Cytb coated wells. After incubation for 3 hours at 4 °C, wells were rinsed with PBS five times. Bound antibody was detected after incubation for 30 min at

37 °C with horseradish peroxidase-conjugated goat anti-rabbit IgG diluted 1:2000 in the blocking buffer. Plates were rinsed five times with PBS and, following exposure to the ABTS/H₂O₂ reagent, color development was measured at 405 nm using SpectraMax 250 micro-plate spectrophotometer supplied with SoftMax Pro 3.1.1 software (Molecular Devices Corp., Sunnyvale, CA).

Human Neutrophil Preparation

Human neutrophils were purified from citrated peripheral blood using gelatin sedimentation followed by lysis of remaining erythrocytes with isotonic ammonium chloride as described (43). Prepared cells were treated with 2 mM diisopropyl fluorophosphate for 15 min on ice, to inactivate serine esterases. The cells were then pelleted by centrifugation and resuspended in PBS.

Flow Cytometric Analysis of Surface Antigens

To detect surface antigens, neutrophils prepared as described above were washed with PBS and incubated with rabbit polyclonal antibody at 10 µg/mL in PBS supplemented with 2% milk protein. After one hour of incubation, the cells were rinsed by centrifugation and resuspension in PBS. Then the cells were labeled with FITC-conjugated goat anti-rabbit secondary antibody diluted 1:1000 in PBS with 2% milk protein for one hour, washed twice as before, and suspended in PBS containing 5 µg/mL

propidium iodide. All the incubations were performed on ice and with solutions pre-cooled to 4 °C.

Flow cytometric analysis was performed on 10,000 cells using a Becton Dickinson FACScan flow cytometer supplied with CONSORT 30 software (Becton Dickinson Immunocytometry Systems Inc., Franklin Lakes, CA). Data analysis was performed using WinMDI v.2.8 software (The Scripps Research Institute, La Jolla, CA). Propidium iodide staining intensity of the cells was used to identify and gate intact cells.

Superoxide Anion Production Assay

To determine the effect of KIS-1 antibody binding on neutrophil superoxide production rate, a ferrocytochrome c (CytC) microplate assay was adapted from Arthur, et al. (44) and Chapman-Kirkland, et al. (45). Neutrophils prepared as described above were degranulated with cytochalasin B and fMLF (8). The cells were then dispensed at 10^6 cells per well in PBS containing 160 μ M CytC and 1000 U/ml catalase in 96-well polystyrene micro-plate (Corning Life Sciences, Acton, MA). The cells then were incubated for 10 min at 37 °C with serial dilutions of antibody KIS-1 or preimmune serum IgG from 0.35 to 50 μ g/mL. Control samples were run without any IgG and also with 100 μ g/ml SOD to verify specificity of CytC reduction. After cells were activated by 0.1 μ M PMA, CytC reduction was monitored for 20 min as the absorbance difference at 550-557 nm using SpectraMax 250 micro-plate spectrophotometer supplied with SoftMax Pro 3.1.1 software (Molecular Devices Corp., Sunnyvale, CA). Initial maximal

superoxide production rate values were estimated from CytC reduction curves and normalized to the control lacking any IgG as a zero level.

Calcium Release Assay

Measurements of cytosolic Ca^{2+} concentrations were performed as described by Miettinen et al. (46). Neutrophils were prepared and degranulated using the same conditions as described for the superoxide anion production assay protocol. The cells were then incubated with 2.5 μM Fura-1/AM in PBS plus 0.9 mM CaCl_2 and 0.5 mM MgCl_2 for 45 min at 37 °C. Cells were centrifuged and resuspended in the above buffer at room temperature, where they were left until the assay. Each measurement contained about 2×10^7 cells in a volume of one milliliter. Cells were preincubated with 50 $\mu\text{g/ml}$ of KIS-1 antibody or preimmune serum IgG or with no IgG added for 10 min at 37 °C. Continuous measurements of calcium-bound and free Fura-2/AM were made at 37 °C with a double excitation monochromator fluorescence spectrofluorometer (Photon Technology International, Monmouth Junction, NJ) with excitation at 340 and 380 nm and emission at 510 nm. To provide a stimulus for calcium mobilization 100 nM fMLF peptide was used, and 10 μM ATP was added as a heterologous ligand to provide a standard stimulus for calcium mobilization.

Results

Computational Transmembrane Topology Predictions

To construct a topological protein model for the Cytb large subunit gp91-phox, results from six protein transmembrane helix and topology predicting tools using different scoring matrixes and algorithms were used in our study to identify transmembrane domains and their orientation. Two of the programs, DAS (47) and TMpred (48), use scales based on statistical analysis of known structure protein database, while PHDhtm (49) uses a system of neural networks to analyze multiple protein sequence alignments. Physicochemical properties of amino acid sequences are analyzed using Fourier transformations by the SOSUI 1.0/10 (50) algorithm, and a hidden Markov model with adjustable or known structure protein database trained parameters for HMMTOP 1.1 (51) and TMHMM 1.0 (52), respectively. Transmembrane helix prediction results for the previously reported gp91-phox amino acid sequence (53, 54) are shown in Table 2.1. Depending on the program used, five to seven hydrophobic regions on the gp91-phox sequence were suggested to form transmembrane α -helices. In addition, four of the programs assess helix orientation and, as a result estimate overall transmembrane topology of the protein. TMHMM 1.0 predictions suggest the gp91-phox N-terminus to be oriented to an extracellular aspect of membrane, while the N-terminus is placed on the cytosolic side of membrane in results of HMMTOP 1.1, PHDhtm and TMpred.

Table 2.1. Results of gp91-phox transmembrane domain computational predictions.

Trans-membrane domain number	Program name					
	DAS	HMMTOP 1.1	PHDhtm	SOSUI 1.0/10	TMHMM 1.0	TMpred
I	9-30	9-30	11-29	11-33	12-30	9-27
II	50-76	45-71	57-74	50-72	50-72	45-72
III	105-117	103-120	104-121	-	103-121	98-120
IV	167-192	168-189	173-191	169-191	167-189	171-194
V	207-222	204-221	206-223	207-229	204-222	204-228
VI	274-282	-	-	-	-	267-289
VII	402-419	-	404-421	403-425	403-425	401-420

Length of transmembrane segments is specified by amino acid residue number in the gp91-phox sequence.

Mass Spectrometry Analysis of Cytb Proteolytic Digests

It was previously reported that an immunoaffinity purified preparation of Cytb reconstituted in phosphatidylcholine lipid vesicles, supports NADPH oxidase activity in cell free superoxide production assays (37). This result suggests that the relipidated protein has a functional native conformation. To distinguish solvent-accessible and membrane-embedded or conformation-sequestered regions on native structure of gp91-phox, the reconstituted protein was used to identify proteolytic enzyme cleavage sites accessible to solution. Two proteolytic enzymes used were trypsin and endoproteinase Glu-C. Cleavage by trypsin is specific, with few exceptions, to peptide bonds at the carboxylic side of lysine and arginine residues, while Glu-C is a specific endoproteinase for the carboxylic side of glutamic acid (with 3,000 or more times lower rate for aspartic

acid depending on buffer used (55)). Following proteolytic digestion and separation from lipid vesicles, cleaved hydrophilic peptides were analyzed using MALDI-TOF mass spectrometry and identified by peptide mass matching to theoretical protease cleavage peptides. Nineteen peptides identified for trypsin and six for Glu-C digests are listed in Table 2.2. Identified peptides represented hydrophilic segments of gp91-phox sequence 2 to 25 residues long and with zero or one (including Lys44-Arg54, Gly81-Arg91, Arg92-Arg96, Asp500-Lys508, Thr509-Lys521, Ser486-Glu498 and Phe520-Glu544) missed protease cleavage site.

Polyclonal Anti-peptide Antibody Binding Studies

The success of producing specific antibodies that react with native protein depends on physico-chemical features and surface-accessibility of the region in the cognate protein (36, 56). Hydrophathy profiles are widely used to identify antigenic sites on proteins lacking three-dimensional structures (57, 58, 59, 60). Antigenic sites tend to occur on protein surfaces, where predominantly hydrophilic residues are both exposed to solvent and accessible for interaction with antibody. Therefore correlation between antigenic sites and regions of high hydrophilicity is anticipated. The method developed by Parker, et al. (36) was used to determine antigenic regions on the amino-terminal part of gp91-phox sequence, including residues 1- 300. The method estimates averaged propensities for each residue in a sliding window of seven amino acids using a combination of three amino acid antigenicity scales: atomic flexibility, hydrophilicity, and experimental HPLC

Table 2.2. Relipidated Cytb proteolytic digestion peptides identified by MALDI mass spectrometry.

Trypsin				Endoproteinase Glu-C			
Observed masses	Theoretical masses	Gp91-phox residue number	Predicted domain	Observed masses	Theoretical masses	Gp91-phox residue number	Predicted domain
509.0	508.3	288-290	VI-C4	604.3	603.8	246-250	E3
683.1	682.4	422-426	C4	1487.7	1488.1	556-568	C4
688.5	687.4	92-96	C2	1520.1	1520.9	486-498	C4
719.4	720.1	248-253	E3	2133.0	2133.8	468-485	C4
733.4	734.1	39-43	E1	2475.3	2475.8	499-519	C4
759.4	759.3	97-102	C2-III	2699.4	2699.8	520-544	C4
828.2	827.5	300-306	C4				
831.4	831.3	32-38	I-E1				
861.9	862.5	74-80	II-C2				
861.9	862.4	307-313	C4				
962.2	961.5	560-567	C4				
1000.3	1001.5	500-508	C4				
1050.6	1051.4	374-381	C4				
1112.7	1113.3	44-54	E1-II				
1125.1	1124.6	522-531	C4				
1126.5	1126.2	81-91	C2				
1162.1	1161.5	549-559	C4				
1213.6	1214.1	319-328	C4				
1640.1	1639.8	509-521	C4				

Experimentally observed and theoretical masses represent a monoisotopic values of singly protonated ions. Topology domains are consistent with gp91-phox topological model based on computational predictions and published experimental data and described in the Discussion section (roman numerals indicate transmembrane, C - cytosolic and E - non-cytosolic (extracellular) domains numbered starting from amino-terminus).

for each residue in a sliding window of seven amino acids using a combination of three amino acid antigenicity scales: atomic flexibility, hydrophilicity, and experimental HPLC retention times of synthetic peptides. Analysis of the amino-terminal portion of gp91-phox suggested nine regions, of two residue or greater, with a propensity value higher than the cutoff value, including Gly2-Ala5, Val27-Arg43, Ser77-Asn97, Cys126-Ser134,

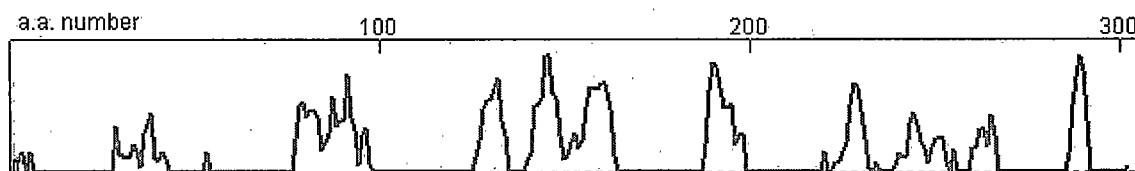


Figure 2.1. Antigenicity profile of gp91-phox amino-terminal half sequence, residues 1 to 300, calculated by the method of Parker, et al. Peaks represent antigenic segments with surface antigenicity value (axis of ordinates) greater than 50% of maximum.

Ala140-Pro163, Leu188-Arg199, Phe205-Trp206, Gly223-Thr232, His239-Lys253

(Figure 2.1)

For antipeptide antibody production, five segments, nine to fifteen amino acids long, were selected from the gp91-phox primary sequence included in the predicted antigenic regions (antibody names specified in brackets were derived from first three residues of the peptide): Met1-Gly9 (MGN), Tyr30-Lys44 (YRV), Glu150-Arg159 (ESY), Ala156-Gly166 (ARK), Lys247-Cys257 (KIS-1 and -2). Synthetic peptides corresponding to the sequence of selected segments were prepared with an additional carboxy-terminal cysteine residue added, with the exception of the KIS peptide, which contained a carboxy-terminal cysteine that was native in the gp91-phox primary sequence. The presence of the cysteine residue allowed coupling of the peptides to carrier protein using a sulfhydryl specific crosslinker.

Serum of immunized rabbits collected 12 to 20 weeks following the first injection was used as a source for antibody purification on peptide affinity columns. Binding of purified antibodies to gp91-phox was then tested by immunoblotting, ELISA, and by

flow cytometry on intact neutrophils. Purified antibodies ESY, ARK, KIS-1, KIS-2 displayed reactivity to denatured purified Cytb on immunoblots (Figure 2.2), demonstrating a diffuse reactive band of about 70 to 100 kDa, corresponding to gp91-phox. There was significantly higher staining intensity of the large subunit band by antibody KIS-1 and ESY compared to antibody ARK and KIS-2 at the same experimental conditions. No binding to Cytb was observed with antibodies MGN, YRV, as well as purified pre-immune serum IgG.

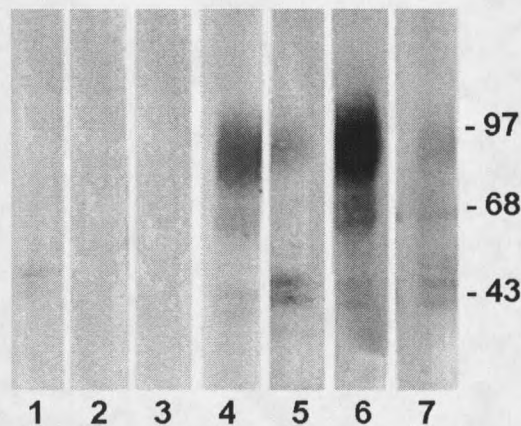


Figure 2.2. Immunoblot analysis of polyclonal antibody binding to Cytb. Each lane contains 0.5 μ g of purified Cytb electroblotted onto the nitrocellulose membrane. 15 μ g/ml of antibodies and purified preimmune IgG were used for blotting followed by detection with alkaline phosphatase-conjugated goat anti-rabbit IgG secondary antibody. Lane 1 represents rabbit IgG purified from preimmune serum and lanes 2-7 polyclonal antibodies MGN, YRV, ESY, ARK, KIS-1 and KIS-2, respectively.

The binding of antibodies to purified, detergent-solubilized purified Cytb was tested by ELISA. Antibodies YRV, ARK and KIS-1 showed stronger affinity to Cytb than MGN, ESY and KIS-2. A modest, but specific increase in color development was

observed at antibody concentrations greater than 12 $\mu\text{g/ml}$ for KIS-2 and about 5 $\mu\text{g/ml}$ for all other antibodies (Figure 2.3).

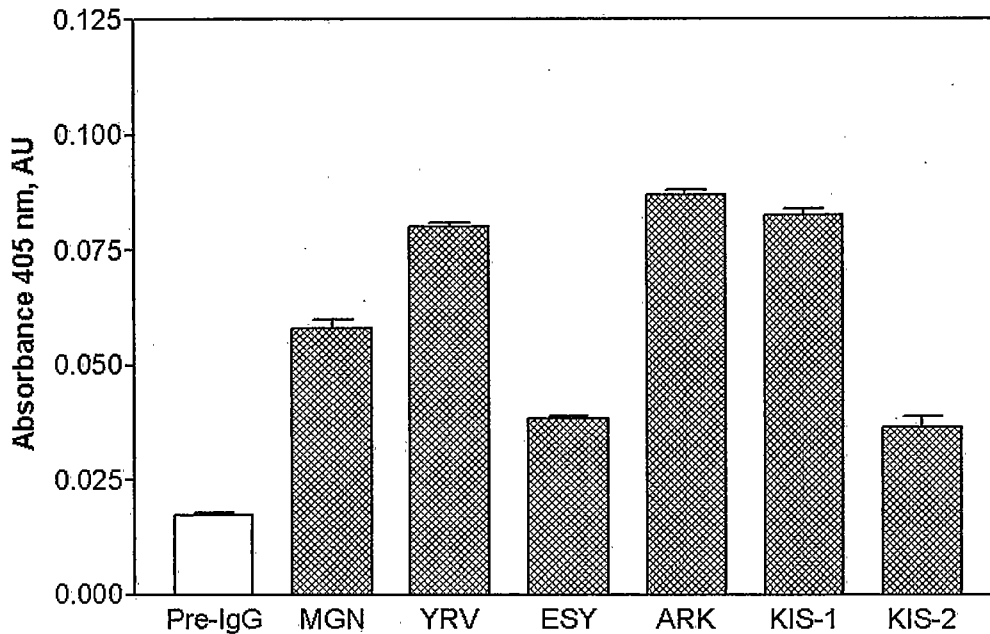


Figure 2.3. Polyclonal antibody ELISA with purified Cytb coated plates. Microplate wells were coated 0.4 pmole of purified Cyt b558 and were incubated with serial dilutions of purified polyclonal antibodies and preimmune serum IgG. Antibody binding was detected with secondary antibody horseradish peroxidase -conjugated goat anti-rabbit IgG. Color intensity in wells incubated with 45 $\mu\text{g/mL}$ of preimmune serum IgG (Pre-IgG) or polyclonal antibodies (specified for each bar) are displayed on the graph. Data is presented as mean \pm SEM of two repeats from an experiment representative of three similar experiments.

Flow cytometry was used to identify immunoreactivity of the purified antibodies to the external aspect of human neutrophils. The neutrophils were labeled with antibodies MGN, YRV, ESY, ARK, KIS-1 and KIS-2, or purified pre-immune serum IgG as a negative control. A shift of intact cell fluorescence intensity compared to the negative control was approximately twelve-fold for antibody ARK, ten-fold for antibodies MGN,

KIS- and approximately two-fold for antibody ESY (Figure 2.4). There was no significant shift in fluorescence for cells labeled with antibody YRV.

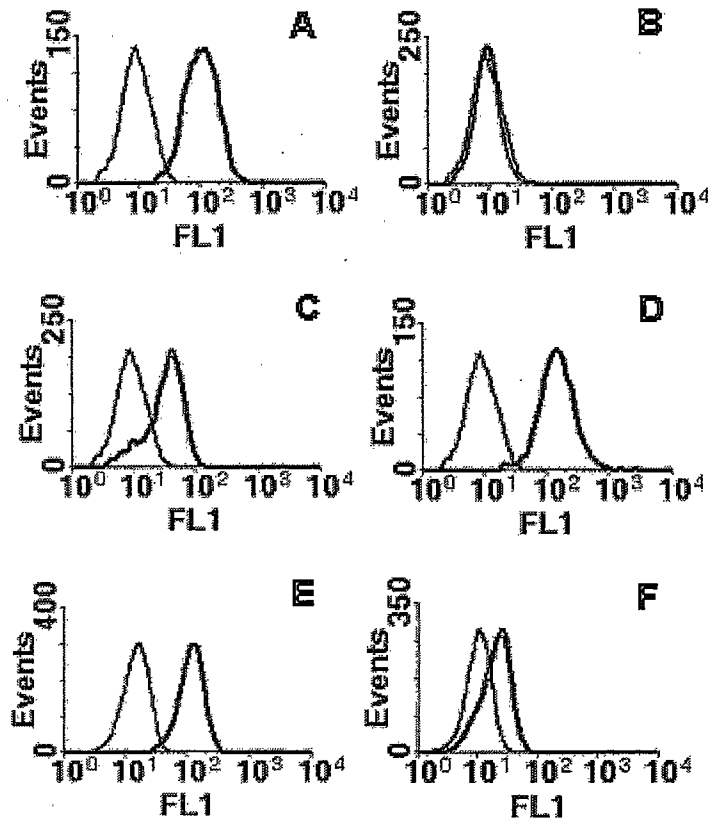


Figure 2.4. Flow cytometry analysis of antibody binding to intact neutrophil cells. Human neutrophils were labeled with purified antibodies, or preimmune serum IgG at 10 μ g/ml, then labeled with FITC-conjugated goat anti-rabbit IgG secondary antibody. Thick lines represent fluorescence intensity data for cells labeled with purified polyclonal antibodies MGN (panel A), YRV (B), ESY (C), ARK (D), KIS-1 (E) and KIS-2 (F). Thin lines correspond to the negative control of purified preimmune serum IgG. Graphs are representative of more than three similar experiments.

Certain X-linked CGD neutrophils have been characterized to have diminished or no expression of the Cytb protein, either because the gp91-phox protein encoding gene CYBB is partially or completely deleted, or because the aberrant protein product (or mRNA) is unstable. Such cells were previously used to show binding specificity of anti-Cytb antibodies on neutrophils (61). In this study, polyclonal antibody labeling of CGD neutrophils (lacking Cytb expression) did not indicate significant differences from results obtained with intact normal neutrophils (data not shown). This result was surprising since antibody YRV in contrast to MGN, ESY, ARK, KIS-1 and KIS-2 showed no reactivity to CGD cells.

Polyclonal Antibody Effect on Oxidase Activity

Antibody KIS-1, which binds gp91-phox on immunoblots, ELISA and possibly the native protein on intact neutrophils, was used to investigate possible functional effects the antibody binding may have on NADPH oxidase activity. Superoxide production was monitored following attachment of KIS-1 to intact, degranulated neutrophils that expose most of the Cytb at the cell surface (8, 62). Addition of Cytb-specific or preimmune IgG had differential stimulatory effects on superoxide production by cells. A concentration-dependent increase was seen in the rate of superoxide production, reaching 40% at 50 $\mu\text{g/mL}$ was observed for KIS-1, as compared to control (Figure 2.5). Purified preimmune serum IgG induced approximately an 8% increase in the superoxide production rate at the same concentration. Ferricytochrome c reduction was inhibitable in all cases by addition of SOD (data not shown) demonstrating that such reduction was due to NADPH oxidase

activity. To examine whether crosslinking of surface molecules by our antibody might be perturbing signal transduction events, fMLF stimulated Ca^{2+} release was monitored in the presence of KIS-1 or preimmune IgG and in the absence of antibody. Measurements of calcium release showed that preincubation of cells with KIS-1 antibody or preimmune serum IgG did not have an effect on neutrophil calcium release after fMLP stimulation when compared to cells preincubated in the absence of IgG (data not shown).

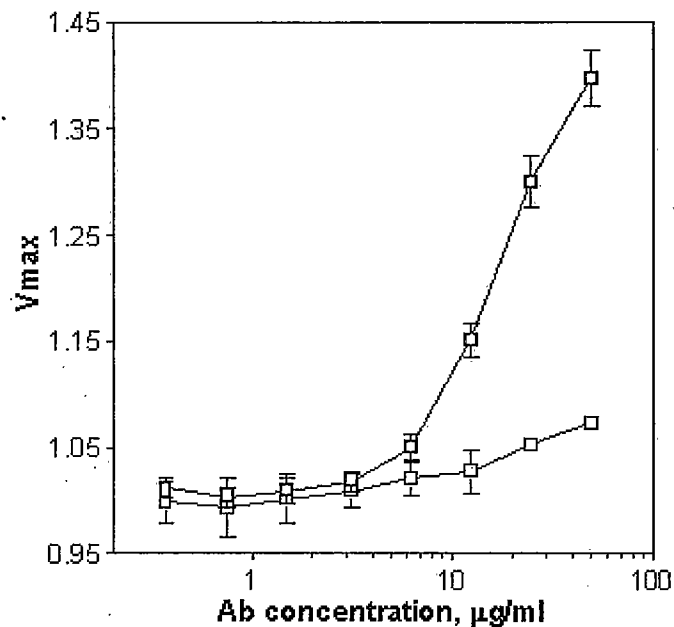


Figure 2.5. The effect of antibody KIS-1 on neutrophil superoxide anion production rate. Antibody KIS-1 or preimmune IgG was preincubated with cells and superoxide production was monitored by CytC reduction assay as described in Materials and Methods. Filled symbols represent data for antibody KIS-1. Empty symbols represent control with preimmune serum IgG. Data was normalized to maximal control (without IgG) superoxide production rate for each point, and presented as mean \pm SEM of six repeats in two separate experiments.

Discussion

Computational Transmembrane Topology Analysis of Gp91-phox

The function of Cytb in the NADPH oxidase is to provide a regulated pathway for high energy electrons to reduce molecular oxygen to superoxide in the extracellular or phagosomal milieu of phagocytes. Thus, to understand the molecular basis of the Cytb function, an understanding of its structure and membrane topology is necessary.

Structural features of proteins can be deduced based on their primary sequence. A significant effort has been put forth to analyze rules governing secondary structure formation (63, 64, 65, 66). Though computational modeling is not often capable of reliably predicting global protein topology without input from experimental data, mathematical transmembrane topological analysis can provide realistic structural estimates for integral membrane proteins (67).

Structure modeling studies have resulted in a wide range of algorithms and scales used to quantify the physicochemical amino acid properties important in shaping the three-dimensional protein structure (68). A key physical feature of proteins is their hydrophathy pattern - the distribution of hydrophobic and hydrophilic amino acid residues in the primary sequence. Hydrophobic interactions provide the primary net free energy required for protein folding (69). In an intact globular protein hydrophobic amino acids are generally shielded from the aqueous environment by coalescing at the center of the molecule, with the more hydrophilic residues exposed at its surface. Transmembrane proteins provide a rather different physical arrangement of hydrophobic residues in which

hydrophobic residues are collected primarily into a segments embedded within a cell membrane. An important application of hydropathy profiles in membrane protein structure studies is their use in conjunction with transmembrane topology prediction tools. In addition to hydropathy scales, there are amino acid membrane preference scales based on statistical distributions of each amino acid in membrane regions (68). Some scales are based solely on physicochemical measurements such as the free energy of side-chain transfer (70, 71). Other scales are based on statistical analysis of three-dimensional structures (72). Moreover, scales have been developed using a combination of both procedures (73). Individual scales were developed for different purposes, such as to identify transmembrane regions (47, 48, 50, 51, 73)

In this study, we used six computer programs available online to predict the transmembrane topology of the large subunit of Cytb. The programs utilizing different prediction methods provided alternative views of the overall protein topology including size of protein regions in the membrane and their transmembrane orientation. Five to seven regions were shown to have a high probability of forming transmembrane helices, mostly located on amino terminal half of gp91-phox. To compile the prediction results into a single topological model of the large subunit of the gp91-phox (Figure 2.6) we used available experimental data to validate and extend the predictions.

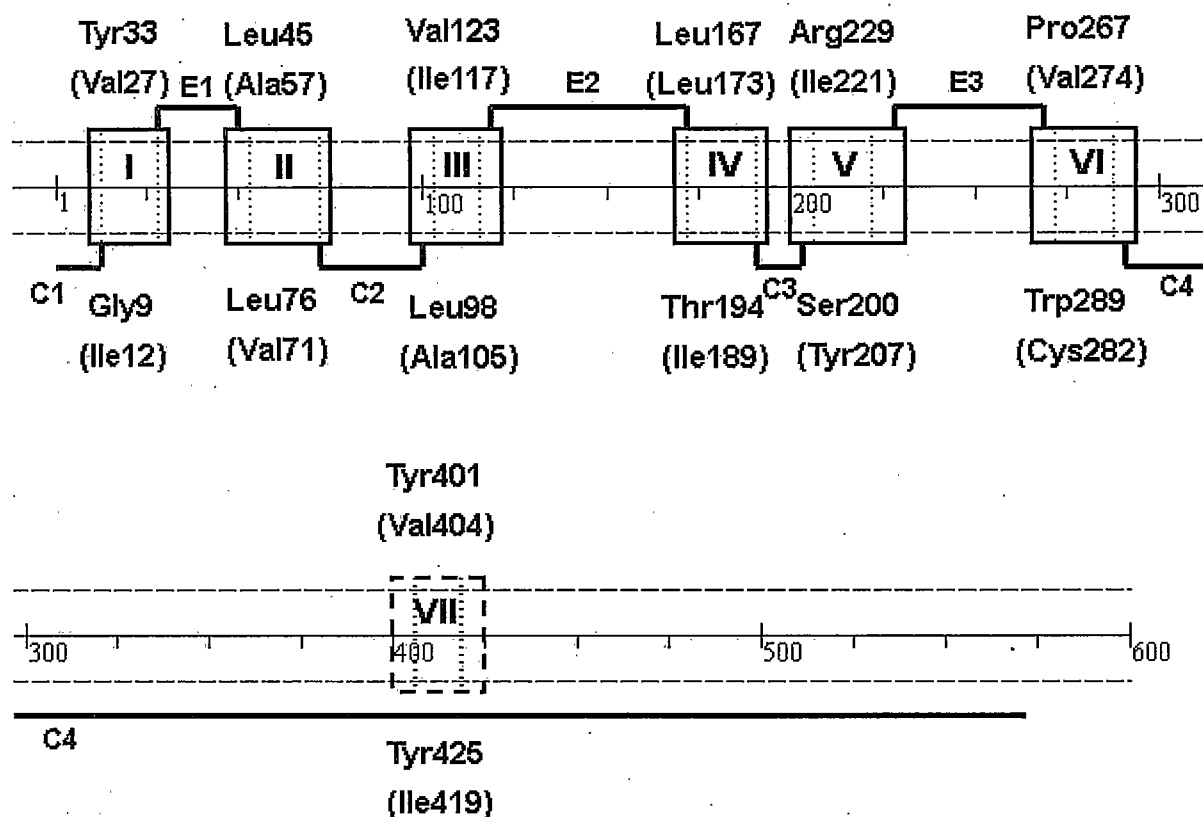


Figure 2.6. The gp91-phox topological model based on computational predictions and published experimental data. Lengths of helical domains were estimated from mathematical predictions and denoted as a starting and ending residue for the longest (solid line rectangles, non-bracketed residue values) and the shortest predicted helix interval (dotted thin line rectangles, text in brackets). Solid lines connecting helical regions represent parts of the protein sequence located in intracellular (top) or intracellular (bottom) aspect of cell membrane (represented as an area between two parallel dashed lines). Since segment Tyr401(Val404)-Tyr425(Ile419) has been identified as a transmembrane helical domain by most of mathematical programs used, but this possibility appears unlikely from experimental data analysis, it is shown here not included into gp91-phox topology model (dotted solid line).

Extracellular Domain

Since gp91-phox is a glycoprotein (8, 74), it must have some extracellular exposure. Yet little direct evidence exists for non-cytosolic regions on the large subunit. Gp91-phox has five potential N-linked glycosylation consensus sites, and glycosylation of three asparagine residues of three asparagine residues (residues 131, 148 and 239) was supported by mutagenesis analysis of these positions in a recombinant expression system (29). The glycosylation data agree with polyclonal antibody binding analyses, which localized region Glu160 - Thr172 outside neutrophil plasma membrane (35). A complex epitope bound by monoclonal antibody 7D5 has also been mapped using phage display analysis (34) and suggests that residues Arg159-Glu164 and Arg226-Gln231 form a discontinuous epitope on gp91-phox. Further, flow cytometry analysis of the antibody binding to intact neutrophils reveals that the regions must be located on extracellular loops of the protein. The described data supports topology predictions of HMMTOP 1.1, PHDhtm and TMPred methods that placed the two loops connecting transmembrane regions III-IV and V-VI (loops E2 and E3 in Figure 2.6, respectively) on the extracellular aspect of cell membrane.

Cytoplasmic Domain

A number of studies have provided evidence for the cytosolic location of specific residues of gp91-phox. Polyclonal antibodies raised against peptides mimicking the carboxy-terminus of gp91-phox and showed intracellular immunostaining of neutrophils

(35, 75). Phage display library binding analyses revealed three regions of gp91-phox as sites for interaction with cytosolic protein p47-phox at residues Ser87-Leu94, Phe451-Leu458, Phe554-Gln564 (32). Those possible interactions were supported by NADPH oxidase inhibition in mutants carrying deletions corresponding to residues Arg91 and Arg92 (31) or addition of synthetic peptides which mimicked regions located at or near putative p67-phox or p47-phox interaction sites (32, 33, 76, 77, 78, 79). Another peptide corresponding to amino acid residues Leu420-Tyr425 of gp91-phox and having an inhibitory effect on the oxidase activity was not shown to be associated with cytosolic protein binding, but rather interrupted electron transfer from NADPH to oxygen (80). Indeed, the sequence of the peptide overlaps with one of the predicted NADPH binding site segments, spanning residue Asp403 to Val423 as predicted by sequence alignment with known structure of ferredoxin-NADP⁺ reductases (18, 19, 27). Additional putative NADPH binding sites, based on the sequence similarity analyses, appear to involve residues Phe441-Ala450, Gly504-Arg513, Lys548-Phe570. Apart from these specific cofactor-binding sites, a general homology with ferredoxin-NADP⁺ reductase family was shown for the distal 250 carboxy-terminal sequence of gp91-phox. This data provides evidence that the region around Ser87-Leu94 (loop C2), and carboxy-end residues starting at approximately Asp403 of gp91-phox must be located in cytoplasm.

Transmembrane Domain

Due to contradicting experimental data and our results of transmembrane predictions (Table 2.1), the boundary between the carboxyl-most transmembrane region

and cytosolic domain may not been adequately defined. Alignments of the amino acid sequence of gp91-phox with previously characterized flavoproteins revealed that there are three possible binding sites for the FAD cofactor near the middle portion of gp91-phox, including regions Ile214-Gln246, Leu335-Ala345 and Phe350-Asp360 (18, 19, 27). Since a portion of antibody 7D5 epitope Arg226-Gln231 is located on extracellular aspect of plasma membrane and Asn239 is likely to be glycosylated, as described above, it excludes region Ile214-Gln246 from potential cytosolic FAD binding sites. With regard to region Cys369-Val398, contradictory evidence has been presented in the literature. This region to was characterized to contain an extracellular papain cleavage site (35), and mutagenesis studies revealed His338 to be critical for FAD incorporation into the oxidase system (81). Thus, placing a FAD binding region at Leu335-Ala345 to cytosolic aspect of the membrane, we conclude that the carboxy-terminal cytosolic domain of gp91-phox is connected to an extracellular loop by a transmembrane helix VI predicted approximately between residues Pro267(Val274) through Trp289(Cys282). This assignment rules out a transmembrane helix VII predicted to lie between Tyr401(Leu406)-Tyr425(Ile419). The latter hydrophobic segment has been identified as a transmembrane helical domain by most of computational methods used in this study, yet it must reside in the hydrophobic core of the cytoplasmic domain.

The Cytb has at least two hemes which are either coordinated by gp91-phox alone (11, 12) or by the sharing of one heme across subunits (9, 14, 15). Although the location of hemes in Cyt b558 heterodimer remains unknown, recent models have suggested residues coordinating hemes are histidines 101, 111, 115, 119, 209, 222 in gp 91-phox

and His94 in p22-phox. Limited proteolysis data also supports heme placement in the amino-terminal half of gp91-phox at a transmembrane or extracellular location (13). As discussed above, the antibody epitopes Arg159-Thr172, Arg226-Gln231, Lys247-Cys257, and potentially glycosylated asparagines 239, 131, 148 are located on non-cytosolic loops (Figure 2.6, E2, E3), and residues Ser87 through Leu94 are cytosolic (C2). Thus, our model suggests that in gp91-phox, the histidines involved in heme coordination must be located on two helices (helix III encompassing residues Leu98(Ala105)-Val123(Ile117) and helix V at Ser200(Tyr207)-Arg229(Ile221)) with their amino-ends starting in cytosol. This restricts helix IV location to be between the latter helices at position Leu167(Leu173)-Thr194(Ile189).

Although there is a lack of experimental data to evaluate topology of the most amino terminal region of gp91-phox (residues 1-87), transmembrane helices are quite likely to an essential component of its structure. The only published data concerning putative structure of this region describes inhibition of NADPH oxidase activity with a synthetic peptide mimicking residues Val27-Leu46, so possible interaction with cytosolic proteins and thus cytosolic location was suggested for the region (33). However, uncertainties exist about the specificity of peptide-protein interactions that reduces the oxidase activity and without independent evidence, one is never certain that added peptides are not affecting intra-protein interactions. For example, inhibitory effects of gp91-phox carboxy-terminus-mimicking peptides were in conflict with results from mutation analysis of the region that showed a lack of the effect on the NADPH oxidase activity (82, 83). Considering this limitations, the topology of the amino-terminal end of

gp91-phox in our model is based on the transmembrane topology predictions, suggesting high probability for two transmembrane helices I and II formation in regions Gly9(Ile12)–Tyr33(Val27) and Leu45(Ala57)–Leu76(Val71). To be consistent with the experimentally-based topology of our model downstream, we tentatively predict, in opposition of our anti-peptide antibody binding results discussed above, that the amino-terminus (C1) of the gp91-phox is located in cytoplasm.

Limited Proteolysis Followed by Mass Spectrometry

To further improve the gp91-phox topological model and identify boundaries between elements of the protein structure, we proteolytically digested relipidated Cytb and identified liberated peptides by MALDI mass spectrometry. Results of identification of solvent exposed domains on native, lipid-reconstituted gp91-phox are summarized in Figure 2.7. The displayed pattern of proteolytic enzyme cleavage sites is mostly restricted to hydrophilic segments of the protein. Some of these segments are located on putative loops connecting transmembrane helices (C2, E1, E3) at the amino-terminal half of our gp91-phox model while others likely represent surface exposed regions on the cytosolic carboxy-terminal domain (C4). Interestingly, we detected trypsin digest products derived from regions in predicted transmembrane helices I, II, III and VI, suggesting an overestimate in the predicted size of the transmembrane α -helices. These residues may be located at capping domain of α -helix extending beyond the membrane bilayer, or possibly located on a integral membrane helical structure with an opening large enough

A

MGNWAVNEGLSIFVILVWLGLNVFLVWYYR VYDIPPK FFYTR KLLGSALALAR APAACLNFCML
 ILLPVCRL NLLSFLR GSSACCSTRVRR RQLDR NLTFHK MVAWMIALHSAIHTIAHLFNVEWCVNARV
 NNSDPYSVALSELGDRQNESYLNFAARKRIKNPEGGLYLAVTLLAGITGVVITLCLILIIITSSTKTIIRRSYF
 EVFWYTHHLFVIFFIGLAIHGAEIRIVRGQTAESLAVHNITVCEQK ISEWVK IKCEPIQFAGNPPMTW
 KWIVGPMFLYLCERLVRFWR SQQKVVITK VVTHPK TIELQMK KKGFK MEVGQYIFVK CPKV
 SKLEWHPFTLTSAPEDFFSIHIRIVGDWTEGLFNACGCDK QEFQDAWK LPKIAVDGPFGTASEDVFS
 YEVVMLVGAGIGVTPPFASILK SVWYK YCNNATNLKLLKIYFYWLCRDTHAFEFWADLLQLLESQMQR
 NNAGFLSYNIYLTGWDESQANHFAVHHDEEK DVITGLKQK TLYGRPNWDNEFK TIASQHPNTR IG
 FLCGPEALAEATLSK QSISNSESGR GVHFIFNK ENF

B

MGNWAVNEGLSIFVILVWLGLNVFLVWYYRVYDIPPKFFYTRKLLGSALALARAPAACLNFCMLILLPV
 CRNLLSFLRGGSSACCSTRVRRQLDRNLTFHKMVAWMIALHSAIHTIAHLFNVEWCVNARVNSDPYSVALS
 ELGDRQNESYLNFAARKRIKNPEGGLYLAVTLLAGITGVVITLCLILIIITSSTKTIIRRSYFVFWYTHHLFV
 IFFIGLAIHGAEIRIVRGQTAESLAVHNITVCE QKISE WGIKICPIQFAGNPPMTWIKWIVGPMFLYL
 CERLVRFRWRSQQKVVITKVVTHPKTI ELQMKKKGFKMEVGQYIFVKCPKVSKEWHPFTLTSAPEDFFS
 IHIRIVGDWTEGLFNACGCDKQEFQDAWKLPKIAVDGPFGTASEDVFSYEVVMLVGAGIGVTPPFASILKSV
 WYKYCNNATNLKLLKIYFYWLCRDTHAFEFWADLLQLLESQMQR RNNAGFLSYNIYLTGWDE SQANHFA
 VHHDEE KDVITGLKQKTLYGRPNWDNE FKTIASQHPNTRIGVFLCGPEALAE TLSKQISISNSE SGPR
 GVHFIFNKE NF

Figure 2.7. Soluble peptides and protease cleavage sites on gp91-phox identified by proteolytic digestion with trypsin (panel A) or endoproteinase Glu-C (panel B) of lipid reconstituted Cytb and MALDI mass spectrometry analysis. Boxed residues on the gp91-phox show potential cleavage sites for protease and the spaces signify detected cleavages. The identified peptides are shaded. Underlined regions represent putative transmembrane domains based on mathematical predictions and experimental data.

to be accessible by trypsin protease. There are also a few cleavage products, resulting from application of trypsin and endoproteinase Glu-C, at or near predicted NADPH binding sites, Gly504-Arg513, Lys548-Phe570, and carboxy-terminal end of Asp403-Val423 (residues Lys421, Lys508, Lys548, Glu556, Arg559, Lys567, Glu568). Figure 7 also shows a number of missed cleavage sites, including residues at the amino-terminal end of Asp403-Val423 assigned as NADPH binding site or other predicted binding sites for NADPH at Phe441-Ala450 and FAD at Leu335-Ala345 and Phe350-Asp360 (residues Glu336, Arg356, Glu403, Glu442, Arg446). Some of the protease-cleaved peptides may not be identified from mass spectrometry data by matching to theoretical protein digest results because of peptide mass increase due to various post-translational modifications. Such masking may be the reason for lack of detectable peptides around potential carbohydrate modified asparagines residues 131, 148 and 239. Additional proof is required to allow these missed cleavage sites to be characterized as part of sequence domains sequestered in a membrane or tertiary protein structure as the sites may become exposed (or hidden) when the protein denatures and possibly aggregates.

Polyclonal Rabbit Anti-peptide Antibodies

Native protein-reactive antipeptide antibodies have been successfully used to identify cytoplasmic or extracellular localization of protein segments by assessment of antibody binding to intact or permeabilized cells using immunofluorescence microscopy or flow cytometry (35, 84, 85, 86). In this study, six polyclonal antipeptide antibodies were raised against five different gp91-phox regions located at the amino-terminal part of

the protein to map its transmembrane topology. The produced antibodies showed various degree of binding to denatured, detergent-solubilized Cytb (Figures 2.2 and 2.3).

Interestingly, comparison of the binding characteristics of two antibodies KIS-1 and KIS-2, raised using two identical peptides, shows that a significantly higher specificity polyclonal antibody could be attained by specific peptide coupling to carrier protein using bifunctional cross-linker.

Labeling of the intact neutrophil extracellular surface with the specific antibodies would suggest what regions of gp91-phox are accessible on the extracellular domain on the native protein *in situ*. Antibody binding to intact neutrophil suggested an extracellular localization of epitope regions Met1-Gly9 (MGN), Glu150-Arg159 (ESY), Ala156-Gly166 (ARK), Lys247-Cys257 (KIS) (Figure 2.4). However, X-linked CGD neutrophils lacking expression of Cytb (used as a negative control) did not indicate significant differences of polyclonal antibody labeling as compared to normal type cell data. This result was particularly surprising since antibody YRV (region Tyr30-Lys44) which was negative in flow cytometry on intact neutrophils was, unlike antibodies MGN, ESY, ARK and KIS, was also negative when tested with neutrophils from CGD patients. This result implies that either CGD cells have unusual properties that makes them non-ideal control cells or that the affinity purified antibodies selectively bind other components of the neutrophil surface. The results also underscores how cautious one must be in the application of immunological probes in human blood cells. Because of this uncertainty, interpretation of gp91-phox topology using the polyclonal antibody binding data must remain suspect until this ambiguity is resolved.

Polyclonal antibody KIS-1 effect on oxidase activity

An interaction of the two subunits of the Cytb has been shown to be essential for function of the Cytb (87). Additionally, important interactions between cytosolic and membrane associated proteins of the NADPH oxidase have been studied showing that specific sites of interaction must exist on the protein surface. The interaction with cytosolic components, and possibly direct Cytb-Cytb interactions, may result in clustering of the molecule or dimerisations of α - β heterodimer to a quaternary structural unit (9, 37, 88). Published immunoelectron microscopy data show aggregates of NADPH oxidase components in a phagosomal or plasma membrane of neutrophils. Using anti-Cytb antibodies for immunocytochemical electron microscopy showed that Cytb translocates from specific granules to the phagosomal membrane in phagocytosing neutrophils, where the protein appeared to be clustered in discrete regions of contact between the bacterial and phagosomal membrane interface (75). Later, immunoelectron microscopy of gp91-phox (89) and other NADPH oxidase proteins, such as p47-phox, p67-phox and Rac2, revealed cluster formation of about 0.03 - 0.1 μm^2 dimensions in a plasma membrane of adherent neutrophils (90). Aggregation of NADPH oxidase complexes in neutrophil and the physiological function of this process has been previously discussed (22). Although other possibilities clearly exist, the hypothesis of interaction between molecules of Cytb in a cluster might provide an explanation how antibody crosslinking could effect the superoxide production rate. Location of hemes of aggregated Cytb molecules might permit not only intramolecular electron transfer, but also intermolecular electron transfer between the hemes of different cytochrome

molecules. Such a pathway could involve direct electron transfer between spatially overlapping hemes. Alternatively, tunneling pathways along specific structures of the protein, such as an alpha helix or a beta sheet, could be coupled to heme by an aromatic side chain of an amino acid in close proximity to the heme, as suggested by Beratan, et al. (91). By this latter interpretation, an electron donated to the cluster by an FAD could reduce an oxygen bound to any one of the Cytb molecules in the cluster, making the electron transport and oxygen reduction process more efficient.

Thus anti-Cytb antibodies might represent tools to cause such clustering experimentally. Our physiological study on neutrophils revealed that the presence of an antibody that possibly binds to an extracellular domain of Cytb has a significant positive effect on the rate of superoxide production (Figure 2.5). Although some increase of superoxide production was caused by presence of nonspecific IgG antibodies in the reaction solution, the effect was one fifth the value of the specific anti-peptide polyclonal antibody effect. The antibody cross-reactivity to components other than Cytb epitopes on intact neutrophil cells interjects uncertainties about mechanism of stimulation of superoxide production. However, the results are consistent with the clustering hypothesis but need still additional investigation that secondary effects of surface protein capping do not result in similar increases for other reasons.

In summary, computational methods used to predict the transmembrane topology for gp91-phox identified five to seven membrane-spanning, α -helical domains on the amino terminal half of the protein. Transmembrane topology model of gp91-phox containing six transmembrane regions at N-terminal half of the protein and carboxy- and

amino-termini located in cytosol was build using computational predictions and published experimental data. Purified, lipid reconstituted Cytb proteolytic enzyme cleavage product analysis by MALDI mass spectrometry identified potentially solvent-accessible, membrane-embedded or conformationally sequestered regions on gp91-phox. In addition, rabbit polyclonal antibodies raised against synthetic peptide mimicking gp91-phox regions binding to intact neutrophils suggested extracellular localization of the corresponding regions 1-9 (MGN), 150-159 (ESY), 156-166 (ARK), 247-257 (KIS-1, KIS-2). Binding of KIS-1 antibody to neutrophils also resulted in an increase in the rate of superoxide production and suggested a possible functional role for Cytb reorganizations and/or clustering in the active NADPH oxidase. However, because the antibodies, with the exception of YRV (region 30-44) and preimmune controls, positively labeled neutrophils from patients missing gp91-phox, the results also suggested that CGD-cells and perhaps normal neutrophils have an unusual crossreactive species in their plasma membranes.

References Cited

1. Clark RA. 1999. Activation of the neutrophil respiratory burst oxidase. *J. Infect. Dis.* 179 Suppl 2:S309-S317
2. Jesaitis AJ. 1995. Structure of human phagocyte cytochrome b and its relationship to microbicidal superoxide production. *J. Immunol.* 155:3286-8
3. Roos D, de Boer M, Kuribayashi F, Meischl C, Weening RS, Segal AW, Ahlin A, Nemet K, Hossle JP, Bernatowska-Matuszkiewicz E, Middleton-Price H. 1996. Mutations in the X-linked and autosomal recessive forms of chronic granulomatous disease. *Blood* 87:1663-81
4. Lambeth JD. 2002. Nox/Duox family of nicotinamide adenine dinucleotide (phosphate) oxidases. *Curr. Opin. Hematol.* 9:11-7
5. Leusen JH, Verhoeven AJ, Roos D. 1996. Interactions between the components of the human NADPH oxidase: intrigues in the phox family. *J. Lab. Clin. Med.* 128:461-76
6. Koshkin V, Pick E. 1994. Superoxide production by cytochrome b559. Mechanism of cytosol-independent activation. *FEBS Lett.* 338:285-9
7. Koshkin V, Pick E. 1993. Generation of superoxide by purified and relipidated cytochrome b559 in the absence of cytosolic activators. *FEBS Lett.* 327:57-62
8. Parkos CA, Allen RA, Cochrane CG, Jesaitis AJ. 1987. Purified cytochrome b from human granulocyte plasma membrane is comprised of two polypeptides with relative molecular weights of 91,000 and 22,000. *J. Clin. Invest.* 80:732-42
9. Parkos CA, Allen RA, Cochrane CG, Jesaitis AJ. 1988. The quaternary structure of the plasma membrane b-type cytochrome of human granulocytes. *Biochim. Biophys. Acta.* 932:71-83
10. Parkos CA, Dinauer MC, Walker LE, Allen RA, Jesaitis AJ, Orkin SH. 1988. Primary structure and unique expression of the 22-kilodalton light chain of human neutrophil cytochrome b. *Proc. Natl. Acad. Sci. U. S. A.* 85:3319-23

11. Yu L, Quinn MT, Cross AR, Dinauer MC. 1998. Gp91(phox) is the heme binding subunit of the superoxide-generating NADPH oxidase. *Proc. Natl. Acad. Sci. U. S. A.* 95:7993-8
12. Finegold AA, Shatwell KP, Segal AW, Klausner RD, Dancis A. 1996. Intramembrane bis-heme motif for transmembrane electron transport conserved in a yeast iron reductase and the human NADPH oxidase. *J. Biol. Chem.* 271:31021-4
13. Foubert TR, Bleazard JB, Burritt JB, Gripenrog JM, Baniulis D, Taylor RM, Jesaitis AJ. 2001. Identification of a spectrally stable proteolytic fragment of human neutrophil flavocytochrome b composed of the NH₂-terminal regions of gp91(phox) and p22(phox). *J. Biol. Chem.* 276:38852-61
14. Parkos CA, Quinn MT, Jesaitis AJ. 1992. The structure of human neutrophil plasma membrane b-type cytochrome involved in superoxide production. In *Molecular Basis of Oxidative Damage by Leukocytes*, ed. AJ Jesaitis, EA Dratz, pp. 45-46. Boca Raton: CRC Press
15. Quinn MT, Mullen ML, Jesaitis AJ. 1992. Human neutrophil cytochrome b contains multiple hemes. Evidence for heme associated with both subunits. *J. Biol. Chem.* 267:7303-9
16. Segal AW, Shatwell KP. 1997. The NADPH oxidase of phagocytic leukocytes. *Ann. N. Y. Acad. Sci.* 832:215-22
17. Escriou V, Laporte F, Vignais PV. 1996. Assessment of the flavoprotein nature of the redox core of neutrophil NADPH oxidase. *Biochem. Biophys. Res. Commun.* 219:930-5
18. Rotrosen D, Yeung CL, Leto TL, Malech HL, Kwong CH. 1992. Cytochrome b558: the flavin-binding component of the phagocyte NADPH oxidase. *Science.* 256:1459-62
19. Sumimoto H, Sakamoto N, Nozaki M, Sakaki Y, Takeshige K, Minakami S. 1992. Cytochrome b558, a component of the phagocyte NADPH oxidase, is a flavoprotein. *Biochem. Biophys. Res. Commun.* 186:1368-75

20. Nisimoto Y, Otsuka-Murakami H, Lambeth DJ. 1995. Reconstitution of flavin-depleted neutrophil flavocytochrome b558 with 8-mercapto-FAD and characterization of the flavin-reconstituted enzyme. *J. Biol. Chem.* 270:16428-34
21. Doussiere J, Brandolin G, Derrien V, Vignais PV. 1993. Critical assessment of the presence of an NADPH binding site on neutrophil cytochrome b558 by photoaffinity and immunochemical labeling. *Biochemistry.* 32:8880-7
22. Jesaitis AJ. 1992. Organization of the leukocyte plasma membrane components of superoxide production. In *Molecular Basis of Oxidative Damage by Leukocytes*, ed. AJ Jesaitis, EA Dratz, pp. 91-98. Boca Raton: CRC Press
23. Ravel P, Lederer F. 1993. Affinity-labeling of an NADPH-binding site on the heavy subunit of flavocytochrome b558 in particulate NADPH oxidase from activated human neutrophils. *Biochem. Biophys. Res. Commun.* 196:543-52
24. Tsunawaki S, Mizunari H, Namiki H, Kuratsuji T. 1994. NADPH-binding component of the respiratory burst oxidase system: studies using neutrophil membranes from patients with chronic granulomatous disease lacking the beta-subunit of cytochrome b558. *J. Exp. Med.* 179:291-7
25. Smith RM, Connor JA, Chen LM, Babior BM. 1996. The cytosolic subunit p67phox contains an NADPH-binding site that participates in catalysis by the leukocyte NADPH oxidase. *J. Clin. Invest.* 98:977-83
26. Dang PM, Johnson JL, Babior BM. 2000. Binding of nicotinamide adenine dinucleotide phosphate to the tetratricopeptide repeat domains at the N-terminus of p67PHOX, a subunit of the leukocyte nicotinamide adenine dinucleotide phosphate oxidase. *Biochemistry.* 39:3069-75
27. Segal AW, West I, Wientjes F, Nugent JH, Chavan AJ, Haley B, Garcia RC, Rosen H, Scrace G. 1992. Cytochrome b-245 is a flavocytochrome containing FAD and the NADPH-binding site of the microbicidal oxidase of phagocytes. *Biochem. J.* 284 (Pt 3):781-8
28. Taylor WR, Jones DT, Segal AW. 1993. A structural model for the nucleotide binding domains of the flavocytochrome b-245 beta-chain. *Protein. Sci.* 2:1675-85

29. Wallach TM, Segal AW. 1997. Analysis of glycosylation sites on gp91phox, the flavocytochrome of the NADPH oxidase, by site-directed mutagenesis and translation in vitro. *Biochem. J.* 321 (Pt 3):583-5
30. Rae J, Newburger PE, Dinauer MC, Noack D, Hopkins PJ, Kuruto R, Curnutte JT. 1998. X-Linked chronic granulomatous disease: mutations in the CYBB gene encoding the gp91-phox component of respiratory-burst oxidase. *Am. J. Hum. Genet.* 62:1320-31
31. Biberstine-Kinkade KJ, Yu L, Dinauer MC. 1999. Mutagenesis of an arginine- and lysine-rich domain in the gp91(phox) subunit of the phagocyte NADPH-oxidase flavocytochrome b558. *J. Biol. Chem.* 274:10451-7
32. DeLeo FR, Yu L, Burritt JB, Loetterle LR, Bond CW, Jesaitis AJ, Quinn MT. 1995. Mapping sites of interaction of p47-phox and flavocytochrome b with random-sequence peptide phage display libraries. *Proc. Natl. Acad. Sci. U. S. A.* 92:7110-4
33. Park MY, Imajoh-Ohmi S, Nunoi H, Kanegasaki S. 1997. Synthetic peptides corresponding to various hydrophilic regions of the large subunit of cytochrome b558 inhibit superoxide generation in a cell-free system from neutrophils. *Biochem. Biophys. Res. Commun.* 234:531-6
34. Burritt JB, DeLeo FR, McDonald CL, Prigge JR, Dinauer MC, Nakamura M, Nauseef WM, Jesaitis AJ. 2001. Phage display epitope mapping of human neutrophil flavocytochrome b558. Identification of two juxtaposed extracellular domains. *J. Biol. Chem.* 276:2053-61
35. Imajoh-Ohmi S, Tokita K, Ochiai H, Nakamura M, Kanegasaki S. 1992. Topology of cytochrome b558 in neutrophil membrane analyzed by anti-peptide antibodies and proteolysis. *J. Biol. Chem.* 267:180-4
36. Parker JM, Guo D, Hodges RS. 1986. New hydrophilicity scale derived from high-performance liquid chromatography peptide retention data: correlation of predicted surface residues with antigenicity and X-ray-derived accessible sites. *Biochemistry* 25:5425-32

37. Taylor RM, Burritt JB, Foubert TR, Snodgrass MA, Stone KC, Baniulis D, Gripenrog JM, Lord C, Jesaitis AJ. 2003. Single-step immunoaffinity purification and characterization of dodecylmaltoside-solubilized human neutrophil flavocytochrome b. *Biochim. Biophys. Acta* 1612:65-75
38. Wilkins MR, Lindskog I, Gasteiger E, Bairoch A, Sanchez JC, Hochstrasser DF, Appel RD. 1997. Detailed peptide characterization using PEPTIDEMASS--a World-Wide-Web-accessible tool. *Electrophoresis* 18:403-8
39. Ausubel FM, Kinston RE, Moore DD, Seidman JG, Smith JA, Struhl K. 1992. Enzyme-linked immunosorbent assay (ELISA): Indirect ELISA to detect specific antibodies. In *Short Protocols in Molecular Biology*, New York: Greene publishing associates and John Wiley & Sons
40. Wisniewski JR, Ghidelli S, Steuernagel A. 1994. Region of insect high mobility group (HMG) 1 protein homologous to helix 2 of the rat HMG1-b box is in close contact with DNA. *J. Biol. Chem.* 269:29261-4
41. Quinn MT, Parkos CA, Jesaitis AJ. 1995. Purification of human neutrophil NADPH oxidase cytochrome b-558 and association with Rap 1A. *Methods Enzymol.* 255:476-87
42. Laemmli UK. 1970. Cleavage of structural proteins during the assembly of the head of bacteriophage T4. *Nature.* 227:680-5
43. Henson PM, Oades ZG. 1975. Stimulation of human neutrophils by soluble and insoluble immunoglobulin aggregates. Secretion of granule constituents and increased oxidation of glucose. *J. Clin. Invest* 56:1053-61
44. Arthur MJ, Kowalski-Saunders P, Gurney S, Tolcher R, Bull FG, Wright R. 1987. Reduction of ferricytochrome C may underestimate superoxide production by monocytes. *J. Immunol. Methods* 98:63-9
45. Chapman-Kirkland ES, Wasvary JS, Seligmann BE. 1991. Superoxide anion production from human neutrophils measured with an improved kinetic and endpoint microassay. *J. Immunol. Methods* 142:95-104

46. Miettinen HM, Gripentrog JM, Mason MM, Jesaitis AJ. 1999. Identification of putative sites of interaction between the human formyl peptide receptor and G protein. *J. Biol. Chem.* 274:27934-42
47. Cserzo M, Wallin E, Simon I, von Heijne G, Elofsson A. 1997. Prediction of transmembrane alpha-helices in prokaryotic membrane proteins: the dense alignment surface method. *Protein Eng* 10:673-6
48. Hofmann K, Stoffel W. 1993. TMbase - a database of membrane spanning protein segments. *Biol. Chem.* 347:166
49. Rost B, Casadio R, Fariselli P, Sander C. 1995. Transmembrane helices predicted at 95% accuracy. *Protein Sci.* 4:521-33
50. Hirokawa T; Boon-Chieng S, Mitaku S. 1998. SOSUI: classification and secondary structure prediction system for membrane proteins. *Bioinformatics.* 14:378-9
51. Tusnady GE, Simon I. 1998. Principles governing amino acid composition of integral membrane proteins: application to topology prediction. *J. Mol. Biol.* 283:489-506
52. Sonnhammer EL, von Heijne G, Krogh A. 1998. A hidden Markov model for predicting transmembrane helices in protein sequences. *Proc. Int. Conf. Intell. Syst. Mol. Biol.* 6:175-82
53. Dinauer MC, Orkin SH, Brown R, Jesaitis AJ, Parkos CA. 1987. The glycoprotein encoded by the X-linked chronic granulomatous disease locus is a component of the neutrophil cytochrome b complex. *Nature* 327:717-20
54. Teahan C, Rowe P, Parker P, Totty N, Segal AW. 1987. The X-linked chronic granulomatous disease gene codes for the beta-chain of cytochrome b-245. *Nature* 327:720-1
55. Sorensen SB, Sorensen TL, Breddam K. 1991. Fragmentation of proteins by *S. aureus* strain V8 protease. Ammonium bicarbonate strongly inhibits the enzyme but does not improve the selectivity for glutamic acid. *FEBS Lett.* 294:195-7

56. Liang TC, Luo W, Hsieh JT, Lin SH. 1996. Antibody binding to a peptide but not the whole protein by recognition of the C-terminal carboxy group. *Arch. Biochem. Biophys.* 329:208-14
57. Hopp TP. 1989. Use of hydrophilicity plotting procedures to identify protein antigenic segments and other interaction sites. *Methods Enzymol.* 178:571-85
58. Hopp TP. 1984. Protein antigen conformation: folding patterns and predictive algorithms; selection of antigenic and immunogenic peptides. *Ann. Sclavo. Collana. Monogr* 1:47-60
59. Hopp TP, Woods KR. 1981. Prediction of protein antigenic determinants from amino acid sequences. *Proc. Natl. Acad. Sci. U. S. A* 78:3824-8
60. Tanaka T, Slamon DJ, Cline MJ. 1985. Efficient generation of antibodies to oncoproteins by using synthetic peptide antigens. *Proc. Natl. Acad. Sci. U. S. A* 82:3400-4
61. Batot G, Martel C, Capdeville N, Wientjes F, Morel F. 1995. Characterization of neutrophil NADPH oxidase activity reconstituted in a cell-free assay using specific monoclonal antibodies raised against cytochrome b558. *Eur. J. Biochem.* 234:208-15
62. Parkos CA, Cochrane CG, Schmitt M, Jesaitis AJ. 1985. Regulation of the oxidative response of human granulocytes to chemoattractants. No evidence for stimulated traffic of redox enzymes between endo and plasma membranes. *J. Biol. Chem.* 260:6541-7
63. Booth PJ, Curran AR. 1999. Membrane protein folding. *Curr. Opin. Struct. Biol.* 9:115-21
64. Dieckmann GR, DeGrado WF. 1997. Modeling transmembrane helical oligomers. *Curr. Opin. Struct. Biol.* 7:486-94
65. Gafvelin G, Sakaguchi M, Andersson H, von Heijne G. 1997. Topological rules for membrane protein assembly in eukaryotic cells. *J. Biol. Chem.* 272:6119-27

66. von Heijne G. 1998. Structural aspects of transmembrane alpha-helices. *Acta Physiol Scand. Suppl* 643:17-9
67. Tsukihara T, Aoyama H, Yamashita E, Tomizaki T, Yamaguchi H, Shinzawa-Itoh K, Nakashima R, Yaono R, Yoshikawa S. 1996. The whole structure of the 13-subunit oxidized cytochrome c oxidase at 2.8 Å. *Science* 272:1136-44
68. Degli EM, Crimi M, Venturoli G. 1990. A critical evaluation of the hydropathy profile of membrane proteins. *Eur. J. Biochem.* 190:207-19
69. Kauzmann W. 1959. Some factors in the interpretation of protein denaturation. *Adv. Protein. Chem.* 14:1-63
70. Nozaki Y, Tanford C. 1971. The solubility of amino acids and two glycine peptides in aqueous ethanol and dioxane solutions. Establishment of a hydrophobicity scale. *J. Biol. Chem.* 246:2211-7
71. Wolfenden R, Andersson L, Cullis PM, Southgate CC. 1981. Affinities of amino acid side chains for solvent water. *Biochemistry* 20:849-55
72. Rose GD, Geselowitz AR, Lesser GJ, Lee RH, Zehfus MH. 1985. Hydrophobicity of amino acid residues in globular proteins. *Science* 229:834-8
73. Kyte J, Doolittle RF. 1982. A simple method for displaying the hydropathic character of a protein. *J. Mol. Biol.* 157:105-32
74. Harper AM, Chaplin MF, Segal AW. 1985. Cytochrome b-245 from human neutrophils is a glycoprotein. *Biochem. J.* 227:783-8
75. Jesaitis AJ, Buescher ES, Harrison D, Quinn MT, Parkos CA, Livesey S, Linner J. 1990. Ultrastructural localization of cytochrome b in the membranes of resting and phagocytosing human granulocytes. *J. Clin. Invest* 85:821-35
76. Adams ER, Dratz EA, Gizachew D, DeLeo FR, Yu L, Volpp BD, Vlases M, Jesaitis AJ, Quinn MT. 1997. Interaction of human neutrophil flavocytochrome b with cytosolic proteins: transferred-NOESY NMR studies of a gp91phox C-terminal peptide bound to p47phox. *Biochem. J.* 325 (Pt 1):249-57

77. Kleinberg ME, Mital D, Rotrosen D, Malech HL. 1992. Characterization of a phagocyte cytochrome b558 91-kilodalton subunit functional domain: identification of peptide sequence and amino acids essential for activity. *Biochemistry*. 31:2686-90
78. Nakanishi A, Imajoh-Ohmi S, Fujinawa T, Kikuchi H, Kanegasaki S. 1992. Direct evidence for interaction between COOH-terminal regions of cytochrome b558 subunits and cytosolic 47-kDa protein during activation of an O(2)-generating system in neutrophils. *J. Biol. Chem.* 267:19072-4
79. Rotrosen D, Kleinberg ME, Nunoi H, Leto T, Gallin JI, Malech HL. 1990. Evidence for a functional cytoplasmic domain of phagocyte oxidase cytochrome b558. *J. Biol. Chem.* 265:8745-50
80. Tsuchiya T, Imajoh-Ohmi S, Nunoi H, Kanegasaki S. 1999. Uncompetitive inhibition of superoxide generation by a synthetic peptide corresponding to a predicted NADPH binding site in gp91-phox, a component of the phagocyte respiratory oxidase. *Biochem. Biophys. Res. Commun.* 257:124-8
81. Yoshida LS, Saruta F, Yoshikawa K, Tatsuzawa O, Tsunawaki S. 1998. Mutation at histidine 338 of gp91(phox) depletes FAD and affects expression of cytochrome b558 of the human NADPH oxidase. *J. Biol. Chem.* 273:27879-86
82. Babior BM. 1999. NADPH oxidase: an update. *Blood*. 93:1464-76
83. Zhen L, Yu L, Dinauer MC. 1998. Probing the role of the carboxyl terminus of the gp91phox subunit of neutrophil flavocytochrome b558 using site-directed mutagenesis. *J. Biol. Chem.* 273:6575-81
84. Burritt JB, Quinn MT, Jutila MA, Bond CW, Jesaitis AJ. 1995. Topological mapping of neutrophil cytochrome b epitopes with phage-display libraries. *J. Biol. Chem.* 270:16974-80
85. Conti-Fine BM, Lei S, Mclane KE. 1996. Antibodies as tools to study the structure of membrane proteins: the case of the nicotinic acetylcholine receptor. *Annu. Rev. Biophys. Biomol. Struct.* 25:197-229

86. Traxler B, Boyd D, Beckwith J. 1993. The topological analysis of integral cytoplasmic membrane proteins. *J. Membr. Biol.* 132:1-11
87. Yu L, DeLeo FR, Biberstine-Kinkade KJ, Renee J, Nauseef WM, Dinauer MC. 1999. Biosynthesis of flavocytochrome b558 . gp91(phox) is synthesized as a 65-kDa precursor (p65) in the endoplasmic reticulum. *J. Biol. Chem.* 274:4364-9
88. Vignais PV. 2002. The superoxide-generating NADPH oxidase: structural aspects and activation mechanism. *Cell. Mol. Life. Sci.* 59:1428-59
89. Rasmusson BJ, Sandoval KB, Magnusson K-E, Petersen NO, Jesaitis AJ. Image correlation spectroscopy of flavocytochrome b559 in neutrophil FcR-mediated adherence footpads. 38th Annual Meeting of the American Society for Cell Biology, San Francisco, CA. 1998.
90. Wientjes FB, Segal AW, Hartwig JH. 1997. Immunoelectron microscopy shows a clustered distribution of NADPH oxidase components in the human neutrophil plasma membrane. *J. Leukoc. Biol.* 61:303-12
91. Beratan DN, Onuchic JN, Winkler JR, Gray HB. 1992. Electron-tunneling pathways in proteins. *Science* 258:1740-1

ANTI-GP91-PHOX ANTIBODIES (CL5 AND 54.1) AS IMMUNOPROBES FOR NOX
FAMILY PROTEINS, GRP58 AND GELSOLIN

Introduction

Human phagocyte flavocytochrome b558 (Cytb) is an integral membrane protein composed of two polypeptides (gp91-phox and p22-phox) with molecular weight of 91,000 and 22,000 (1, 2). Cytb serves as the electron transferase of the NADPH oxidase complex (3, 4, 5). This membrane localized enzyme plays an important role in the host defense function of phagocytic cells, including neutrophil granulocytes, monocytes, macrophages and eosinophils (6, 7). During phagocytosis, macrophages and neutrophils produce a variety of toxic products that help to kill the microorganisms engulfed into phagosomes (8, 9). Superoxide anion ($O_2^{\cdot-}$) is the common precursor for the production of such reactive oxygen species and is generated by the NADPH oxidase in the plasma membrane, phagosomal membrane and at discrete internal membrane sites.

Homologues of human gp91-phox have been identified in a variety of tissues. Based on their sequence similarity four different mammalian proteins were identified and assigned to the Nox family, while two larger proteins were identified and assigned to the Duox family (10, 11, 12, 13). All of the identified homologues contain a cluster of up to six putative hydrophobic transmembrane domains similar to the gp91-phox transmembrane helices at amino-terminal part of the protein including conserved histidine residues implicated in heme ligation by gp91-phox. Also, there is significant

similarity in the carboxy-terminal domain of Nox/Duox family proteins with consensus sequences comprising putative flavin- and NAD(P)H-binding sites found in a variety of FAD-bound redox proteins. Nox5, Duox proteins and homologous plant proteins also contain a larger hydrophilic N-terminal domain not present in other Nox proteins (including gp91-phox) (14, 15, 16, 17, 18). This domain contains two Ca^{2+} -binding EF-hand motifs possibly involved in regulation of catalytic activity. In addition, Duox proteins possess a unique, amino-terminal hydrophobic transmembrane α -helix and putative extracellular domain homologous to peroxidase (14, 15).

Anti-Cytb antibodies have found variety of applications in research related to NADPH oxidase structure and function. Such antibodies have been widely used for identification and quantitative analysis in Cytb expression experiments and chronic granulomatous disease (CGD) studies (19, 20, 21, 22, 23, 24, 25). Due to the absence of crystallographic data, a variety of experimental approaches have been utilized to explore structural aspects of Cytb. Biochemical analysis combined with epitope mapping of monoclonal antibodies has confirmed aspects of transmembrane topology and has revealed intramolecular interaction features in the tertiary structure of the protein (26, 27, 28, 29, 30). Moreover, such antibodies are finding important application in studies involving biochemical and physiological assays of Cytb and NADPH oxidase function (28); (Taylor, RM and Jesaitis, AJ, unpublished data).

The structural similarities among Nox family members suggest that anti-Cytb antibodies may be cross-reactive with some of the other members of this family and might be of use in their detection. In this study we analysed the potential of two

monoclonal antibodies for use as immunoprobes for Nox family proteins and detection of possible short forms of gp91-phox expressed in CGD neutrophils. In addition, the mAb CL5 epitope was mapped and proteins which specifically cross-react with mAbs 54.1 and CL5 have been partially purified and identified.

Materials and Methods

Materials

The pBluescript KS+ vector containing the full-length gp91-phox gene insert was kindly provided by M. Dinauer.

Mouse anti-ERp57 mAb was obtained from Stressgen Biotechnologies Corporation (Victoria, BC, Canada) and mouse anti-gelsolin mAb was obtained from Sigma-Aldrich (St. Louis, MO). Alkaline phosphatase conjugated goat anti-mouse IgG was obtained from BioRad Laboratories (Hercules, CA). *E. coli* XL1-Blue, *E. coli* BL21(DE3) and *E. coli* BL21(DE3)pLysS strains were obtained from Invitrogen (Carlsbad, CA), and the expression vector pET-14b from Novagen (Madison, WI). Restriction enzymes EcoRI, NdeI, BamHI were purchased from New England Biolabs (Beverly, MA). 5-bromo-4-chloro-3-indolyl phosphate/nitro blue tetrazolium (BCIP/NBT) chromogen was purchased from Kirkegaard and Perry Laboratories (Gaithersburg, MD). GammaBind Plus Sepharose was obtained from Pharmacia Biotech (Piscataway, NJ). ProSieve Protein Markers were obtained from BMA (Rockland, ME). IEF carrier ampholytes pH 3-10 and immobilized pH gradient strips Immobiline DryStrip

were purchased from Amersham Biosciences (Piscataway, NJ). Mass spectrometry grade trypsin was purchased from Promega Corporation (Madison, WI). Luria-Bertani medium was purchased from EM Science (Gibbstown, NJ). Acetonitrile and trifluoroacetic acid were from Mallinckrodt Baker (Philipsburg, NJ). Unless otherwise specified, all other reagents were purchased from Sigma-Aldrich (St. Louis, MO).

Monoclonal antibody CL5 was produced using standard hybridoma technology (28). Briefly, the X-CGD mutant mouse strain C57 Bl/6JxE129 (Genentech Inc, South San Francisco, CA) was immunized three times with 50 μ g of partially purified Cytb solubilized in 10 mM HEPES, 10 mM NaCl, 100 mM KCl, pH-7.4, containing 40 mM octylglucoside. Hyperimmune splenocytes were fused with 3PU1 myeloma cells and screened for mAb production by ELISA using octylglucoside-solubilized Cyt b. Hybridoma clones producing anti-Cytb antibodies were cloned twice by limiting dilution and grown in RPMI-1640 medium containing 5% FBS. Following growth of positive clones antibody was purified from hybridoma culture supernatant on Gammabind Plus Sepharose as described by manufacturer and dialyzed against 150 mM NaCl, 10 mM Na₂HPO₄, pH-7.4. The name of this antibody is derived from the abbreviation C for CGD mouse strain immunized animal, L for Large Cytb subunit gp91-phox, and 5 for clone number 5.

Cloning, Transfection, Cell Culture and Preparation

Cloning of the cytoplasmic portion of gp91-phox (residues 293-570) into the *E. coli* expression vector pET-14b was conducted as follows. Using the initial pBluescript

KS+ vector containing the full length gp91-phox gene (inserted into the Bam HI site) as the source of DNA, the Quickchange Mutagenesis kit (Stratagene, La Jolla, CA) was used according to the manufacturers instructions to introduce a unique NdeI restriction site at residue 292 in the gp91-phox gene (5' mutagenic primer: 5' GGTTTTGGCGATCTCATATGAAGGTGGTCATCACC 3'; 3' mutagenic primer: 5' GGTGATGACCACCTTCATATGAGATCGCCAAAACC 3'). Following PCR mutagenesis, the resulting products were electroporated into *E. coli* XL1-Blue and resulting transformants were grown for purification of plasmid DNA using a QIAprep Spin Miniprep kit (Qiagen, Valencia, CA). Restriction digest analysis with NdeI was used to screen for transformants which contained the desired mutation. Plasmid containing the desired mutation was then double digested with NdeI/BamHI and the resulting fragments of gp91-phox were gel purified using a QIAquick Gel Extraction kit (Qiagen, Valencia, CA). Since the resulting N- and C-terminal fragments of gp91-phox co-migrated on agarose gels, the two fragments were simply gel purified together and then ligated into pET-14b (that had also been double digested with NdeI/BamHI and gel purified). The ligation reactions were electroporated into *E. coli* XL1-Blue and resulting colonies screened for the desired construct. Plasmid DNA was isolated from colonies containing insert and these constructs were restriction mapped with EcoRI (which produces a ~0.8 kb fragment for constructs containing the C-terminal portion of gp91-phox) for identification of the desired ligation product.

For expression of Nox protein fragments, pET-14b containing the C-terminal portion of gp91-phox was electroporated into *E. coli* BL21(DE3)pLysS and pET32a(+)

vectors containing the C-terminal fragments of Nox1, Nox3 and Nox4 were transformed to *E. coli* BL21(DE3) using One Shot BL21 Star(DE3) chemically competent cell kit (Invitrogen, Carlsbad, CA). Colonies resistant to ampicillin and both, ampicillin and chloramphenicol in case of the *E. coli* BL21(DE3)pLysS strain, were then isolated. Transformed cells were grown at 37 °C in Luria-Bertani medium containing the antibiotics to an OD₆₀₀=0.4-0.6 and then induced for 4 h with 1 mM IPTG. Following induction, cells were centrifuged and resuspended in 10 mM HEPES, 10 mM NaCl, 100 mM KCl, pH-7.4 and then disrupted by probe sonication.

The Nox1 cDNA cloning from a human colon cDNA library and transfection into NIH 3T3 cells using the pEF-PAC vector was described by Suh Y.A., et al. (31). The stably transfected NIH 3T3 cells (American Type Culture Collection, Manassas, VA) were maintained at 37 °C in 5% CO₂ in DMEM medium containing 10% FBS, penicillin (100 U/mL), and streptomycin (100 µg/mL). Medium for pEF-PAC-Nox1 transfected cells was supplemented with 1 µg/mL puromycin. For harvesting, cells were detached by incubating with 0.05 g/L porcine trypsin and 0.5 mM EDTA in 150 mM NaCl, 10 mM Na₂HPO₄, pH-7.4 for a few minutes and resuspended in growth medium. After washing with in 10 mM HEPES, 10 mM NaCl, 100 mM KCl, pH-7.4, the cells were incubated 15 min on ice with 2 mM DFP to inactivate serine esterases. The washed cells were then pelleted by centrifugation and resuspended in membrane resuspension buffer MRB (10 mM HEPES, 10 mM NaCl, 100 mM KCl, 1 mM EDTA, 0.1 mM dithiothreitol, 1 mM PMSF, 10 µg/ml chymostatin, pH-7.4). Membrane fractions were prepared as described by Parkos et al. (1). Briefly, the cells were disrupted by nitrogen cavitation and unbroken

cells and nuclei were separated by low speed centrifugation ($1,000 \times g$, 5 min). The supernatant fraction was then centrifuged in a 60 Ti rotor (Beckman Instruments, Fullerton, CA) at $114,000 \times g$ for 30 min. The resultant membrane pellet was resuspended in MRB buffer and the supernatant saved as a cytosolic fraction.

For Nox protein expression in HEK-293H cells gp91-phox gene was subcloned from EST clone AA996282 to pcDNA3 expression vector and the sequence was confirmed by sequencing. Nox3 was cloned as described before (32). The HEK-293H cells were grown to ~40% confluence and were transfected with 5 μ g of the pcDNA3 vector without insert or harboring gp91-phox or Nox3 using Fugene 6 (Roche, Indianapolis, IN) according to the manufacturer's instructions. After 48 hours, cells were removed from the plate, washed twice with cold PBS, centrifuged to pellet and stored at -70°C until use. Cell membrane fractions were separated as described above for NIH 3T3 cells except that the cells were disrupted by sonication.

Human neutrophils were purified from citrated peripheral blood using gelatin sedimentation followed by lysis of remaining erythrocytes with isotonic ammonium chloride as described by Henson P.M. and Odes Z.G. (33). The isolated cells were disrupted and separated into membrane and cytosolic fractions by the method of Parkos C.A. et al. (1).

CGD neutrophil plasma membrane fractions were prepared by density gradient centrifugation in Percoll (34). The membranes were washed and resuspended in 10 mM PIPES, 100 mM KCl, 3 mM NaCl, 3.5 mM MgCl_2 , 1 mM ATP, 1.25 mM EGTA, 340

mM sucrose, pH-7.3. The CGD neutrophil membrane samples used in this study contained mutations in the CYBB gene described in the legend of Figure 3.4.

Phage-display Epitope Mapping

Monoclonal antibody was subjected to epitope mapping as previously described (35, 36) by selecting peptide sequences that mimic the natural Cyt b epitope from the J404 nonapeptide library (37). Three rounds of selection and amplification of phage display peptide library clones were conducted using a mAb CL5 immunoaffinity matrix as described previously (35, 36). For phage DNA sequencing, 100 μ L of phage from the final column eluate were used to infect starved K91 cells. Serial 100-fold dilutions of infected cells were used to inoculate LB agar plates containing the appropriate dilution, which were then incubated overnight at 37 °C. Isolated colonies were used to inoculate 2 mL of 2 x YT (38) containing kanamycin (75 μ g/mL), and the tubes were incubated overnight at 37 °C in a shaking water bath. DNA from the isolated phage was prepared and sequenced according to the directions of the Sequenase version 2.0 kit (U.S. Biochemical Corp., Cleveland, OH). An oligonucleotide primer with the sequence 5'-GTT TTG TCG TCT TTC CAG ACG-3' was used to determine the nucleotide sequence of the unique region of the phage, and autoradiographs were viewed using PhosphorImager model 400E (Molecular Dynamics/Amersham Biosciences, Piscataway, NJ).

Flow Cytometry Analysis of Surface and Intracellular Antigens

To detect surface antigens with mouse monoclonal antibodies, cells were washed with PBS (10 mM phosphate, 150 mM NaCl, pH-7.4) and incubated with mouse monoclonal antibody at 30 $\mu\text{g}/\text{mL}$ in PBS supplemented with 2% milk protein. After one hour of incubation, the cells were rinsed by centrifugation and resuspension in PBS. Then the cells were labeled with FITC-conjugated goat anti-mouse IgG secondary antibody diluted 1:1000 in PBS with 2% milk protein for one hour, washed twice as before, and suspended in PBS containing 5 $\mu\text{g}/\text{mL}$ propidium iodide. All the incubations were performed on ice and with solutions pre-cooled to 4 $^{\circ}\text{C}$.

For detection of intracellular antigen cells were prepared using the same protocol as described above, except that the PBS buffer was supplemented with 0.1% (w/v) saponin, and cells were preincubated in the saponin-containing buffer for 10 minutes prior to addition of primary antibody.

Samples for paraformaldehyde fixation were rinsed twice with PBS by centrifugation and then incubated with 1% (w/v) paraformaldehyde in PBS for 10 minutes at 22 $^{\circ}\text{C}$. Fixed cells were rinsed twice with PBS and then labeled with antibody as described above for detection of intracellular antigens.

Flow cytometric analysis was performed on 10,000 cells using a Becton Dickinson FACScan flow cytometer supplied with CONSORT 30 software (Becton Dickinson Immunocytometry Systems Inc., Franklin Lakes, CA). Data analysis was performed using WinMDI software (The Scripps Research Institute, La Jolla, CA).

Propidium iodide staining intensity of the cells was used to identify and gate intact or permeabilized cells.

Protein Purification

Proteins representing the bands of molecular weights 57,000 and 91,000 (later in this section indicated by A and B, respectively) on antibody 54.1 (A) and CL5 (B) immunoblots were partially purified from human neutrophil cytosolic fractions prepared as described before (1). In both cases, the protein purification procedure included precipitation with ammonium sulfate followed by chromatographic separation, on DEAE-Sepharose and Heparin-Sepharose. All procedures for protein purification were conducted at 4 °C or in an ice bath.

Ammonium sulfate precipitation: Solid ammonium sulfate was slowly added with stirring to 60% (A) or 40% (B) saturation to 200 mL of the neutrophil cytosol fraction. The solution was stirred for 10 min and centrifuged at $2,000 \times g$ for 1 h to remove precipitate. Additional ammonium sulfate was then added to supernatant to 80% (A) or 60% (B) saturation and after stirring for 10 min the precipitated protein was centrifuged to pellet ($2,000 \times g$ for 1h). The resulting precipitate was dissolved in 10 mL of low salt buffer (10 mM HEPES, 20 mM NaCl, pH-7,4) and dialyzed against 200 volumes of the low salt buffer for 24 h.

DEAE-Sepharose chromatography: Following dialysis the protein solution was loaded on a column of DEAE-Sepharose (1 \times 15 cm) previously equilibrated with low salt buffer. Proteins were eluted with a 100 mL linear salt gradient from 20 to 500 mM

NaCl in 10 mM HEPES, pH-7.4. Fractions containing the protein of interest were identified by immunoblotting with either mAb 54.1 or CL5 as described and pooled fractions were diluted with 10 mM HEPES, pH-7.4 to adjust NaCl concentration to approximately 20 mM.

Heparin-Sepharose chromatography: The diluted protein solution from the DEAE-Sepharose separation step was loaded on a column of Heparin-Sepharose (1 × 10 cm) equilibrated with low salt buffer. Proteins were eluted and fractions were analyzed exactly as described above. Pooled fractions were concentrated using Centricon centrifugal filter devices (Millipore Corporation, Bedford, MA) with molecular weight cut-off 30,000 (A) or 50,000 (B), then extensively dialyzed against 10 mM Hepes, pH-7.4 containing 0.02% (w/v) sodium azide.

SDS-PAGE Electrophoresis

Protein samples were mixed with an equal volume of SDS-PAGE sample buffer (3.3% (w/v) SDS, 167 mM Tris-HCl, pH-6.8, 33% (v/v) glycerol, 0.03% (w/v) bromphenol blue, and 500 mM 2-mercaptoethanol) and boiled for 1 min. The samples were separated by SDS-PAGE on 12% or 7-15% Tris/glycine polyacrylamide slab gels containing 0.1% (w/v) SDS as described (39) and electrophoretic mobility of the sample proteins was compared to prestained protein standards. Proteins were visualized on slab gels by staining with 0.125% Coomassie Blue G 250 in 50% methanol, 10% acetic acid as described (40), silver stained under basic conditions as described (41) or prepared for immunoblotting as described below.

Two-dimensional Gel Electrophoresis

2-DE was performed according to Rabilloud T. et al. (42). For IEF 50 μ L protein sample was mixed with 200 μ L of the rehydration solution (8 M urea, 2 M thiourea, 20 mM DTT, 0.4% carrier ampholytes pH 3-10, 4% (w/v) CHAPS, 2% (w/v) ASB-14, 0.03% (w/v) bromphenol blue, 1mM EDTA in 50 mM Tris-HCl, pH-8.0) and applied to 130 mm immobilized pH gradient (nonlinear gradient from 3 to 10) strips overnight. The following running conditions were then used in the IEF system (Amersham Biosciences, Piscataway, NJ): 0 to 500 V in 4 h, 500 V for 3 h, 500 V to 3500 V in 4 h, and 3500 V for 9 h. After the IEF step, the IPG gel strips were incubated at room temperature for 15 min in 6 M urea, 30% (w/v) glycerol, 4% (w/v) SDS, 13 mM DTT, 50 mM Tris-HCl, pH-6.8. The following equilibration step in preparation for SDS-PAGE was carried out for 15 min in the above solution, except that DTT was replaced by 2.5% (w/v) iodoacetamine and 0.03% (w/v) bromphenol blue. The strips were then mounted at the top of the 1.5 \times 150 mm vertical 12% acrylamide second-dimension gel with a 10 mm stacking gel. Electrophoresis was conducted using a vertical slab gel electrophoresis system (Bio-Rad, Richmond, CA) at 40 V while the bromphenol blue tracking dye migrated through stacking gel and then at 80 V until the tracking dye reached the bottom of the gel. The resolved gels were then either silver stained under basic conditions as described (41), stained with 0.125% Coomassie Blue G 250 in 50% methanol as described (40) for mass spectrometry analysis, or prepared for immunoblotting as described below.

Immunoblotting

Following electrophoresis, protein samples were transferred to nitrocellulose membranes as described previously (1). Monoclonal antibodies were diluted in diluting buffer (3% (v/v) normal goat serum, 1% (w/v) BSA, 0.2% (v/v) Tween 20, 10 mM sodium phosphate, 150 mM NaCl, pH-7.4) and incubated with the nitrocellulose membrane blots for 1 h at room temperature with continuous rocking. The blots were then rinsed with wash buffer (250 mM NaCl, 10 mM Hepes, 0.2% (v/v) Tween 20, pH-7.4) and incubated with a alkaline phosphatase-conjugated secondary antibody diluted 1:1000 ratio in diluting buffer. The blots then were rinsed three times with wash buffer, equilibrated in 250 mM NaCl, 30 mM Tris-HCl, pH-8.0, and developed using a BCIP/NBT phosphatase substrate system.

Protein Identification by MALDI Mass Spectrometry

2-DE separated protein samples were excised from gels and in-gel digested with trypsin as described (43) with several modifications. The acetonitrile dehydrated gel slices were rehydrated in 20 μ L of 40 mM NH_4CO_3 /10% (v/v) CH_3CN containing 25 $\mu\text{g/ml}$ mass spectrometry grade trypsin. An additional 50 μ L of 40 mM NH_4CO_3 /10% CH_3CN were added and digestion was carried out at 37 $^\circ\text{C}$ for 15 h. The resulting peptides were extracted with 50 μ L of 50% (v/v) CH_3CN /1% (v/v) trifluoroacetic acid by bath sonication for 15 min followed by 1 h incubation at room temperature. Samples were diluted at 1:1 ratio in α -cyano-4-hydroxy-cinnamic acid saturated solution and 1 μ L

was spotted on a MALDI target. MS analysis was performed with a Bruker Biflex III MALDI-TOF spectrometer (Bruker Daltonics, Billerica, MA). Peak masses were extracted from the generated spectra and used for protein identification using on-line MASCOT peptide mass fingerprint tool (Matrix Science Ltd., London, UK; URL: <http://www.matrixscience.com>) (44). The interrogation was performed against NCBI nr database with restriction to *Homo sapiens* sp.

Results and Discussion

Monoclonal Antibody Epitope Identification and Characterization of Binding Specificity

A novel mAb, termed CL5, was produced against detergent solubilized Cytb in gp91-phox deficient mice. Following affinity purification, mAb CL5 was used for immunoblotting analysis using human neutrophil membrane and cytosol fractions (1) as a test antigen. Its reactivity was compared to that of mAb 54.1, previously shown to recognize the peptide region 382-PKIAVDGP of gp91-phox (35). The results of the current study show that mAb CL5 recognizes a broad species similar to that recognized by mAb 54.1 in the neutrophil membrane fractions (Figure 3.1, lanes 2 and 4).

Interestingly, mAb CL5 also recognizes a strong band with a molecular weight of 91,000 in the cytosolic fraction that is absent on mAb 54.1 immunoblots. Monoclonal antibody

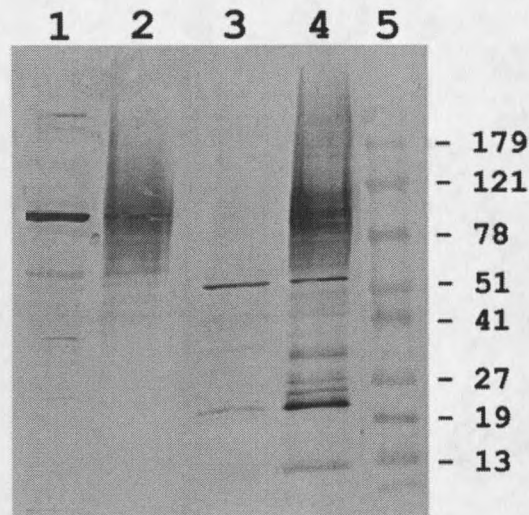


Figure 3.1. Monoclonal antibody CL5 and 54.1 immunoreactivity to neutrophil cytosol and membrane fractions. Samples of neutrophil cytosol (lanes 1 and 3) and membranes (lanes 2 and 4) were resolved (at approximately 3×10^6 cell equivalents per lane) by SDS-PAGE and immunoblotting was performed with mAbs CL5 (lanes 1 and 2) and 54.1 (lanes 3 and 4) at $5 \mu\text{g}/\text{mL}$ concentration as described in Materials and Methods section. Molecular weight standards are shown in lane 5. The data are representative of at least two separate analyses.

54.1 recognizes an additional band with molecular weight of 58,000 in both fractions and a strong band with molecular weight of 25,000 in membrane fraction. The bands with molecular weight of 91,000 and 58,000 were identified as gelsolin and GRP58, as described below. The Mr 25,000 band is attributed to a degradation reduction of gp91-phox (29). It has been demonstrated that the 54.1 antibody does not bind intact or permeabilized neutrophils (35). In the current study, flow-cytometry analysis performed on human neutrophils shows that mAb CL5 does not bind to intact cells (data not shown), though it displays a positive signal in permeabilized neutrophils (Figure 3.2). This analysis suggests that mAb CL5 may serve as an important probe for gp91-phox

detection by immunoblotting but caution need to be exercised in its application since additional reactivities exist for mAb CL5 and also for mAb 54.1.

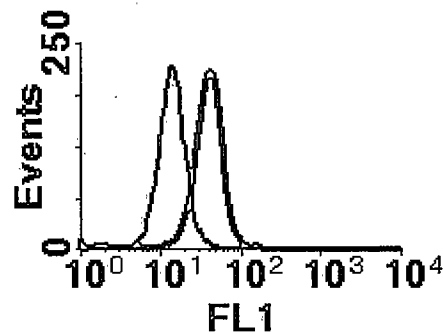


Figure 3.2. Antibody CL5 flow cytometry analysis of permeabilized neutrophils. Human neutrophils were permeabilized by treatment with 1% saponin and exposed to mAb CL5 (thick line) or irrelevant control antibody (thin line) at a 30 $\mu\text{g}/\text{mL}$ concentration on ice for 1 h before washing and labeling with goat-anti-mouse IgG FITC-conjugated secondary antibody. The data are representative of at least three separate experiments.

Monoclonal Antibody CL5 Epitope Identified by Phage Display Epitope Mapping

To precisely define the epitope recognized by mAb CL5, phage display analysis was applied. A total of twenty nine unique peptide sequences were obtained by sequencing 68 selected phage clones from second and third round immunoselections (Figure 3.3). In these selections there was an unusually high number of phage clones with mutations in the constant pIII protein region adjacent to the unique peptide sequence (Figure 3, sequences number 1-5, 14-16, 22, 23, 25, 26, 28, 29) suggesting that the mutated residues might be important, directly or indirectly, for antibody interaction with the pIII protein. Subsequently, for sequence alignment the unique phage nine residue

peptides were extended to include an additional six residues from the pIII constant sequence where most of the mutations were observed. The alignment of the sequences matched to gp91-phox region 135-DPYSVALSELGDR and this peptide was identified as an epitope for mAb CL5.

The identified mAb CL5 epitope is located on the predicted extracellular loop of 30 residues connecting two hydrophobic transmembrane regions of gp91-phox protein. The extracellular placement of this region has been confirmed by previous independent studies examining glycosylation and the binding of antipeptide polyclonal and monoclonal antibodies. Gp91-phox has five potential N-linked glycosylation consensus sites, and glycosylation of three asparagine residues, including Asn148 located immediately at the carboxy-terminal end of the identified mAb CL5 epitope, has been supported by mutagenesis analysis of these positions in a recombinant expression system (45). Polyclonal antibody binding analyses have previously localized the region Glu160 - Thr172 of gp91-phox to the extracellular aspect of the neutrophil plasma membrane (30). In addition, a complex epitope bound by the Cytb-specific mAb 7D5 has been mapped using phage display analysis (27), and suggests that the discontinuous regions of gp91-phox including residues Arg159-Glu164 and Arg226-Gln231 are localized on the extracellular aspect. Nevertheless, our flow cytometry results with intact neutrophil cells were negative, suggesting that the CL5 epitope was latent or sequestered on the native protein structure, contributed possibly by glycosylation. The labeling of saponin-permeabilized cells with mAb CL5 is possibly attributed to the antibody cross-reactivity

to cytosolic protein gelsolin, identified to contain an epitope for mAb CL5 as described below.

Truncated Gp91-phox Fragments are not Stably Expressed in CGD Neutrophils

Phagocytic leukocytes (neutrophils, eosinophils, monocytes and macrophages) affected by the immunodeficiency syndrome, CGD, are unable to activate the NADPH oxidase and generate the reactive oxygen compounds needed for the killing of phagocytosed microorganisms (46, 47, 48, 49). More than two thirds of all cases of CGD are X-linked recessive and result from defects in the CYBB gene that encodes the gp91-phox subunit. The 30-kb CYBB gene consists of 13 exons located at Xp21.1 (50). A broad distribution of defects in patients with X-linked CGD include small and large deletions, insertions, nonsense and missense mutations, splice-site defects and mutations in the 5' regulatory region. (51). Some of the CGD mutations cause premature termination of gp91-phox synthesis, and expression of stable shorter peptides of the defective gp91-phox might be possible. Such truncated species might be immunodetectable using the combination of CL5 and 54.1 mAbs. The mAb 54.1 epitope is located near the carboxy-terminus of gp91-phox at a region encoded on exons 9 and 10. The mAb CL5 epitope is located relatively close to amino-terminal end of the protein, on the region encoded on exon 5.

In this study, membranes of CGD neutrophils, carrying different types of mutations in the CYBB gene, were examined by immunoblotting with mAb CL5 and 54.1. Two of the neutrophil samples contained single amino acid substitution (Arg54Ser)

or deletion (Lys315) mutations (Figure 3.4, lanes 3 and 8). These latter samples were reactive to both of the monoclonal antibodies and showed similar gp91-phox glycoform distribution patterns as control neutrophil samples. However, mAbs 54.1 and CL5 failed to bind smaller size protein fragments from four samples with translation termination signals at exons 8 or 9 (lane 5-7, 9), consistent with the idea that the truncated gp91-phox species are not stably expressed in neutrophils. Similar negative profiles were observed with the samples containing mutations resulting in exon 2 deletion (lane 1), translation termination in exon 3 (lane 4) or entire gene deletion (lane 10). The bands having molecular weights similar to those detected on mAb CL5 and 54.1 immunoblots with neutrophil cytosol or membrane fractions (Figure 3.1) were also detected with varying degrees in the CGD neutrophil samples. The bands with molecular weight of 91,000 and 58,000 were identified as gelsolin and GRP58, as described below. We conclude from these results that there are no stable short-form gp91-phox peptides present in the CGD patients examined.

Epitope Alignment with Nox Family Proteins

Nox family proteins have a high degree of amino acid sequence similarity to gp91-phox, with highly conserved regions in cytosolic and transmembrane domains (10). All of the identified homologues contain a cluster of up to six putative transmembrane domains similar to the gp91-phox transmembrane helices in the amino-terminal half of the protein. This region also includes conserved histidine residues implicated in heme ligation by gp91-phox. There is also a significant similarity in carboxy-terminal domain

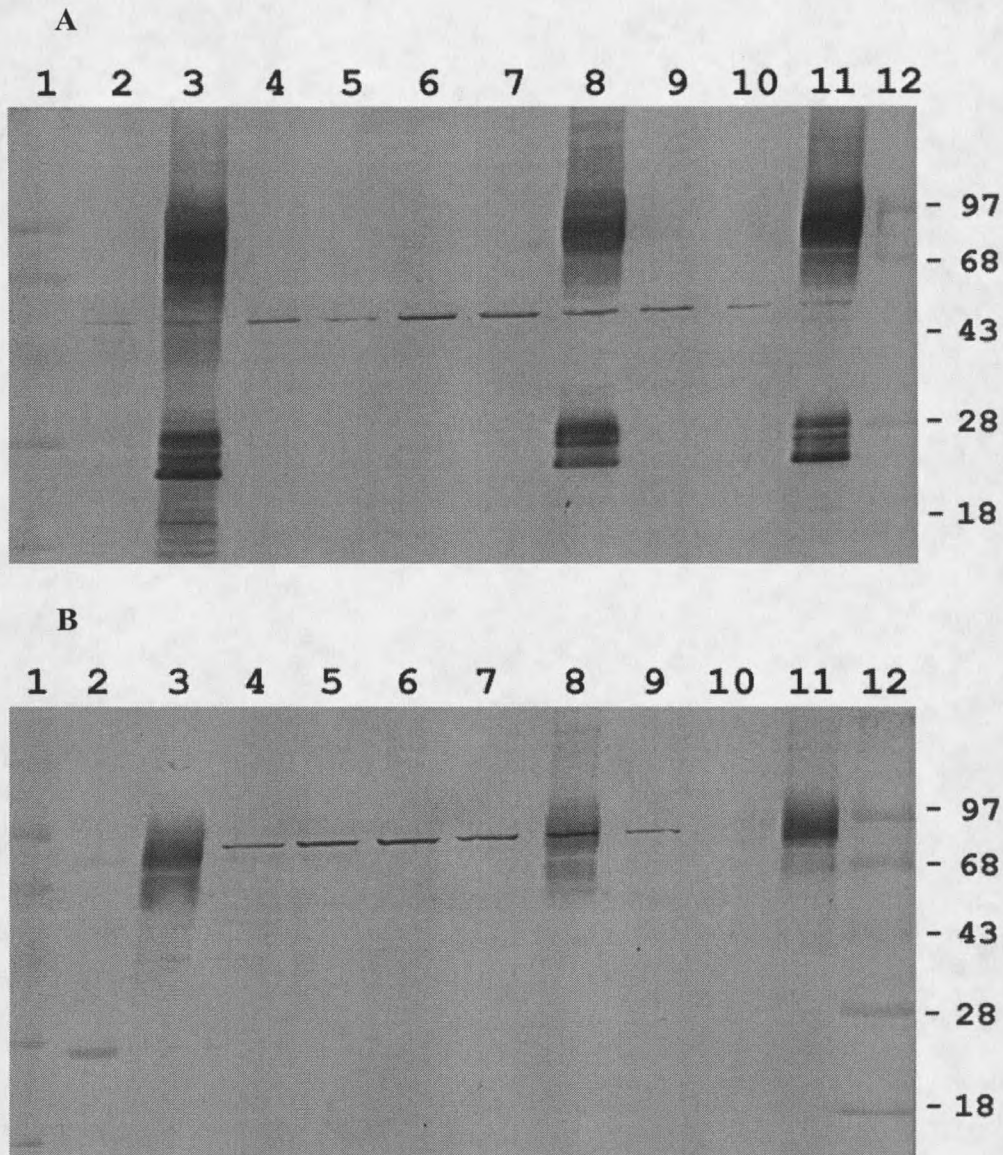


Figure 3.4. CGD neutrophil membrane immunoblotting with mAbs 54.1 (A) and CL5 (B). SDS-PAGE was used to resolve the samples loaded at 3×10^6 cell equivalents per lane. Lane 11 represents control neutrophil samples containing the full length gp91-phox protein. Samples in lanes 2-10 represent CGD mutations and subsequent mRNA transcription or translation effects described in parenthesis as follows: 2 – splice site mutation in intron 2 (exon 2 deletion), 3- G174C (Arg54Ser mutation), 4 – splice site mutation in intron 3 (not determined), 5 – insertion A after A754 (stop in exon 8), 6 – insertion A after A772 (stop in exon 8), 7 – nonsense mutation C880T (stop in exon 8), 8 – AAG955-957 deletion (Lys315 deletion), 9 – nonsense mutation G1151A (stop in exon 9), 10 – exons 1-13 deleted (entire gene deleted). Lanes 1 and 12 – molecular weight standards. The data represent at least three similar analyses.

of Nox family members with consensus sequences comprising putative flavin- and NAD(P)H-binding sites.

To examine the possibility that mAb CL5 or 54.1 might cross-react with other Nox family members, and thus provide valuable probes for these proteins, the sequences of Nox (1-4) were compared. The alignment of the gp91-phox (Nox2) sequence with those of the three other Nox family proteins revealed regions with sequence correspondence to the epitopes of mAbs 54.1 and CL5 (Figure 3.5). The 54.1 epitope and surrounding residues are a part of highly conserved region showing 70% identity for Nox1 and Nox3, and 50% identity for Nox4. A similar comparison of the region recognized by mAb CL5 shows a three to six residue identity in other Nox proteins. However, such identities represent only 23 to 46% sequence conservation making it more likely that the mAb 54.1 would be a better cross-reactive immuno-probe for all of the analyzed Nox proteins.

Monoclonal Antibody 54.1 Recognizes the Conserved Carboxy-terminal Domain of Nox Family Proteins in Immunoblots

To assess the suitability of mAb 54.1 as an immunoprobe for Nox family proteins, Nox protein C-terminal fragments were individually expressed in *E. coli*. The fragments were designed with sequences corresponding to amino acid residue numbers as follows: Nox1 268-564, Nox2 293-570; Nox3 304-568; Nox4 320-428. Results obtained from

A. Ab 54.1

gp91-phox : DAWKL PKIAVDGP FGTAS
 (NOX-2) : PKIAVDGP
 NOX-1 : QYSP I P R I E V D G P F G T A S
 NOX-3 : EPWSL PRLAVDGP FGTAL
 NOX-4 : QSRNYPKLY IDGP FGSPF

B. Ab CL5

gp91-phox : RVNNS DPYSVALSELGDR QNESY
 (NOX-2) : DPYSVALSELGDR
 NOX-1 : RQATD G S L A S I L S S L S H D E K K G G
 NOX-3 : QSEEA Q G L L A A L S K L G N T P N E S Y
 NOX-4 : YSEDFVELN A A R Y R D E D P R K ---

Figure 3.5. Sequence alignment of gp91-phox and Nox 1, 3 and 4 regions corresponding to mAb 54.1 (A) and CL5 (B) epitopes identified by phage-display. The alignment includes epitope sequences on gp91-phox (marked with border) and five surrounding residues from each end. The consensus residues are shaded.

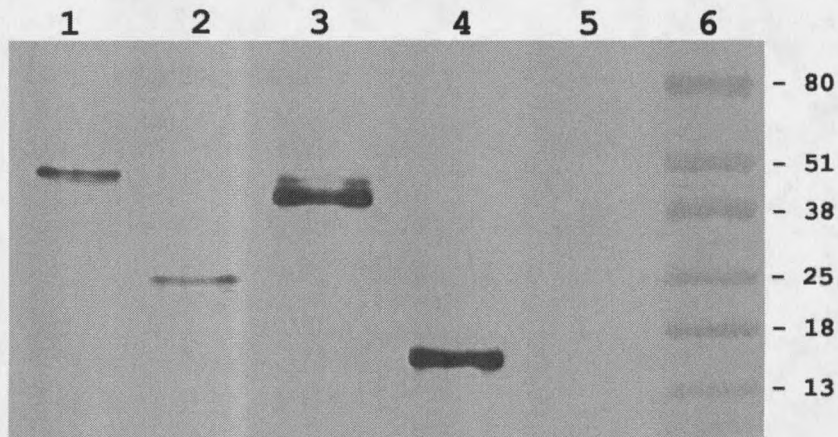


Figure 3.6. Antibody 54.1 immunoblotting of Nox 1-4 fragments (lanes 1-4, respectively). Samples of control cells not transfected with Nox protein fragment is shown in lane 5. Pre-stained protein molecular weight standards are shown in lane 6. Bacterial cell lysates were prepared, resolved by SDS-PAGE and immunoblotted as described in Materials in Methods section. Relative amounts of protein loading was not adjusted and varies depending on Nox protein expression levels in the bacterial cells and other factors. The data are representative of at least three separate experiments.

immunoblotting *E. coli* cell lysates expressing the Nox fragments with mAb 54.1 are shown in Figure 3.6. Specific bands corresponding to the anticipated molecular weight of the Nox protein fragments were observed (lane 1-4) with no positive staining of the control cell lysates (lane 5). The results showed reactivity of mAb 54.1 to epitopes contained in the primary structure of Nox1, Nox2, Nox3 and Nox4. Since these recombinant fragments represented only the carboxy-terminal regions of the Nox proteins, mAb CL5 binding was not examined.

Attempts at Immunodetection of Nox Protein in Membrane Fraction of HEK-293H and NIH 3T3 Using CL5 and 54.1 on SDS-PAGE and 2-DE Gels.

Membrane fractions of HEK-293H cell lines transfected with Nox3 or gp91-phox were analyzed by immunoblotting with mAbs 54.1 and CL5 as shown in Figure 3.7 A and B, respectively. As compared to control cells, transfected with DNA vector without an insert, gp91-phox was detected by both of the antibodies as a broad band with molecular weight of 85,000 to 100,000, corresponding to a glycosylated protein form similar to that observed in neutrophils shown in Figure 3.1. The other broad band, with molecular weight of approximate 60,000 to 70,000, could be assigned to previously identified precursor of gp91-phox biosynthesis that contains smaller, high-mannose carbohydrate chains (lane 2 on panels A and B) (52, 53). A Nox3 translation product was detected by mAb 54.1 as a relatively sharp band with molecular weight of approximately 35,000 and as heterogeneous species of a possibly glycosylated protein observed at a

molecular weight ranging between 45,000 and 50,000 (panel A, lane 1). The observed Nox3 molecular weight of 35,000 is considerably lower than theoretical molecular weight of 66,744. Also, the detected heterogenous forms of the protein with molecular weight of 45,000 to 50,000 are also smaller than the molecular weight of intact protein could be expected. These results suggest that the mAb 54.1 detected bands represent truncated forms of the Nox3 protein that contains the mAb 54.1 epitope. Immunoblots with mAb CL5 do not contain any bands specific for Nox3 expressing cells (panel B, lane 1), suggesting that mAb CL5 does not recognize similar epitope region on Nox3 protein or

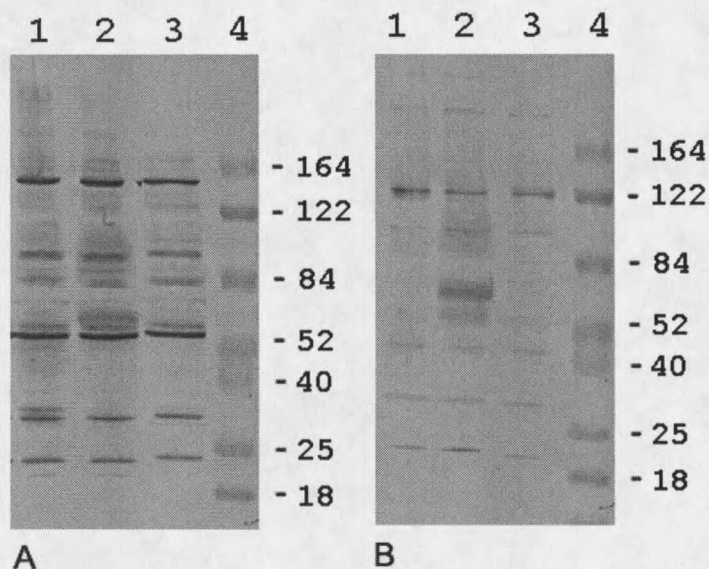


Figure 3.7. Antibody 54.1 and CL5 immunoblots with HEK-293H cell membrane samples. Membrane fractions from Nox3-(lanes 1) or gp91-phox (lane 2) expressing HEK-293H cells and control cells carrying only transfection vector (lane 3) were prepared and resolved by SDS-PAGE at approximately 10^5 cell equivalents per lane. Immunoblotting was performed with mAbs 54.1 (panel A) and CL5 (panel B) at $5 \mu\text{g/mL}$ concentration. Pre-stained protein molecular weight standards are shown in lane 4. The data are representative of two separate analyses.

that the antibody binding affinity is lower and amounts of the protein expressed in the HEK-293H cells could not be detected in this assay.

Immunodetection of Nox1 with the mAbs 54.1 and CL5 was also analyzed using the NIH 3T3 cells expressing the Nox1 long variant as previously described (31). The theoretical molecular weight of Nox1 long variant is 58,972. The immunoblotting results shown in Figure 3.8 indicate that mAb CL5 is reactive to a protein band of Mr 91,000 observed in both Nox1 expressing and control cells, but otherwise the antibody did not show reactivity to proteins of other molecular weights (lanes 3 and 4). A similar band was observed in neutrophil fractions, shown in Figures 3.1 and 3.3. Immunoblots probed with mAb 54.1 display bands of the same approximate molecular weight in both Nox1-expressing and control cells (lanes 1 and 2), including a strong band with molecular weight approximately 58,000, similar to that observed in the neutrophil samples.

Since it has previously been shown that Nox1 mRNA is absent in control cells (31), the immunoblotting result suggested that the antibodies cross-reacted with some other proteins expressed in NIH 3T3 cells. The Mr 58,000 protein was identified as GRP58 as described below. Because of the similar molecular weights of Nox1 and the positive band in these immunoblots it is conceivable that the cross-reactive protein might interfere with binding of 54.1 to Nox1. GRP58 has a theoretical molecular weight of 56,782 with a pI of 5.98. Nox1 on the other hand, has a pI equal to 9.02. Thus a good separation of the two proteins should be achieved by isoelectrical focusing. This possibility was examined by employing two-dimensional gel electrophoresis.

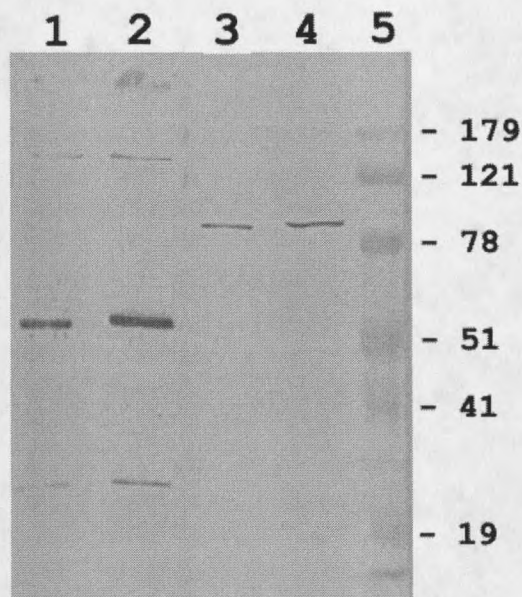


Figure 3.8. Antibody 54.1 and CL5 immunoblots with NIH 3T3 cell membrane samples. Membrane fractions from Nox1-expressing NIH 3T3 cells (lanes 1 and 3) and control cells carrying only transfection vector (lanes 2 and 4) were prepared and resolved by SDS-PAGE at approximately 10^6 cell equivalents per lane. Immunoblotting was performed with mAbs 54.1 (lanes 1 and 2) and CL5 (lanes 3 and 4) at $5 \mu\text{g/mL}$ concentration. Pre-stained protein molecular weight standards are shown in lane 5. The data are representative of at least three separate analyses.

The strongly staining species detected by immunoblotting with mAb 54.1 had a pI in the acidic range that corresponded to pI value of GRP58 (Figure 3.9, panel A). However, the Nox1 with a basic pI could not be detected in this immunoblotting assay. Thus, the results suggest that the antibody did not recognize the epitope on the immunoblotted, full length Nox1 protein or that the protein expression level is below the detection limits of the assay used. The immunoblotting assay detection limit for gp91-phox was determined by serial dilution of purified Cytb at approximately 10 and 45 fmole/lane for mAbs 54.1 and CL5, respectively. Assuming that the assay sensitivity with mAb 54.1 would be

